國立臺灣大學生物資源暨農學院生物科技研究所

碩士論文

Institute of Biotechnology
College of Bio-Resources and Agriculture
National Taiwan University

Master's Thesis

探討 TAOK1 在 SH-SY5Y 神經母細胞中的神經毒性及神經炎症效應

Elucidating the Neurotoxic and Neuroinflammatory Effect of TAOK1 in SH-SY5Y Neuroblastoma Cells

吳靖敏

Jing Min Goh

指導教授：林劭品 博士

Advisor: Shau-Ping Lin, Ph.D.

中華民國 113 年 7 月

July 2024

doi:10.6342/NTU202402516

Acknowledgements

It is the most horrifying thing when someone becomes a stranger right before your eyes. It is never all of a sudden, and you can almost always recall when it was that they were not themselves. There would be memories where they were asking if you've eaten just not too long ago, and now accusing you of being a stranger and breaking into their room. At first, your chest becomes heavy, knowing all the while that this could happen. Then sometimes, a lump appears in your throat, your ears burn, and words that you would never have spoken form at the tip of your tongue. You might begin to look forward to the next fair-weathered day, after all, it always came. But more often than not, the skies would be full of dark clouds, and you cannot remember when you last saw the sun. There would be one day when the storm finally passes. At first, you may feel happy and light, and there would be days when you'd miss the rain. This thesis is dedicated to all the primary caregivers who have weathered storms, some of which were mild and gentle, while others leave only ruins in their wake. One day, we will build shelters, and drizzles will never become a storm. But before then, do not feel guilt when you have to hold an umbrella in your hand, or when someone holds one above your heads.

This thesis is also dedicated to my closest companion for 16 years. I have held you in my hands since you were the size of my palm, yet my wilfulness have brought me away from you in your final days. My dear Fluffy, with you, a part of me is lost forever.

Thank you to all the Professors, my classmates and companions who have made these two years like a marathon full of cheers and treats. None of this work would have been possible without you.

doi:10.6342/NTU202402516

中文摘要

神經退行性疾病 (Neurodegenerative Diseases)，如阿爾茨海默症（Alzheimer's Disease）和帕金森病（Parkinson's Disease），其特徵是神經元和突觸的喪失，通常由於異常蛋白質沉積和神經炎症引起。TAOK1（一種絲氨酸/蘇氨酸激酶）被確定為 AD 和 PD 患者認知障礙的生物標誌物，並在血漿來源的細胞外囊泡中積累。TAOK1 已知會促進細胞死亡、病理性 tau 蛋白磷酸化，進而調節微管動態。儘管 TAOK1 在許多研究中與神經發育障礙有關，但其在神經退行性疾病中的作用較少研究。在初步研究中，TAOK1 過度表達會降低細胞活力和 ATP 產量，增加 tau 蛋白磷酸化，並增加可轉座元件（Transposable Elements）的活動性。為了更好地研究 TAOK1 在通過 tau 蛋白誘導的微管失調和 TE 釋放的神經毒性後果中的作用，我們在人的神經母細胞瘤 SH-SY5Y 細胞中建立了一個可誘導的 TAOK1 過度表達細胞株。在本研究中，我們證明了 TAOK1 過度表達促進了 tau 蛋白的過度磷酸化，可能導致微管的不穩定。這表現為在神經分化過程中無法維持神經突起的生長。還觀察到了與突觸和微管相關基因表達的補償性變化。神經突起的喪失，加上細胞凋亡的增加，表明 TAOK1 過度表達與神經毒性有關。進一步分析發現，TAOK1 過度表達的細胞在儘管抗氧化基因上調的情況持續顯示出活性氧水平的升高，，這表明氧化壓力是促使炎症反應的驅動因素。還發現內質網應激反應通路基因上調，暗示 TAOK1 介導的 tau 蛋白過度磷酸化在病理性蛋白質聚集中的作用。此外，TAOK1 過度表達上調了幾個 TE 家族。隨著 STING 和 TBK1 表達的增加，數據表明細胞質雙鏈 DNA 的檢測增加，並可能通過 I 型干擾素通路激活炎症(IFN-I)反應，表明 TE 釋放的神經毒性後果。總體而言，這些發現

doi:10.6342/NTU202402516

闡明了 TAOK1 過度表達如何引起神經毒性並促進促炎機制，可能促進神經退行性疾病的進展。

關鍵字：神經退行性疾病，阿茲海默症，帕金森氏症，Tau 蛋白磷酸化，微管動態，神經毒性，可轉座元件，氧化壓力，發炎反應

doi:10.6342/NTU202402516

Abstract

Neurodegenerative diseases (NDs) like Alzheimer's (AD) and Parkinson's (PD) are characterised by neuron and synapse loss, often due to abnormal protein deposition and neuroinflammation. TAOK1, a serine/threonine kinase, was identified as a biomarker for cognitive impairment in AD and PD, accumulating in plasma-derived extracellular vesicles. TAOK1 is known to contribute to cell death, pathological tau phosphorylation, and by extension, regulation of microtubule dynamics. While TAOK1 has been implicated in neurodevelopmental disorders in many studies, its role in neurodegeneration is less studied. In preliminary studies, TAOK1 overexpression reduces cell viability and ATP production, increases phosphorylated Tau, and transposable elements (TEs) derepression. To better investigate TAOK1's role in inducing neurotoxicity, therefore promoting neuron and functional loss, we established an inducible TAOK1-overexpressing cell line in human neuroblastoma SH-SY5Y cells. In this study, we have demonstrated that TAOK1 overexpression increases phosphorylated Tau, potentially leading to the destabilisation of microtubules. This was evidenced by inability to maintain neurite outgrowths during neuronal differentiation accompanied by changes in expression of synapse and microtubule-associated genes. Neurite loss, coupled with increased apoptosis, indicates neurotoxic effects linked to TAOK1 overexpression. TAOK1-overexpressing cells also exhibited elevated reactive oxygen species coupled with downregulation of mitochondria protein-coding genes, suggesting mitochondrial dysfunction as a driver of oxidative stress and neurotoxicity. Upregulation of endoplasmic reticulum stress response pathway genes was also discovered, implicating TAOK1-mediated tau hyperphosphorylation in pathological protein aggregation as a source of cellular stress. Additionally, TAOK1 overexpression upregulated several TE families. With increased STING and TBK1 expression, a heightened detection of cytosolic dsDNA

doi:10.6342/NTU202402516

and potential activation of inflammatory responses via class I Interferon pathways may be occurring as potential neurotoxic consequences of TE de-repression. Collectively, these findings elucidate how TAOK1 overexpression induces neurotoxicity and promotes pro-inflammatory mechanisms, contributing to the progression of neurodegenerative diseases.

Keywords: TAOK1, biomarker, cell death, neuron loss, neurite maintenance, abnormal protein deposition, tauopathy, tau phosphorylation, neurodegenerative diseases, dementia, cognitive impairment, neurotoxicity, neuroinflammation

doi:10.6342/NTU202402516

Table of Contents

doi:10.6342/NTU202402516

doi:10.6342/NTU202402516

doi:10.6342/NTU202402516

doi:10.6342/NTU202402516

Table of Figures

doi:10.6342/NTU202402516

doi:10.6342/NTU202402516

doi:10.6342/NTU202402516

1. Introduction

1.1. Neurological Health and Neurodegenerative Diseases

1.1.1. Introduction

Throughout history, diseases have posed a significant threat, repeatedly devastating civilizations. When considering the burden of disease on life, one might first think of epidemics such as smallpox, the bubonic plague, or, more recently, the COVID-19 pandemic. However, it is easy to overlook the more insidious players whose constant presence poses an increasing threat to human health. These persistent and often unnoticed diseases quietly but steadily impact our well-being, highlighting the need for ongoing vigilance and research to mitigate their effects.

In 2024, a public health study on the Global Burden of Diseases (GBD) was published by The Lancet, detailing the health challenges faced by 204 countries and territories from 1990 to 2021. According to this study, approximately 3.4 billion people out of the global population of 7.9 billion in 2021 were affected by neurological disorders (GBD 2021 Nervous System Disorders Collaborators, 2024). Neurological disorders encompass a broad range of diseases, including neurodevelopmental disorders such as autism spectrum disorders (ASD) and attention deficit hyperactivity disorder (ADHD), and neurodegenerative diseases (NDs) such as multiple sclerosis, Parkinson's disease (PD), Alzheimer's disease (AD), and other dementias. Neurodegenerative diseases contribute substantially to the global burden, accounting for 14.5% of disability-adjusted life years (DALYs) and 30.9% of deaths within the neurological disorders group. Alarmingly, these values are expected to increase. As life expectancy rises due to advancements in various technologies, the burden of disorders that develop with aging is also likely to grow. For example, AD, which was ranked 22nd in the leading causes of

doi:10.6342/NTU202402516

disease burden worldwide in 2022, is predicted to rise to 8th by 2050 (GBD 2021 Forecasting Collaborators, 2024). These trends illustrate the pressing need to address the growing impact of neurodegenerative diseases on public health.

1.1.2. Neurodegenerative Diseases & Diagnosis

Brain-associated NDs are characterised by hallmarks such as inflammation, pathological protein aggregation, synaptic and neuronal network deficits and neuronal cell death. These contribute towards impairment in brain communication and regular brain function that could present as symptoms including cognitive impairment, behavioural changes and psychological disturbances (Wilson, et al. 2023). In the largest subgroup of NDs as detailed by the GBD study, AD and other dementias are primarily characterised by cognitive impairment in affected individuals. This are identified as deficits in various areas of cognition such as executive function, language, and memory (American Psychiatric Association, 2022).

Current clinical diagnostic approaches include observing familial history, neuropsychological tests that assesses cognitive function, such as the mini-mental state examination (MMSE) and neuroimaging, where PET scans can identify protein deposits or neural injury (Hugo & Ganguli, et al. 2014). However, many of these methods are reactive towards the onset of cognitive symptoms that reached at a mid to late stages of degeneration (Malek-Ahmadi, et al. 2020). However, as scientific research advances, methods such as laboratory tests and genetic testing have emerged as a form of proactive screening to identify risk factors and changes in molecule deposition that can cause neurodegeneration. These are known as biomarkers and can be in the form of genetic biomarkers like genetic single nucleotide polymorphisms (SNPs), protein or metabolic biomarkers that reflect changes in gene expression and accumulation of proteins. These

doi:10.6342/NTU202402516

may be identified through genetic testing, neuroimaging and detection through various body fluids. Genes such as ApoE4 and SNCA carry the potential for highlighting genetic susceptibility (Corder, et al. 1993; Polymeropoulos, et al. 1997). On the other hand, others such as TREM2 whose shifts in gene expression, reflects disease progression (Lue, et al. 2015). Biomarkers that can accurately reflect specific disease subtypes or disease progression is critical in not only early detection, but also reduce misdiagnosis due to similar presentation of clinical symptoms. Hence, leading us to a discovery analysis for biomarkers that can identify cognitive impairment in diseased individuals to allow a more tailored approach to treatment.

1.2. TAOK1: Discovery, Functions and Implications

1.2.1. TAOK1 as a Protein Biomarker for Cognitive Impairments

Thousand and one amino acid kinase 1 (TAOK1) was first regarded as a protein of interest in our laboratory during the discovery analysis of potential biomarkers that can differentiate dementia patients presenting cognitive impairments. It was found to be enriched in the extracellular vesicles (EV) in the blood of patients with AD and PD-Dementia (PDD). Statistical analysis reveals a significant difference in TAOK1 concentration in patient plasma EVs between those with cognitive impairment and healthy controls, as well as PD patients without cognitive impairment (Unpublished Data). These findings prompt an investigation into the molecular significance of TAOK1 in the neuronal context, which may contribute to shared characteristics observed between these patient groups.

1.2.2. Functions of TAOK1 in the Neuronal Context

TAOK1 is a serine-threonine protein kinase known primarily for its regulatory role in several cellular pathways such as the mitogen activated protein kinase (MAPK)

doi:10.6342/NTU202402516

pathway and Hippo signalling pathways (Hutchison, Berman and Cobb, 1998; Zheng and Pan, 2019). TAOK1 plays a direct role in regulating cellular function Its ability to phosphorylate serine and threonine residues on proteins such as Tau, Rnd3, and MAP2Ks grants it significant regulatory functions in various pathways (Giacomini, et al. 2018; Gard, et al. 2020). Additionally, it is involved in programmed cell death (apoptosis) and mitotic segregation, processes that vital to cellular homeostasis and division (Byeon and Yadav 2024).

In neurodevelopmental studies, TAOK1 has been implicated in neurite formation and development through its influence on microtubule dynamics. Depletion of *TAOK1* results in reduced axon and dendrite branching and impaired synapse establishment (van Woerden, et al. 2021). This may be through TAOK1 phosphorylation of synaptic proteins such as Septin 7, or through the regulation of Tau phosphorylation (Byeon & Yadav, 2021). Abnormal *TAOK1* expression has been linked to impaired neurodevelopment and observed in numerous clinical studies of neurodevelopmental diseases, implicating it in deficits in neurodevelopment and behavioural changes. (Dulovic-Mahlow, et al. 2019; (Beeman, et al. 2023). *TAOK1* itself is recognized as a potential candidate gene for neurodevelopmental disorders, with *de novo* variations coinciding with various developmental abnormalities (Hunter, et al. 2022). It is also through the regulation of Tau phosphorylation, that TAOK1 has been implicated in neurodegeneration, where TAOK1 activity has been found to co-localise with pathological Tau aggregates (Giacomini, et al. 2018). Taken together, these highlights the significance of TAOK1 in the neuronal context.

1.2.3. TAOK1 and the MAPK Signalling Pathway

The MAPK pathway is one of the pathways regulated by TAOK1 function. TAOK1 is a member of the MAPK kinase kinase (MAP3K) family, otherwise known as

doi:10.6342/NTU202402516

MAP3K16. By phosphorylating downstream MAP2Ks, TAOK1 can function via the ERK, p38 and JNK-MAPK pathways, activating transcription factors such as TCF, SRF, AP1 and ATF2 to lead to downstream cellular processes (Nair, et al. 2010; Fang, et al. 2020). Dysregulation in the MAPK pathway is known to promote various neurotoxic properties, including the activation of apoptotic pathways, dysregulated microtubule dynamics, synaptic plasticity, inflammation, redox homeostasis and mitochondrial dysfunction (Reszka, et al. 1995; Moens, Kostenko and Sveinbjørnsson 2013; Son, et al. 2013; Yue and López 2020). These are processes that has the potential to contribute to neuronal loss and dysfunction. The MAPK signalling pathways are also highly conserved pathways that are pivotal to immune cell inflammatory responses, and their roles in immune cells have been widely studied to manipulate immune responses in various diseases. The activation of p38-MAPK, and JNK-MAPK signalling can regulate the expression of various pro-inflammatory cytokines through its downstream transcription factors. For example, the expression of various interleukin genes, including *IL1A*, *IL1B*, *IL12*, *IL6*, and type I interferons (IFN-Is), is widely known to be regulated by these MAPKs in response to upstream activation (Platanias 2003; Majoros, et al. 2017; Canovas and Nebreda 2021).

MAPK signalling itself can be affected by various sources of cellular stress such as elevated ROS levels. For example, MAPK regulators, such as MAPK phosphatases (MKPs) or dual-specificity phosphatases (DUSPs), are not only dysregulated in neurological diseases but are also highly sensitive to changes in intracellular ROS levels (Low and Zhang 2016; Xu, et al. 2019). Elevated ROS levels can disrupt the balance of MAPK signalling by affecting the activity of these phosphatases, leading to aberrant MAPK pathway activation. Hence, increased oxidative stress mediated by TAOK1

doi:10.6342/NTU202402516

overexpression can further exacerbate the cytotoxic consequences regulated by the MAPK signalling pathway.

The extensiveness of the MAPK pathway in cellular health highlights the importance of its regulators and pathway components, such as TAOK1. Any abnormalities in its function could result in drastic consequences on neuronal health. Given TAOK1's role within this pathway, abnormal expression of TAOK1 could trigger a cascade of events exacerbating neurotoxicity within the cell. Therefore, we aim to observe the effects of dysregulated TAOK1 expression on the various cellular pathways downstream in MAPK signalling.

1.2.4. TAOK1, Tau Phosphorylation and Microtubule Dynamics

TAOK1's ability to phosphorylate Tau proteins directly or indirectly through kinases like MARK2 and PAR-1 has been well documented in several studies (Timm, et al. 2003; Tavares, et al. 2013). TAOK1 phosphorylation at its microtubule-binding domains and its flanking regions disrupts Tau binding to microtubules and consequently, regulating cytoskeletal dynamics (Gong and Iqbal 2008).

Abnormal Tau aggregation underlies tauopathies like AD, where hyperphosphorylated tau dissociates from microtubules and forms neurofibrillary tangles (Tavares, et al. 2013; Huang, et al. 2021). TAOK1 may exacerbate this process promoting Tau hyperphosphorylation either directly or through intermediaries, disrupting neuronal function and contributing to disease progression. Most importantly, increased TAOK1 activity and Tau hyperphosphorylation has been found by studies to correlate with neurodegenerative disorders such as AD (Giacomini, et al. 2018). However, specificities on how TAOK1 expression changes later in life due to neurodegenerative disease progression, and its direct effects on neuronal health, have yet to be properly established.

doi:10.6342/NTU202402516

Further research is needed to elucidate the exact mechanisms and impact of TAOK1 in the progression of these diseases.

doi:10.6342/NTU202402516

1.3. Protein Aggregation and its Effects on Neuronal Health

Deficits in normal cellular function that contribute to neurodegeneration are often caused by the abnormal accumulation of cellular components. Misfolded proteins, resulting from genetic variations or defective protein clearance mechanisms, can accumulate due to genetic or environmental factors, leading to neuronal dysfunction and loss (Sweeney, et al. 2017). This accumulation of protein aggregates is implicated in many common neurodegenerative disorders, such as PD, AD and amyotrophic lateral sclerosis (ALS). In AD, hyperphosphorylated tau forms neurofibrillary tangles, while in PD, alpha-synuclein aggregates into fibrils (Thal and Tome 2022; Vidovic and Rikalovic 2022). In ALS, TDP-43 aggregates accumulate in inclusion bodies within neurons (Prasad, et al. 2019). Aggregated proteins disrupt cellular processes by physically obstructing the cytoplasm and overwhelming the cell's clearance systems, such as ubiquitination. This accumulation of misfolded proteins promotes cellular stress, particularly in the mitochondria and endoplasmic reticulum (ER). Mitochondrial stress exacerbates the production of reactive oxygen species (ROS), while ER stress triggers the unfolded protein response (UPR). Persistent cellular stress ultimately activates pro-inflammatory responses and cell death pathways, contributing to the progressive neurodegeneration observed in the aforementioned diseases.

TAOK1 regulates Tau phosphorylation, by the indirect or direct phosphorylation of serine/threonine at multiple sites either at or adjacent to its microtubule binding domains. Hyperphosphorylation can cause Tau detachment from microtubules and subsequent aggregation into neurofibrillary tangles. This abnormal tau hyperphosphorylation and tangle formation are hallmarks of AD and contribute to

doi:10.6342/NTU202402516

neuronal dysfunction and degeneration. Therefore, it is crucial to elucidate TAOK1's contributions to tau-mediated toxicity and its effects on neuronal health.

1.4. Reactive Oxygen Species and Neurotoxicity

Another source of cellular toxicity that is associated with abnormal protein accumulation is reactive oxygen species (ROS). ROS are chemically reactive molecules that are produced during regular cellular events that are essential to cellular function like aerobic respiration, or as part of host cell defences. Common ROS include hydrogen peroxide (H_2O_2), superoxide anions (O2●-) and hydroxyl radicals (●OH). ROS are closely associated with the mitochondria, as they are primarily generated as byproducts of the mitochondrial electron transport chain (ETC) during ATP production. However, they can also increase with sources of cellular stress like protein aggregates.

The accumulation of misfolded proteins and aggregates in the cell can trigger the ER's unfolded protein response (UPR) to restore normal function by enhancing protein folding and the degradation of misfolded proteins (Hetz, 2012). The protein folding process itself is a major source of ROS production during the formation of disulfide bonds, forming H_2O_2 as a byproduct (Cao and Kaufman, 2014). A contact site between the mitochondria and ER, known as the mitochondria-associated membrane (MAM), facilitates crosstalk between these organelles. (van Vilet & Agostinis, 2018). Through the MAM, stress signals are conducted between the organelles, and increased ER stress will inevitably promote mitochondria stress (van Vilet, Verfaille and Agostinis, 2014). Ca^{2+} leakage from the ER during stress, can also be taken up by mitochondria and promote ROS generation (Zeeshan, et al. 2016). Thus, abnormal protein aggregation is often associated with increased mitochondrial stress and increased ROS production in neurodegeneration (Abramov, et al. 2020). Additionally, pathological Tau

doi:10.6342/NTU202402516

hyperphosphorylation in causing transposable element (TE) de-repression which has been gaining traction in recent years have also been found to be associated with increased oxidative stress (Ramirez, et al. 2022). TE de-repression of various families, such as the human endogenous retroviruses (HERVs) and Alu, can elevate ROS levels through mechanisms like deficits in iron trafficking and endolysosome deacidification responses (Halcrow, et al. 2024).

Under normal circumstances, antioxidant pathways like the Nrf2 pathway, which is regulated by MAPK signalling, are upregulated, activating intrinsic antioxidants such as catalase, superoxide dismutases (SODs) and glutathione peroxidases (GPXs) to maintain stable ROS levels (Kovac, et al. 2015). This balance between ROS production and removal is known as redox homeostasis. However, these mechanisms can become overwhelmed or be disrupted by misfolded proteins like hyperphosphorylated Tau in AD (Tejo & Quintanilla, 2021). In dysregulated redox homeostasis, excessive ROS accumulate abnormally and result in prolonged oxidative stress. This can damage essential macromolecules such as nucleic acids, lipids, proteins, as well as the mitochondria (Pizzino, et al. 2017).

Neurons are particularly vulnerable to ROS-induced damage due to their high energy requirements, making redox homeostasis critical for their survival and function (Olunfunmilayo, Gerke-Duncan & Holsinger, 2023). The accumulation of oxidative damage in neural cells, particularly in aging has been associated with impairment in cognitive function in AD (Massaad & Klann, 2011). Studies over the years have explored the use of various antioxidants introduced through the diet such as vitamin E, C, molecular hydrogen, caffeine and α-lipoic-acids, to mitigate oxidative damage and promote the activity of endogenous antioxidants (Moretti, Fraga & Rodrigues, 2017;

doi:10.6342/NTU202402516

Casati, et al. 2020; Banks & Rhea, 2021; Pritam, et al. 2022; Ramanathan, et al. 2023). Several of these antioxidants have yielded positive results against tau and Aβ-mediated neurotoxicity, further alluding to the synergistic relationship between pathological protein aggregation, oxidative stress and inflammation (Keshavarz, Farrokhi & Amiri, 2017; Nguyen, et al 2022).

TAOK1 activity may exacerbate risk factors for oxidative stress, such as abnormal Tau phosphorylation, and at the same time, may be involved in pathways like MAPK-Nrf2 that are responsive towards oxidative stress. Dysregulation in TAOK1 activity will create a vicious cycle that can generate more cellular stress and perpetuating cellular damage. Understanding TAOK1's role in redox homeostasis is crucial for elucidating its contribution to oxidative stress and neuronal damage in neurodegenerative disorders.

doi:10.6342/NTU202402516

1.5. Transposable Elements and Cellular Function

Transposable elements (TEs) are mobile DNA sequences that can move and integrate into various parts of the genome. TEs are found in virtually all organisms and are estimated to comprise of about 45% of the human genome (Hoyt, et al. 2022) In normal circumstances, TEs can help promote genetic variability, and are controlled through highly conserved pathways such as the PIWI-piRNA pathway. However, their activity can become dysregulated due to various factors including stress, aging and cellular events causing chromatin relaxation (Breton, Bettencourt and Gendrel 2024). When uncontrolled, TE de-repression is a source of major cellular stress and toxicity, not only through genetic instability, but also triggering of inflammatory pathways to drive cellular dysfunction and death (Bravo, et al. 2020).

In recent years, many studies have observed dysregulated TE expression to not only coincide but drive neuronal dysfunction. Major families such line interspersed nuclear element 1 (LINE-1s), endogenous retroviruses (ERVs) and Alu were amongst the most affected by pathogenic tau aggregation (Guo, et al. 2018). This increased Tau burden was also associated with increased inflammation, and neurotoxicity (Sun, et al. 2018; Ochoa, et al. 2023). Other proteins aggregates in neurodegenerative diseases such as TDP-43 has also been associated with TE de-repression and neurotoxicity (Li, et al. 2012; Krug, et al. 2017). TAOK1 regulates several critical signalling pathways associated with cellular stress such as the MAPK and Hippo pathways, and at the same time, is closely associated with Tau phosphorylation. Hence, it is likely that TAOK1 may promote neurotoxicity through Tau-mediated dysregulation of TEs.

doi:10.6342/NTU202402516

1.6. Neuroinflammation

Neuroinflammation is the inflammatory response within the central nervous system (CNS) and is primarily mediated by glial cells, including microglia and astrocytes (Yang & Zhou, 2019). Neuroinflammatory responses in the CNS are primarily mediated by the secretion of pro-inflammatory cytokines, chemokines, ROS and prostaglandins by CNS cells like microglia and astrocytes (Norden, et al. 2017). These pro-inflammatory molecules can amplify inflammatory responses, recruit and activate additional immune cells to the site of inflammation. While many associate it with glial function, there are many intrinsic sources of neuroinflammation within neurons themselves. Abnormal protein accumulation, TE de-repression and increased oxidative stress can all promote the activation of pro-inflammatory pathways within neurons (Wu, et al. 2020; Mingione, et al. 2021; Nopparat, et al. 2023; Li, et al. 2023). Thus, underlying the importance of investigating its relevance in TAOK1-mediated neurotoxicity. While acute inflammation is a protective mechanism against infection and injuries, chronic inflammation associated with persistent activation of microglia and astrocytes is detrimental and can lead to behavioural deficits and impaired cognitive function particularly in the aged brain (DiSabato, Quan & Godbout, 2016; Xia, et al. 2023).

Previous research suggests that TAOK1 relation to inflammatory responses is primarily associated with MAPK-NF-κB signalling and IL-17 signalling (Zhang, et al. 2018). However, little is known about TAOK1's association with inflammatory responses in neurons.

In this study, we aim to take a more holistic approach to uncover the effects of TAOK1 activity on inflammatory responses through abnormal protein aggregation, oxidative stress and TE de-repression. Ultimately, understanding how TAOK1 can affect

doi:10.6342/NTU202402516

various neuroinflammatory pathways is essential for elucidating TAOK1's overall impact on neuronal health.

1.6.1. The Inflammasome Signalling Pathway

One of the pathways of the innate immune response against pathogens and cellular stress is the inflammasome signalling pathway. Inflammasomes are multiprotein complexes that ultimately lead to the cleavage and release of pro-inflammatory cytokines, such as interleukin-1β (IL-1β) and interleukin-18 (IL-18), and pyroptosis, a form of inflammatory cell death, through the activation of caspase-1 (Kelley, et al. 2019). The inflammasome pathway is often divided into two steps: priming and activation (Yang, et al. 2019). During the priming step, pattern recognition receptors (PRRs) can trigger various pathways to induce the transcription of pro-inflammatory genes, including those encoding cytokines and inflammasome components. This prepares the cell for a rapid response when it detects the activation signal (Gritsenko, et al. 2020). The activation step involves the detection of a second signal, which drives the formation of the inflammasome complex. This complex recruit and activates Caspase-1, leading to the cleavage and activation of pro-inflammatory cytokines and the induction of pyroptotic cell death. Increased TE transposition activity can lead to an accumulation of TE-derived nucleic acids in the cytoplasm (Miller, et al. 2021). These abnormal increase in cytosolic nucleic acids can be sensed by various nucleic sensors, such as cGAS and AIM2 for dsDNA. These receptors initiate a series of pro-inflammatory reactions like IFN-I responses and the activation of the canonical NLRP3 inflammasome pathway (Rathinam, et al. 2010; Pothlichet, et al. 2013; da Costa, et al. 2019; Radzikowska, et al. 2023; Liu, et al. 2024). For instance, Alu elements have been shown to induce NLRP3

doi:10.6342/NTU202402516

inflammasome priming, increasing the expression of NLRP3 and IL-18 mRNA (Lee, et al. 2022).

Given the associations between Tau and TE de-repression, we aim to investigate the NLRP3 inflammasome as a source of neuroinflammation mediated by TAOK1. Understanding how TAOK1 affects inflammasome signalling could provide insights into the mechanisms driving chronic neuroinflammation and neuronal damage.

1.7. Neuron and Synapse Loss in Neurodegenerative Diseases

The loss of neurons and synapses can lead to a loss of neural connectivity, affecting regular brain function, leading to cognitive and motor deficits observed in various neurodegenerative diseases. In AD, the loss of neurons and synapses in the hippocampus and cortex disrupts pathways critical for memory and learning, such as the glutamatergic signalling pathway (Fjell, et al. 2014). The accumulation of amyloid-beta plaques and Tau neurofibrillary tangles also interferes with synaptic function, leading to reduced synaptic plasticity and neuronal death (Spires-Jones and Hyman 2014). On the other hand, the degeneration of dopaminergic neurons in the substantia nigra impairs the dopaminergic pathway, which is essential to motor control, causing the characteristic symptoms of PD (Damier, et al. 1999). Neuron and synapse loss in different regions of the brain may be fostered by genetic variations that develop as these diseases progress. Although AD primarily affects the hippocampus and cortex and PD targets the substantia nigra, they are both plagued with neuronal and synaptic degeneration.

This study proposes that TAOK1 overexpression could reflect general deterioration in neuronal health, which *in vivo,* may contribute to neurodegeneration in various brain regions depending on the specific disease. Thus, TAOK1 overexpression might not be confined to a single neurodegenerative disorder but could represent a

doi:10.6342/NTU202402516

common pathway through which neuronal and synaptic loss occurs, regardless of the initial pathological trigger or the specific brain regions involved.

At this point, we cannot yet determine the pathways where TAOK1 can directly or indirectly contribute towards the deterioration of neuronal health. However, it's regulatory role in tau phosphorylation and involvement in the MAPK signalling pathway clues us into possible sources where it promote neuronal toxicity. Hence, this study aims to elucidate the effect of TAOK1 on neuronal health, exploring various neurotoxic pathways that may contribute towards neuronal and synaptic loss

1.8. Preliminary Studies

Preliminary studies were conducted in our lab by Pin-Jui Kung, to shed light on the molecular mechanisms behind the apparent TAOK1 accumulation in dementia patients. TAOK1 overexpression in differentiating SH-SY5Y was introduced through transient transfection of TAOK1-containing extracellular vesicles. Results from those studies were able to model the in vitro increase of phosphorylated Tau with TAOK1 overexpression, reduce cell viability and ATP production. A reduction in neurite length was also observed, and it was suggested that TAOK1 may induce neurotoxicity through tau hyperphosphorylation to induce synaptic dysfunction through microtubule destabilisation and mitochondrial dysfunction. The expression of several transposable element (TE) families were also found to increase in cells overexpressing TAOK1. (Kung, 2021)

It was postulated that TAOK1 may contribute towards the tau-mediated increase in TE activation observed in other studies and promote downstream immune responses that is detrimental to neuronal health.

doi:10.6342/NTU202402516

1.9. Elucidating the Neurotoxic and Inflammatory Potential of TAOK1 Overexpression in SH-SY5Y Neuroblastoma Cells

1.9.1. Project Aims

The function and impact of TAOK1 activity in neurons remain largely unexplored in the neurodegenerative context. TAOK1 is known for its regulatory role in various cellular pathways due to its ability to phosphorylate various targets. Microtubule destabilisation due to TAOK1 phosphorylation at microtubule binding sites of Tau has been implicated in neurodevelopmental diseases to affect neurite branching and synaptic establishment. Additionally, the propensity for hyperphosphorylated Tau to aggregate into neurofibrillary tangles are amongst the most well-known hallmarks of neurodegenerative diseases like AD. This abnormal protein aggregation can also promote cellular stress, increasing mitochondrial and ER burdens to disrupt redox homeostasis. TE de-repression can also be affected by this protein aggregation in several neurodegenerative diseases. Together, increased oxidative stress and TE de-repression can affect various cellular pathways to drive inflammatory processes. Additionally, TAOK1 can also operate through the MAPK signalling pathway to mediate cellular stress, cell survival and function. Hence, dysregulated TAOK1 activity can drive a cascade of neurotoxic events in the cell, contributing to the perpetuation of neurodegeneration in diseases (**Figure 1**). However, studies have yet to prove that TAOK1 can affect these cellular events to cause neurotoxicity in neurodegenerative diseases.

We hypothesise that TAOK1 overexpression can induce neurotoxicity in the cell directly through Tau phosphorylation, and indirectly perpetuate cellular stress that can be identified through mitochondrial and ER stress, inducing inflammation and ultimately lead to loss of neuronal function and cell death.

doi:10.6342/NTU202402516

This study aims to shed light on the effects of TAOK1 overexpression on neuronal health by looking at cell death and neuronal function. Hence, revealing the molecular mechanisms behind the neurotoxic consequences of TAOK1 accumulation in dementia patients experiencing cognitive impairment. Our objectives include:

(1) Overexpressing TAOK1 endogenously in an inducible SH-SY5Y model to address deficits in transfection models

(2) Characterizing cell death due to TAOK1-mediated pathways

(3) Neurite maintenance in differentiating TAOK1-overexpressing cells and potential implications on neuronal function

(4) Cellular stress and neurotoxic consequences caused by TAOK1-mediated pathways

doi:10.6342/NTU202402516

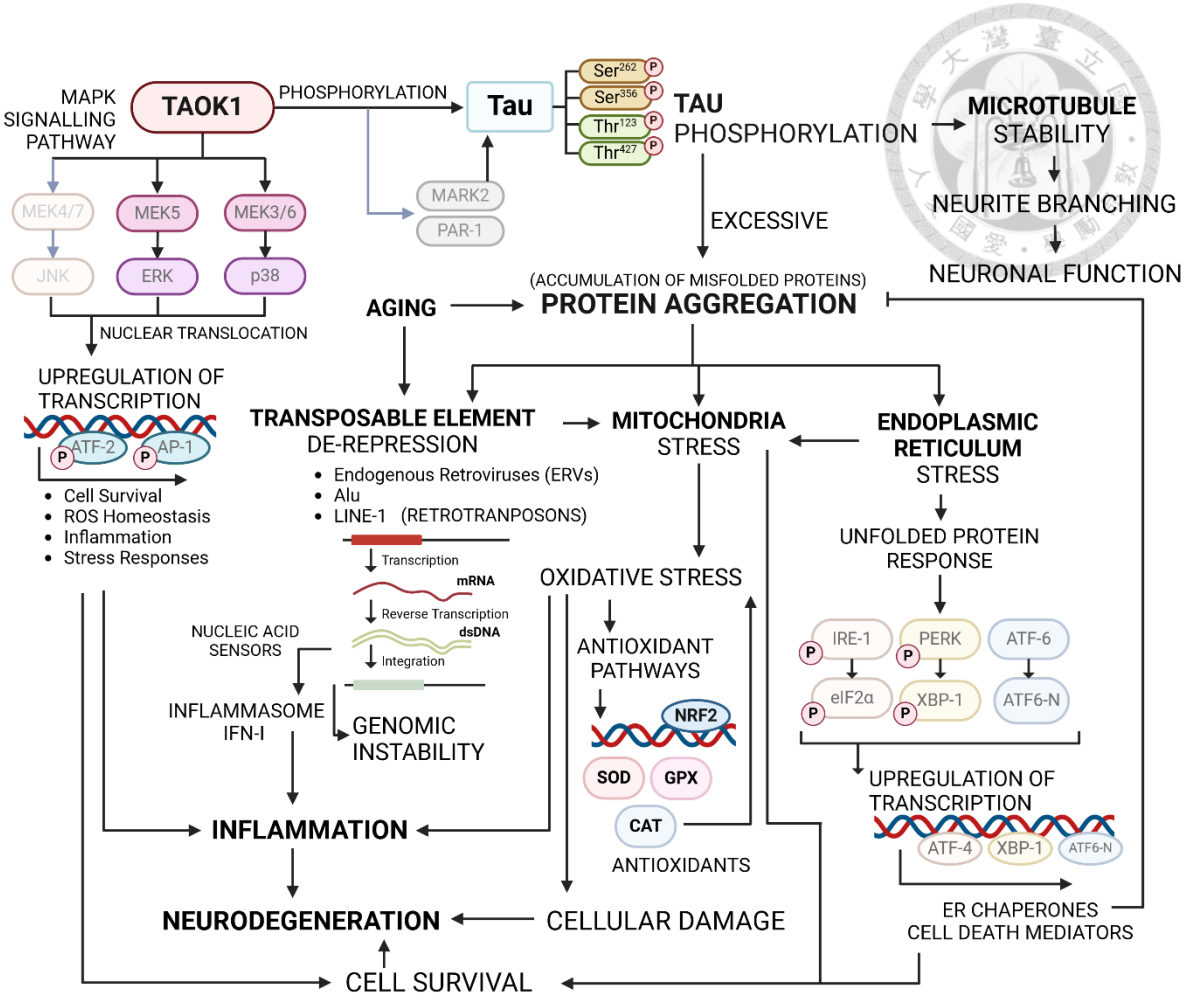

Figure 1. Summary figure of the potential interplay between TAOK1 and neurodegeneration. TAOK1's relationship with MAPK signalling and Tau phosphorylation, can be detrimental to neuronal health and function through interconnected pathways between MAPK signalling, Tau hyperphosphorylation, TE motility, mitochondria and the ER. (Created with BioRender.com)

doi:10.6342/NTU202402516

1.9.2. Experimental Design

In this study, we employed a Tet-On inducible system to overexpress TAOK1 in the SH-SY5Y neuroblastoma cell line. This endogenous TAOK1-inducible SH-SY5Y was generated by Pin-Jui Kung in our laboratory, up to the selection and expansion of single clones before the handover for this study (Kung, 2024).

Mixed and single clones were cultured under both undifferentiated and differentiating conditions, followed by induction of TAOK1 overexpression with doxycycline treatment. Various assays were used to assess protein and RNA expression, including western blot, RT-qPCR, and transcriptome analysis through RNA sequencing. These techniques allowed us to quantify changes in gene and protein expression associated with neurotoxicity pathways, such as apoptosis, oxidative stress, and inflammation. Cell count, viability and ROS levels were measured using Trypan Blue, CCK-8 and DHE assays, respectively. The CCK-8 assay provided insights into cell viability and proliferation, while the DHE assay helped quantify ROS levels, indicating oxidative stress. Immunofluorescence microscopy was used for cell imaging, enabling us to visualize changes in cellular morphology and identify target structures. This approach allowed us to investigate the effects of TAOK1 overexpression on neuronal health and elucidate the underlying mechanisms of neurodegeneration (**Figure 2**).

doi:10.6342/NTU202402516

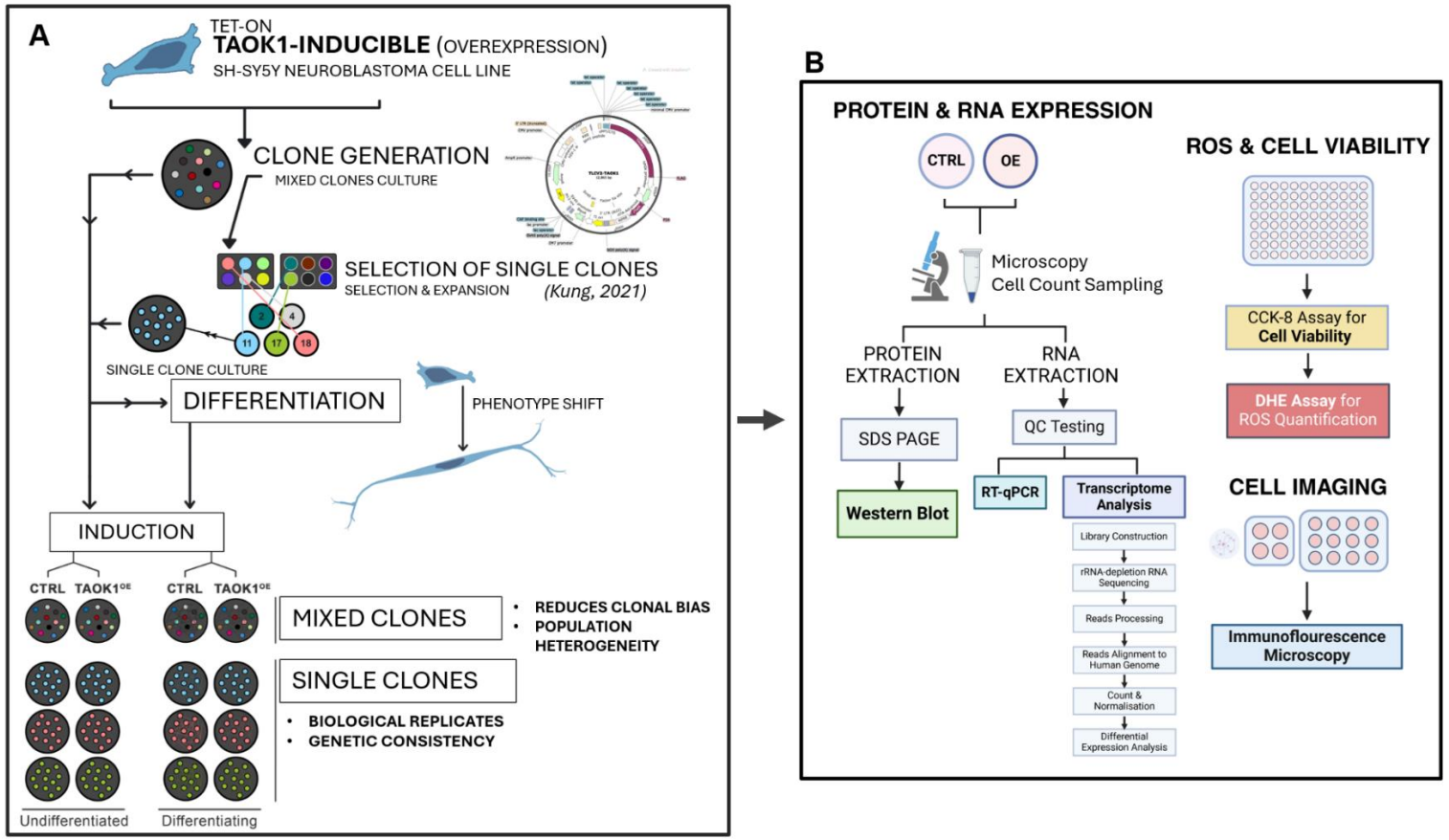

Figure 2. Schematic of experimental workflow to assess effects of TAOK1 Overexpression on molecular and morphological characteristics. (A) Cell culture of TAOK1-inducible SH-SY5Y neuroblastoma cells and selection of clones. **(B)** Experimental procedures to assess RNA and protein expression, cell count and viability sampling, ROS quantification and immunocytochemistry. (1B Created with BioRender.com)

doi:10.6342/NTU202402516

1.9.2.1. SH-SY5Y Neuroblastoma as a Neuronal Model

This study uses the human neuroblastoma cell line SH-SY5Y as a neuronal model to examine the morphological and molecular changes that indicate and affect neuronal health in response to TAOK1 overexpression. The SH-SY5Y is a human-derived neuroblastoma cell line subcloned from the SK-N-SH cell line, originally isolated from the bone marrow biopsy of a four-year old (Biedler, et al. 1978). SH-SY5Y cells are adherent cells that can be distinguished into the more neuron-like neuroblastic (N) or the substrate adherent Wachwannian (S)-types (Quaglia and Manchester 1996). When treated with differentiation agents such as retinoic acid (RA), these N-type cells can differentiate into neuron-like cells, displaying morphology reflective of neuronal differentiation (Encinas, et al. 2000). These include the growth of neurite-like projections, which depend on the formation and stability of microtubule structures. In our study, when exposed to differentiation media for five to seven days, SH-SY5Y cells show a differentiated phenotype, with typical neuronal features such as visible neurite extension and the expression of differentiation marker TUBB3 (**Figure 3**). In this study, these cells will be referred to as “differentiating” rather than “differentiated” to acknowledge that they may not be terminally differentiated. Experiments will be conducted on differentiating SH-SY5Y cells that exhibit and maintain these differentiated phenotypes.

The differentiation into a more neuron-like phenotype provides a model for studying neuronal development and function, particularly processes such as neurite outgrowth during differentiation. This is particularly valuable for modelling neurodegenerative diseases like AD and PD, diseases whose mechanisms manifest after neuronal maturation. This will facilitate the study of cellular processes including protein aggregation and the activation of various pathways, and how they can progress into neuron and synapse loss.

doi:10.6342/NTU202402516

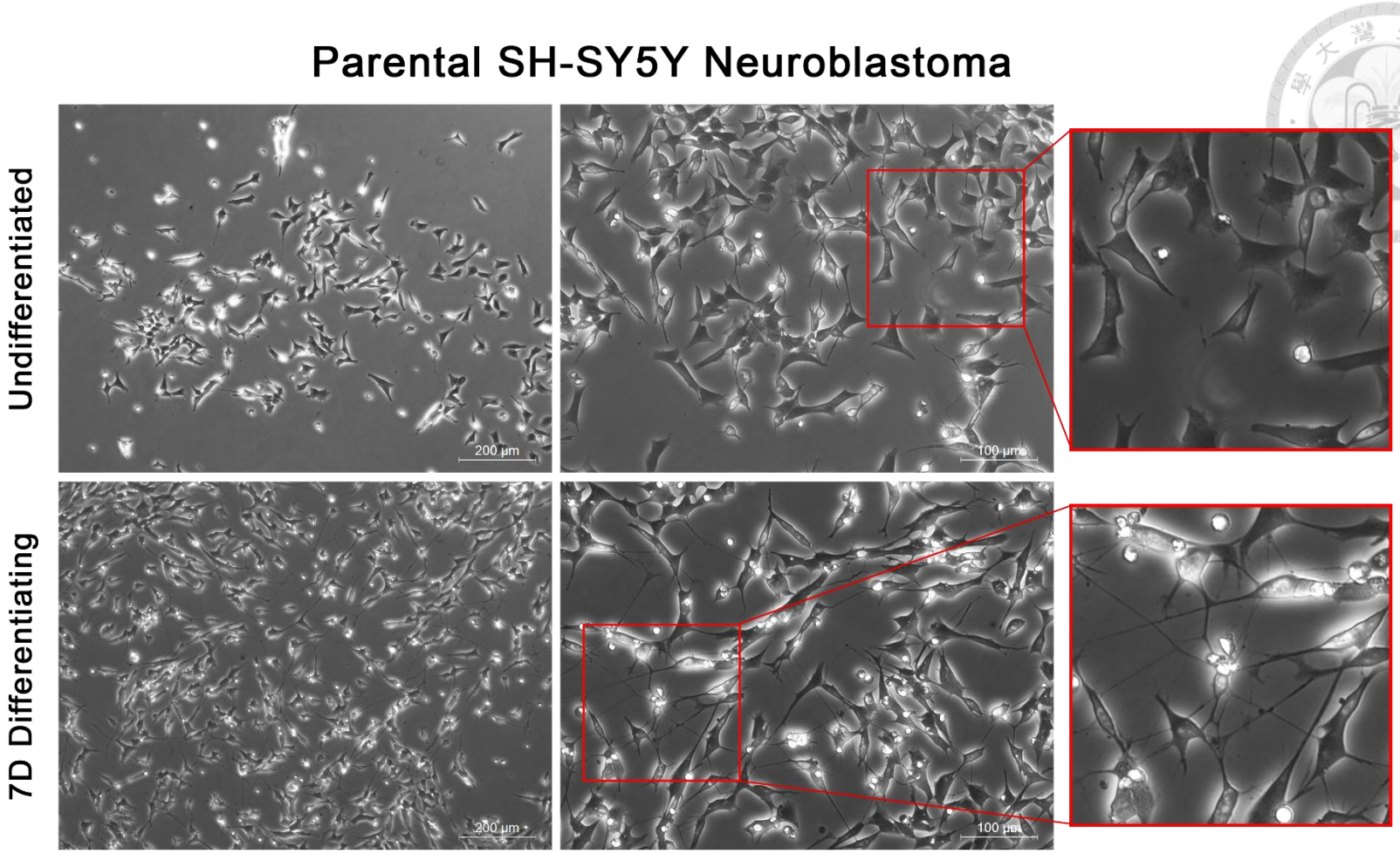

Figure 3. Brightfield images of undifferentiated and differentiating SH-SY5Y cells. Differentiating SH-SY5Y cells exhibit a narrower cell body and significant neurite outgrowth compared to undifferentiated cells. (Top and bottom left: 10X objective magnification. Top and bottom middle: 20X objective magnification. Top and bottom right: magnified detail from 20X objective image).

doi:10.6342/NTU202402516

1.9.2.2. TAOK1 Overexpression in SH-SY5Y using the Tet-On System

This study makes use of an endogenous expression system known as the Tet-On Inducible system in the SH-SY5Y cell model to overexpress TAOK1. This is in contrast to the transfection method used in the preliminary studies for elucidating the effects of TAOK1 overexpression in SH-SY5Y cells.

In the preliminary studies, parental SH-SY5Y cells were transiently transfected with TAOK1-containing extracellular vesicles (EVs). However, using the Tet-On system, the gene of interest, TAOK1 is integrated into the host cell genome and placed under the control of a tetracycline-responsive promoter (TRE). Doxycycline, a tetracycline analogue can be introduced through the culture medium, and in its presence, it will undergo a conformation change and bind to the reverse tetracycline trans-activator which allows it to bind to the TRE and transcribe the gene of interest. Through this, we are able to overexpress TAOK1 at any time, allowing a high degree of temporal control over TAOK1 overexpression. The system is also incredibly stable, allowing for the long-term expression of the gene of interest compared to the temporary expression in transient transfection. Selection of single clones also eliminates expression heterogeneity which is highly dependent on plasmid uptake by the cells, which we cannot control accurately in an experiment setting. This uniform expression will allow for more reliable results, where differences between clones can be attributed to differences in integration site. However, leaving us less variables. In addition, parts of this study assesses neuronal health in areas of cellular stress and neurotoxicity. Transient transfection procedures are known to induce cellular stress, creating artefacts when gathering results.

Overall, making use of the Tet-On system, we are able to achieve better efficacy, stability and control while reducing variability affecting cellular health. This way, we can

doi:10.6342/NTU202402516

produce more robust and reliable results that can be attributed to TAOK1 overexpression in SH-SY5Y.

doi:10.6342/NTU202402516

2. Materials and Methods

2.1. TAOK1-Overexpressing SH-SY5Y

2.1.1. Tet-On System

To study the effects of TAOK1 overexpression of SH-SY5Y cells, the Tet-On system was used as a means of driving TAOK1 overexpression at specific times. Transgene expression is driven by the TRE, through doxycycline in the culture medium. In this study, 5 μg/mL of doxycycline was added to the culture medium to induce the expression of TAOK1 at specific differentiation stages of SH-SY5Y cells. An M2 FLAG label was designed at the end of the TAOK1 sequence, allowing us to selectively identify TAOK1 that has been transcribed through this system. This would allow us to detect leakage in expression. To facilitate the selection of cells which has successfully integrated the system, we incorporated a puromycin resistance gene into the expression vector. Puromycin is an antibiotic that can effectively kill cells that do not carry any resistance gene. By introducing puromycin into the culture medium, we can eliminate any cells that do not carry the integrated system. This helps us establish a stable cell line that expresses TAOK1 under the Tet-On system, that we can ensure over several generations.

2.1.2. Cell Culture and Maintenance

Cells in this study were cultured on cell culture vessels containing appropriate volumes of culture medium of Dulbecco's Modified Eagle Medium/Nutrient Mixture F-12 (DMEM/F-12; Gibco™, #11320033) with 10% heat-inactivated FBS (Gibco™, #10437-028). 1μg/mL puromycin was introduced into the medium of single and mixed clones of the TAOK1-inducible SH-SY5Y cell line to select for cells that express the integrated TAOK1 construct. Culture vessels were placed into humidified incubators

doi:10.6342/NTU202402516

maintained at 37ºC and 10% CO2. Culture medium was replaced every 3 – 4 days and passaged at 70-80-% confluency if not subjected to experimental treatment.

To culture undifferentiated cells, cryovials containing the desired cell line was thawed in a 37ºC water bath until visibly thawed. Contents of the cryovial was added into a 15 mL centrifuge tube containing 5 mL of culture media and centrifuged at 1000g for 5 minutes at room temperature. Supernatant was removed, and the cell pellet was resuspended into appropriate volume of cell media before introduction into the appropriate culture vessel. Feed was conducted every 3 – 4 days with the complete replacement of fresh culture media. Passage was conducted when cells have reached 80 – 90% confluency. In treatment groups, the culture was completely replaced with fresh media at 60-70% confluency, with the addition of 5ug/mL of doxycycline into the treatment group to induce TAOK1 overexpression.

Differentiation was conducted by replacing the regular culture medium with Neurobasal™ Medium (Gibco™, #21103049) containing 1X B-27™ (Gibco™, #17504044), 1X GlutaMax™ (Gibco™, #35050061) and 10 uM of Retinoic Acid (RA) (Sigma, R2625), when undifferentiated cells in their culture vessels have reached 60 – 70% confluency. Feed was conducted by replacing 50% of the culture medium with freshly prepared differentiation medium, to make 10 uM of RA. After 7 days, medium was completely replaced with fresh media, with the addition of 5 μg/mL of doxycycline into the treatment group to induce TAOK1 overexpression.

doi:10.6342/NTU202402516

2.2. Cell Count & Viability Assays

2.2.1. Trypan Blue Exclusion Method

The trypan blue exclusion method was used as a cell count method during harvest. Cells were harvested by aspirating spent culture media from the culture vessel, followed by washing with DPBS without Ca^{2+} and Mg^{2+}. After aspirating the DPBS, TrypLE was added, ensuring complete coverage of the adherent cells and allowed to sit for a maximum of 10 minutes. Culture vessel was tapped lightly to encourage the detachment of cells, before being quenched with equal volume of cell culture media. Cell suspension was collected into a 15 mL centrifuge tube and mixed thoroughly to ensure homogeneity. A 20 µL aliquot was taken into a new 1.5 mL microcentrifuge tube and mixed with an equal volume of trypan blue solution and incubated for 1 – 2 minutes at room temperature. 10 µL of the mixture was loaded onto the hemacytometer chamber. Total cell concentration and viability were counted under a 10X objective lens under the following formulae: ·

$$Total\ Cells\ per\ mL = \text{Average Cell Count per Square} \times \text{Dilution Factor} \times 10^4$$

$$Viable\ Cells\ (\%) = \frac{Viable\ Cells}{Total\ Cells} \times 100$$

2.2.2. Cell Counting Kit-8 Assay

Cell viability was assessed using the Dojindo CCK-8 assay kit (CK04) based on vendor's instructions. The CCK-8 assay is a colorimetric assay that can determine cell viability based on the cell's dehydrogenase activity. In the assay's dye, a water-soluble tetrazolium salt, WST-8, will be reduced by dehydrogenase in live cells. This would form a highly soluble formazan dye that can be measured using a microplate reader at 450 nm.

doi:10.6342/NTU202402516

The amount of formazan is directly proportional to the number of viable cells in the well, which means that a higher absorbance is indicative of higher number of viable cells.

In this study, 5,000 cells were seeded into each well of a 96-well plate. After an appropriate period of growth and treatment, 10 μL of the CCK-8 solution is added to each well containing 100 μL of culture medium. The plate was then incubated for 1 – 4 hours at 37°C. Following incubation, the absorbance of each well was measured at 450 nm using a microplate reader.

2.3. RNA Expression

The expression of specific genes were assessed using Reverse Transcription – quantitative Polymerase Chain Reaction (RT-qPCR) and rRNA-depletion RNA sequencing.

2.3.1. RNA Extraction from Adherent Cells

Total RNA was extracted from cells at 72 hours post-doxycycline treatment. After the aspiration of spent media, cells were washed twice with 0.22uM filtered 1X DPBS without Ca^{2+} and Mg^{2+}. QIAzol™ was added directly onto the cells to lyse the cells for RNA purification using the Qiagen RNeasy Mini Kit (74104) according to manufacturer's instructions. The lysate was either stored at -80°C for long-term storage or processed immediately. For phase separation, one-fifths volume of chloroform (140 μL chloroform for every 700 μL of the sample) was added to the lysate. The mixture was incubated at room temperature for two to three minutes and then centrifuged at 12,000 x g for 15 minutes at 4°C. The aqueous layer was carefully removed and transferred to a new tube. To precipitate the RNA, 1.5X volumes of 100% ethanol were added to the aqueous phase and mixed thoroughly. A maximum of 700 μL of the mixture was then applied to the provided RNeasy spin column with a collection tube. The column was

doi:10.6342/NTU202402516

centrifuged at ≥ 8000 x g for 15 seconds at room temperature, and the flow-through was discarded. This step was repeated until the entire sample had been processed. The column was then washed by adding 350 µL of RWT buffer and centrifuging for 15 seconds at ≥ 8000 x g. For on-column DNase digestion, a mix of 10 µL DNase I and 70 µL RDD buffer was directly applied to the membrane and incubated at room temperature for 15 minutes to remove any contaminating DNA. Following DNase treatment, 500 µL of RPE buffer was added to the column, which was then centrifuged for 15 seconds at ≥ 8000 x g. The flow-through was discarded, and an additional empty spin at maximum speed was performed to ensure all ethanol was removed. The RNA was eluted into a new collection tube by adding 35-50 µL of nuclease-free water directly to the membrane and centrifuging. The eluted RNA was kept on ice, and its concentration and purity were measured using a NanoDrop spectrophotometer. The RNA samples were then aliquoted and stored at -80°C for future use.

2.3.2. Quality Control Analysis via RNA Bioanalyzer

In-house quality control (QC) was assessed using the Agilent 2100 Bioanalyzer following manufacturer's instructions. Only RNA samples of RNA Integrity Number (RIN) of more than 8 was used in later RT-qPCR and sequencing work to ensure purity and integrity of the RNA samples.

2.3.3. Reverse Transcription

cDNA was generated from the purified RNA extracted from cells through reverse transcription using the SuperScript™ IV Reverse Transcriptase system (Invitrogen, #18090010). 1000 ng of total RNA from the previous RNA extraction step was used as starting material for the reverse transcription. The RNA was topped up to a final volume of 8 µL with RNase-free water.

doi:10.6342/NTU202402516

To ensure the removal of any contaminating genomic DNA, a DNase treatment was performed. The DNase treatment mixture consisted of 8 µL RNA sample, 1 µL DNase, and 1 µL RDD buffer (Qiagen, #79254). This mixture was incubated at room temperature (RTP) for 30 minutes. Following DNase treatment, the enzyme was inactivated by adding 1 µL of 25 mM Ethylenediaminetetraacetic acid (EDTA) to the sample, and the mixture was incubated at 75°C for 10 minutes using a polymerase chain reaction (PCR) machine (Biometra TAdvanced Twin PCT Thermal Cycler). This step ensured the complete inactivation of DNase before proceeding to the reverse transcription. EDTA is a chelating agent that chelates divalent cations such as Mg^{2+} and Ca^{2+}, which are cofactors for DNase enzymatic activity that are present in the RDD buffer. Addition of EDTA will chelate and sequester these cations to inactivate DNase activity. For primer annealing, 1 µL of random primers/hexamers and 1 µL of deoxyribonucleotide triphosphate (dNTP) mix were added to the RNA sample. The mixture was incubated at 65°C for 5 minutes using the PCR machine to allow the primers to anneal to the RNA template.

To create a non-reverse transcription (non-RT) control, which is essential for verifying the absence of genomic DNA contamination, the following components were added to 13 µL of the treated RNA sample: 1 µL of Dithiothreitol (DTT), 4 µL of 5x SSIV Buffer, and 2 µL of RNase-free water. This control mixture did not contain the RT enzyme and was processed in parallel with the RT sample. DTT reduces disulfide bonds and can help stabilise RT to ensure the efficacy of the enzyme during the reverse transcription process. DTT can also help protect RNA molecules from oxidative damage and degradation by providing a reducing environment. Overall, creating an optimal environment for reverse transcription.

doi:10.6342/NTU202402516

For the reverse transcription reaction, 1 μL of DTT, 4 μL of 5x SSIV Buffer, 1 μL of SSIV reverse transcriptase, and 1 μL of RNase-free water were added to 13 μL of the treated RNA sample. The reaction mixture was then subjected to the following thermal cycling conditions in the PCR machine: 23°C for 10 minutes, 50°C for 30 minutes, 80°C for 10 minutes, and finally cooled to hold at 4°C. These steps ensured the synthesis of complementary DNA (cDNA) from the RNA template, which was then ready for further downstream RT-qPCR.

2.3.4. Real Time Quantitative Polymerase Chain Reaction (RT-qPCR)

RT-qPCR was conducted using the cDNA synthesized in the earlier reverse transcription step. The cDNA was diluted to a concentration of 2 ng/μL with RNAse-free water.

The forward primer (FP) and reverse primer (RP) were prepared in a 1:1 ratio with nuclease-free water to form the primer mix. The ratio of the primer mix was FP:RP:H_2O (1:1:18). The prepared primer mix was then combined with SYBR Green Master Mix in a ratio of 1:9 to make the Primer-SYBR mixture. A 384-well PCR Plate was used for the reaction. For each well, 5 μL of the Primer-SYBR mixture was added. 5 μL of the diluted cDNA sample (2 ng/μL) was added to each well, bringing the total reaction volume to 10 μL per well. Each condition included one non-RT control and three RT samples (triplicates). These samples were loaded onto a 384-well plate for analysis. The 384-well plate was sealed with an adhesive film to prevent evaporation and contamination. The plate was then gently tapped to thoroughly mix the reaction components. The sealed plate was centrifuged at 4°C at 1000g for 1 minute to ensure that the reaction components settled at the bottom of the wells and to eliminate any air bubbles. The prepared 384-well plate was then placed in a qPCR machine (Bio Rad C1000 Touch™ Thermal Cycler, CFX483™ Real-Time System) with the following cycling conditions:

doi:10.6342/NTU202402516

The expression levels of target genes were normalised to the expression of housekeeping genes Glyceraldehyde-3-Phosphate Dehydrogenase (GAPDH) and Xaa-Pro Aminopeptidase 1 (XPNPEP1). The glycolytic pathway enzyme GAPDH is a popular housekeeping gene due to its ubiquitous expression in various cell and tissue types, and typically stable in response to experimental treatments. On the other hand, XPNPEP1 is another housekeeping gene known for its stability in human brain tissue and has no known neuroinflammatory or neurodegenerative associations (Durrenberger, et al. 2012), marking its suitability as an internal control. Relative gene expression was calculated using the ΔΔCt method, where Ct values of target genes were normalised to the Ct value of the housekeeping gene. Results are presented as fold changes in gene expression relative to the control group.

2.3.5. rRNA-Depletion RNA Sequencing

RNA QC, library construction and subsequent Illumina rRNA-Depletion RNA sequencing (RNA-seq) of selected RNA samples were conducted by Jilong Mix Biotechnology Co., Ltd.

rRNA-depletion RNA sequencing was used to analyse the gene expression changes between our control and TAOK1 overexpression groups. In this study, total RNA was extracted from the cells and subjected to rRNA depletion to enrich for messenger RNA and other non-ribosomal RNA species. rRNA constitutes majority of total RNA and can obscure the detection of less abundant transcripts like mRNA and piRNA, which can serve regulatory functions that are of interest to our study. Sequencing was performed on an Illumina commercial platform, with sequencing depth set to 20G reads per sample, the equivalent of 20 billion reads. This will ensure the detection of both highly expressed and

doi:10.6342/NTU202402516

less abundant reads to increase the resolution and robustness of the data, allowing us to detect even minimal gene expression changes.

Differential gene expression analysis was performed to compare the transcriptomes of the control and treatment groups with TAOK1 overexpression. For the analysis of individual clones in both undifferentiated and differentiating populations, the edgeR package was used to calculate the log2-fold change (log2FC) values and identify differentially expressed genes (DEGs). In parallel, DESeq2 was employed to analyse multiple single clones, treating them as biological replicates. For individual clones where we only have one matched control-treatment sample, edgeR was used as it can effectively handle small sample sizes and provide accurate normalisation using the trimmed mean of M-values (TMM). For the undifferentiated population where we have biological replicates in the form of multiple single clones, DESeq2 was used. DESeq2 is designed to handle biological variability and increases statistical power by treating the single clones as replicates. It uses the Wald test for significance and corrects for multiple tests with the Benjamini-Hochberg method. This combined approach allowed us to accurately identify differentially expressed genes in this study based on the log2FC value. A positive log2FC value indicates upregulation of a gene, while a negative log2FC value indicates downregulation. A log2FC value of 1 corresponds to a two-fold increase in gene expression, whereas a log2FC value of -1 corresponds to a two-fold decrease in gene expression. Similarly, a log2FC value of 2 indicates a four-fold increase, and a log2FC value of -2 indicates a four-fold decrease in gene expression.

Hypothesis testing was conducted within the packages to obtain p-values for statistical significance. P-values are used to determine the statistical significance of the observed changes in gene expression. A lower p-value indicates that the observed change is less likely to be due to random variation. However, when conducting multiple

doi:10.6342/NTU202402516

comparisons, the risk of false positives increases. To address this, adjusted p-values (padj) are calculated to control for the false discovery rate (FDR). Adjusted p-values provide a more stringent measure of significance by accounting for the number of tests performed. In our analysis, we consider genes with a padj value of less than 0.05 to be differentially expressed.

doi:10.6342/NTU202402516

2.4. Western Blot Analysis

2.4.1. Protein Extraction from Adherent Cells

The lysis buffer was prepared using 100 µL of 10X RIPA buffer, 10 µL of phosphatase inhibitor A (PhIA), 10 µL of phosphatase inhibitor B (PhIB), 10 µL of protease inhibitor (ProI), 10 µL of PMSF, and 860 µL of water were combined to a total volume of 1000 µL.

The cell culture medium was aspirated from the culture vessel, and the cells were washed twice with the addition of ice-cold DPBS without Ca^{2+} and Mg^{2+}. For protein extraction, 250 - 500 µL of ice-cold lysis buffer was added directly onto the cells, ensuring full coverage with the lysis buffer. After a short period of incubation, the cells were scraped using a clean plastic cell scraper, and cell suspension was collected into microcentrifuge tubes. The contents of the microcentrifuge tubes were sonicated for 10 minutes on high for two cycles. Following this, the tubes were centrifuged at 16,000 x g for 20 minutes at 4°C. The supernatant was collected in a fresh tube and placed on ice, while the pellet was discarded.

2.4.2. Bicinchoninic acid Assay (BCA)

The Pierce™ BCA Protein Assay Kit (Thermo Scientific, #23225) was used quantify the protein concentration of the supernatant collected in the previous section, based on manufacturer's instructions.

To generate a standard curve, a series of bovine serum albumin (BSA) standards were prepared at the following concentrations: 2000 ng/mL, 500 ng/mL, 125 ng/mL, 31.25 ng/mL, 0 ng/mL, and a blank. The BCA working reagent was prepared by mixing reagent A and reagent B in a 25:1 ratio. 200 µL of the working reagent was added to 15 µL of each protein sample and standard. Protein samples were prepared at 1X and 5X

doi:10.6342/NTU202402516

dilutions, to ensure that the protein concentrations fell within the range of the standard curve.

15 μL of each protein sample was mixed with 200 μL of the BCA working reagent in a microplate well and mixed carefully with a pipette to ensure homogeneity. The microplate was incubated at 37°C for 30 minutes for the reaction to occur. The absorbance of each well was measured at 562 nm using a microplate reader. A standard curve was plotted using the absorbance values of the BSA standards and used to determine the protein concentrations of the unknown samples.

2.4.3. SDS-PAGE & Western Blot

Sodium dodecyl sulphate-polyacrylamide gel electrophoresis (SDS-PAGE) was used to separate proteins based on their molecular weight. Depending on the molecular weight of the target protein, 10%, 12%, and 15% polyacrylamide gels were prepared. Protein samples, ranging from 10-20 ng, were prepared by adding loading dye at a concentration of (stock: 2-mercaptoethanol 3:1) in a 1:4 ratio to the protein sample. The mixture was then heated on a heat block at 90°C for 10 minutes to denature the proteins. After denaturation, the samples were loaded into the wells of a 10- or 15-well gel. 5 μL of PageRuler^{TM} Prestained Protein Ladder (Thermo Scientific^{TM}, #26616) was added to the first lane of the well. Gel electrophoresis was performed at 80V for 20 minutes followed by 110V for 1 hour in 1XSDS running buffer (Omics Bio, #IB3372) to separate the proteins based on their size.

Following SDS-PAGE, the proteins were transferred to a polyvinylidene difluoride (PVDF) membrane (0.2 μm & 0.45 μm pore size). The PVDF membrane was first activated by soaking it in 100% methanol for 5-10 minutes. The protein transfer was conducted in 1X Transfer Buffer (Omics Bio, #IB3352) at 0.25A for 60 minutes. After the transfer, the membrane was blocked for 1 hour in blocking buffer of 5% BSA

doi:10.6342/NTU202402516

dissolved in PBST (1X PBS with 0.1% Tween-20), or 5% skimmed milk in TBST (1X TBS with 0.1% Tween-20) at room temperature with gentle shaking to prevent non-specific binding of antibodies. The membrane was then washed three times for 5-10 minutes each with PBST. The membrane was incubated overnight at 4°C with the primary antibody diluted in blocking buffer. The next day, the membrane was washed three times for 5-10 minutes each with PBST to remove any unbound primary antibody. The membrane was then incubated for 1 hour at room temperature with the secondary antibody diluted in the blocking buffer. Following secondary antibody incubation, the membrane was washed three times for 5-10 minutes each with PBST. For detection, a chemiluminescence reagent was prepared by mixing equal volumes of the Enhanced Luminol Reagent and the Oxidizing Reagent and added to the membrane (PerkinElmer Western Lightning^{TM} Plus, PK-NEL105). The membrane was incubated in the chemiluminescence reagent for one minute with gentle agitation. Excess reagent was removed by draining or blotting, and the membrane was then placed on an appropriate surface for imaging. The membrane was imaged using the GeneGenome XRQ-chemiluminescence imaging system. Intensities of western blot bands were quantified using ImageJ.

For re-probing, the membrane was stripped by adding stripping buffer (Omics Bio, AR0001) to the membrane and incubated for 20 minutes at room temperature with shaking. The membrane was then washed three times for 10 minutes each with PBST, followed by blocking and re-incubation with primary and secondary antibodies as described previously.

doi:10.6342/NTU202402516

2.5. Microscopy

2.5.1. Brightfield Imaging

Brightfield imaging was used to visualise the morphological features of the cells in their respective culture vessels during culture. The Leica DFC360 FX microscope was used to view and take images under 4x, 10x and 20x objective lens.

2.5.2. Immunocytochemistry

For immunocytochemistry, cells were cultured on 100 mm glass discs in a standard culture vessel. Glass discs containing adherent cells were washed three times with PBS without Ca^{2+} and Mg^{2+}, then followed by fixing in 4% (v/v) paraformaldehyde (PFA) for 20 minutes. Following fixing, the samples were washed again with PBS. Next, the samples permeabilized with 0.5% Tween-20 in PBST for 20 minutes. They were then washed with PBS prior to clocking with 1% BSA in PBST for one hour at room temperature. After washing with PBS, the slides were incubated with primary antibodies (**Table 1**) overnight at 4ºC. Next, the glass discs were washed with PBST, then incubated with secondary antibodies for one hour at room temperature in the dark (**Table 2**). Hoechst was added along with the secondary antibody to counterstain the nuclei. Finally, the glass discs were washed in PBS with increasing wash times (5 minutes, 10 minutes, and 15 minutes) on a shaker to ensure thorough removal of unbound primary antibody.

Ca^{2+} and Mg^{2+} can promote cell-cell adhesion by stabilising cadherin-mediated junctions and other cell adhesion molecules. Removal of these ions prevents unwanted cell aggregation and detachment. During permeabilization step, the absence of Ca^{2+} and Mg^{2+} helps to ensure increased cell membrane permeability to detergents such as Tween-20. This allows for more effective entry of antibodies into the cell.

doi:10.6342/NTU202402516

2.6. Dihydroethidium Assay

The DHE assay was conducted using abcam's DHE (Dihydroethidium) Assay Kit – Reactive Oxygen Species (ab236206), with reagent preparation following manufacturer's instructions. 5,000 cells were seeded into each well of a 96-well cell culture plate. The spent media was aspirated from each well, followed by the addition of 150 μL of Cell-Based Assay Buffer, which was subsequently aspirated, leaving 10-20 μL in each well. Next, 130 μL of ROS Staining Buffer was added to each well, and 10 μL of N-acetyl Cysteine Assay Reagent was added to the designated negative control wells. The plate was covered and incubated for 30 minutes at 37°C in a humidified chamber, protected from light. Following this, 10 μL of Antimycin A Working Reagent was added to the designated positive control wells and incubated for 1 hour at 37°C, protected from light. After incubation, the ROS Staining Buffer was aspirated, and 100 μL of Cell-Based Assay Buffer was added to each well. Fluorescence was measured using a fluorescent plate reader with an excitation wavelength between 480-520 nm and an emission wavelength between 570-600 nm.

DHE is a fluorescent probe that detects superoxide anions, a primary form of ROS. When DHE enters the cell, the reaction between superoxide anions and DHE generates a highly specific red fluorescent product, 2-hydroxyethidium (2-OH-E^+), to produce a red fluorescent signal. The intensity of this fluorescence is directly proportional to the amount of superoxide present, allowing for quantitative measurement of ROS levels. While more specific towards superoxide anions, DHE can also react with other ROS like H_2O_2 and hydroxyl radicals. Hence DHE staining is widely regarded as a reliable indication of the overall ROS levels within cells.

doi:10.6342/NTU202402516

2.7. TUNEL Assay

The TUNEL assay was performed using the Click-iT™ Plus TUNEL Assay Kit (C10617) for In Situ Apoptosis Detection (Alexa Fluor^{TM} 647) to detect apoptotic cells. Cells were cultured on 100 mm glass discs in a standard culture vessel. The cells were fixed with 4% (v/v) PFA in PBS for 15 minutes at room temperature. Following fixation, the cells were washed twice with PBS without Ca^{2+} and Mg^{2+}. Next, the cells were permeabilized with 0.25% Tween-20 in PBS for 20 minutes at room temperature. The permeabilization step was followed by washing the cells twice with PBS. The reaction buffers, mixtures and cocktail was prepared according to the manufacturer's instructions. 100 µL of TdT reaction buffer was added to each sample, followed by a 10-minute incubation at 37°C in a humidified chamber protected from light. The buffer was then aspirated, and 50 µL of TdT reaction mix (TdT reaction buffer, EdUTP, TdT enzyme) and incubated for 60 minutes at 37°C. Following this, the slides were washed with 3% BSA in PBST (0.1% Tween-20) for 5 minutes. The TUNEL reaction cocktail, consisting of TUNEL Supermix (1X reaction buffer, copper protectant, AlexaFluor^{TM} 647 picolyl azide) and 10X reaction buffer additive, was prepared and 50 µL of this cocktail was added to each sample. The samples were incubated for 30 minutes at 37°C in the dark to facilitate the labelling of DNA strand breaks. After this incubation, the slides were washed with 3% BSA in PBS for 5 minutes, followed by a 1X PBS rinse.

For antibody staining, the cells were blocked with 3% BSA in 1X PBS for 1 hour at room temperature. Following the blocking step, the slides were washed with 3% BSA in PBS. The primary antibody was then applied and incubated overnight at 4°C. The next day, the slides were washed with PBS and incubated with the secondary antibody for 1 hour at room temperature in the dark. Hoechst stain was added together with the secondary antibody to counterstain the nuclei. Finally, the glass discs were mounted on

doi:10.6342/NTU202402516

glass slides using an antifade mounting medium (ProLong™ Gold, #P36934) to preserve the fluorescence signal. The slides were then examined under a fluorescence microscope using the appropriate filter settings for Alexa Fluor™ 647 and Hoechst to detect TUNEL-positive cells and visualize the nuclei, respectively.

2.8. Statistical Analysis

Statistical analysis was performed to assess the significance of the experimental results. For comparisons between two independent groups, the non-parametric Mann-Whitney unpaired t-test was utilized. All statistical analyses were conducted using GraphPad Prism. A p-value of less than 0.05 was considered statistically significant.

doi:10.6342/NTU202402516

2.9. Antibodies

Table 1. Primary Antibodies used in Western Blot and Immunocytochemistry (ICC)

Antibody Target	Species of Origin	Catalogue Number	Manufacturer	Application	Dilution
TAOK1	Mouse	26250-1-AP	Santa Cruz	Western Blot	1:100
TAOK1	Rabbit	sc136094	Proteintech	Western Blot	1:1000
M2 FLAG	Mouse	F2165	Sigma Aldrich	Western Blot	1:1200
M2 FLAG	Rabbit	#2368	Cell Signalling Technology	Western Blot	1:1000
Cleaved Caspase-3	Rabbit	#9662	Cell Signalling Technology	Western Blot	1:1000
Caspase-3	Rabbit	25546-1-AP	Proteintech	Western Blot	1:500
Caspase-1	Mouse	sc56036	Santa Cruz	Western Blot	1:200
P-Tau (Ser 262)	Rabbit	GTX50175	GeneTex	Western Blot	1:1000
TUBB3/Tuj1	Mouse	66375-1-Ig	Proteintech	Western Blot /Immunocytochemistry	1:5000 (WB) 1:500 (ICC)
a-Tubulin	Mouse	Ab7291	AbCam	Immunocytochemistry	1:1000

doi:10.6342/NTU202402516

β-actin	Rabbit	IR2-7	iReal	Western Blot	1:10000
GAPDH	Mouse	60004-1-Ig	Proteintech	Western Blot	1:5000

Table 2. Secondary Antibodies & Hoechst used in Western Blot and ICC

Antibody Name	**Species of Origin**	**Manufacturer**	**Catalogue Number**	**Dilution (Usage)**
Mouse IgG HRP	Goat	ThermoFisher	31430	1:5000 (WB)
Rabbit IgG HRP	Goat	ThermoFisher	31460	1:5000 (WB)
Alexa fluor Mouse 488	Goat	Invitrogen	A11029	1:800 (ICC)
Alexa fluor Rabbit 546	Goat	Invirtogen	A11035	1:800 (ICC)
Hoechst		Sigma	14533	1:500 (ICC)

doi:10.6342/NTU202402516

2.10. Primers

Table 3. Primer Sequences used in RT-qPCR[1]

Gene Symbol		Primer Pair
GAPDH	F	GGA GCG AGA TCC CTC CAA AAT
	R	GGC TGT TGT CAT ACT TCT CAT GG
TAOK1	F	GGC GTC ATA ACT TAG AGC AGG AC
	R	TTG TGT TGA GGT GGC GGA ACT C
Caspase-3	F	GGA AGC GAA TCA ATG GAC TCT GG
	R	GCA TCG ACA TCT GTA CCA GAC C
TDP43	F	CAA GCC ATT CAG GGC CTT TG
	R	TGC TTA GGT TCG GCA TTG GA
STING	F	CCT GAG TCT CAG AAC AAC TGC C
	R	GGT CTT CAA GCT GCC CAC AGT A
XPNPEP1	F	GAC AAA GCT GAG GAG TTT CGC AG
	R	GAC AAG GTC CTA TTC GTC TCA GG
HERV-k-gag	F	AGC AGG TCA GGT GCC TGT AAC ATT
	R	TGG TGC CGT AGG ATT AAG TCT CCT
HERV-Fc1	F	TTG TCA GAG GCG AGG CAA AT
	R	TTA ACG GCA AGA GAG GCT GG
L1HS	F	ACC AGA GGT ACA AGG AGG AA
	R	CTC TGC CTG GCT TTG GTA TAA
L1MB4	F	AGA CCA CCT AAA GCC TGG GA
	R	GGC ACT CCC CTT CAA CAC TT
AluSX	F	TGG CCA ACA CGG TGA AA
	R	TCA AGC AAT TCT CCC ACC TC
AluYc5	F	GGA GAT CGA GAC CAC GGT GA
	R	ACT GCA AGC TCC GCC TTC CG

[1]All primers were synthesised by Jilong Mix Biotechnology Co., Ltd.

doi:10.6342/NTU202402516

3. Results

3.1. TAOK1 Overexpression can be Stably Induced through Doxycycline Treatment throughout Differentiation

In order to verify stable TAOK1 overexpression through doxycycline in our cell model, we conducted a western blot analysis and RT-qPCR to identify and quantify TAOK1 expression at both the protein and mRNA level. Firstly, we had to verify if doxycycline treatment of SH-SY5Y cells can cause significant toxicity to the cells that may affect later analysis of cell death. Treatment of both undifferentiated and differentiating parental SH-SY5Y at concentrations 0.0, 2.5, 5.0, 7.5 and 10.0 μg/mL of doxycycline revealed a slight decrease in cell count from 7.5 towards 10.0 μg/mL of doxycycline (**Supplementary Figure 1**). Hence, cells in this study was subjected to 5.0 μg/mL of doxycycline for treatment.

Western blot analysis revealed an increase in TAOK1's protein expression levels after doxycycline treatment across multiple single clones and in the mixed clone population regardless of differentiation status **(Figure 4A, B)**. The M2-FLAG which was introduced at the end of the transgene sequence, was identified only in only the treatment group. RT-qPCR analysis has also shown the relative increase in TAOK1 mRNA expression levels in the treatment group compared to the non-treated control group **(Figure 4C, D)**. Taken together, our model for TAOK1 overexpression in SH-SY5Y neuroblastoma is able to stably overexpress TAOK1 across multiple clones and differentiation statuses with the introduction of 5 μg/mL doxycycline in the cell culture media.

doi:10.6342/NTU202402516

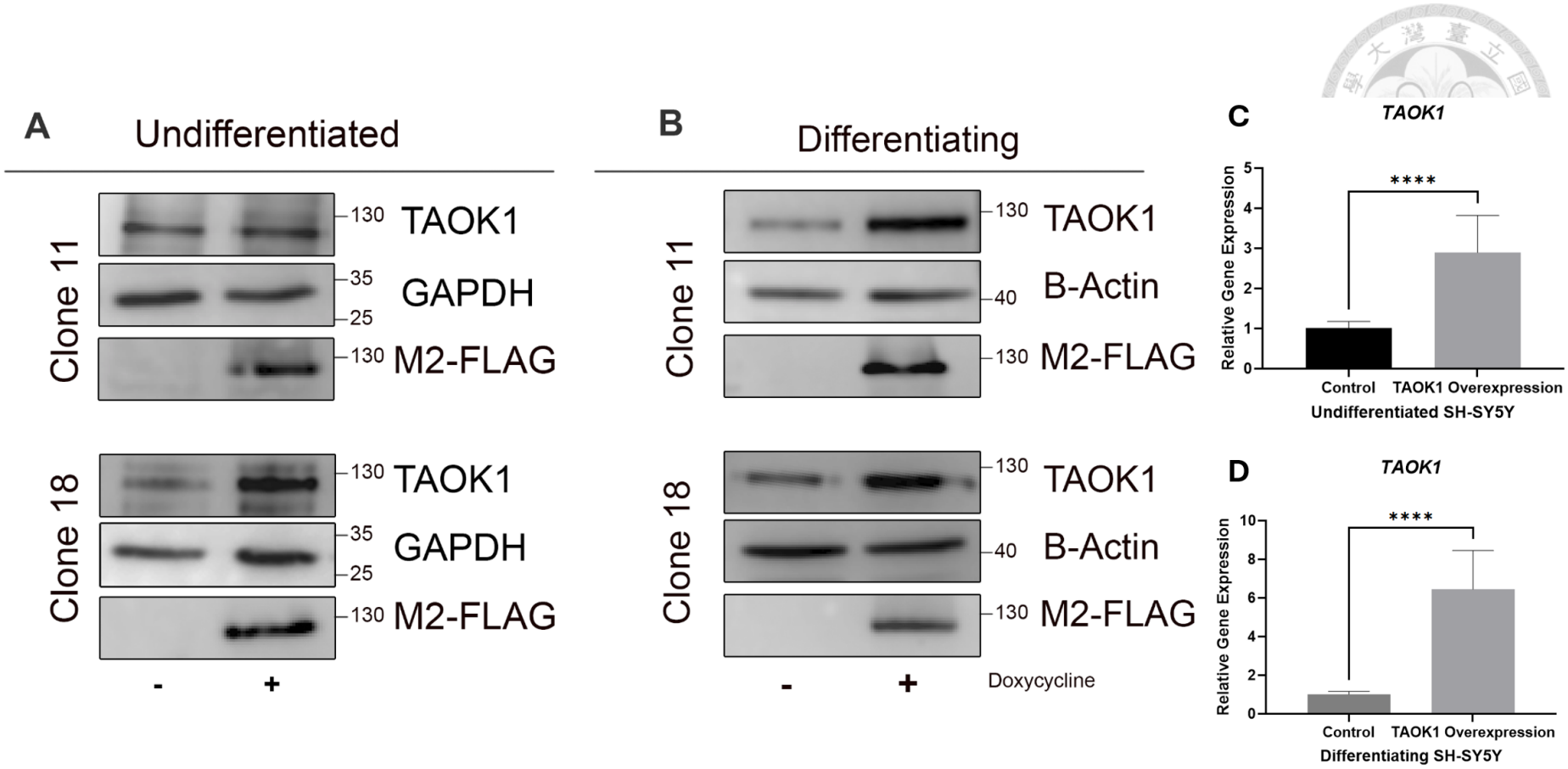

Figure 4. TAOK1 overexpression was maintained stably across multiple clones in the TAOK1-inducible SH-SY5Y cell line throughout differentiation without leakage. (A, B) Doxycycline exposure at 5ug/mL increased protein levels of TAOK1, with successful induction of TAOK1 identified via a M2-FLAG tag. **(C, D)** RT-qPCR analysis shows increase in relative gene expression of TAOK1 with 5 ug/mL doxycycline treatment of SH-SY5Y in both undifferentiated and differentiating SH-SY5Y.

doi:10.6342/NTU202402516

3.2. TAOK1 Overexpression results in Neuron loss

Having established that our model is able to stably overexpress TAOK1 across differentiation statuses, we wanted to observe if TAOK1 overexpression in our neuronal model is sufficient to induce neurotoxicity.

Overexpressing TAOK1 in undifferentiated SH-SY5Y has reduced confluency and harvest cell counts of multiple single clones in this study (**Figure 5B**). Assessment of cell viability using the CCK-8 assay has also revealed a significant reduction in cell viability in mixed clones overexpressing TAOK1 after three days of induction (**Figure 5D**). To model the effect of TAOK1 in differentiating neurons, we also conducted the same observations after seven days of differentiation. Initial observation of the cells through brightfield imaging show an obvious reduction in cell confluency, and a relative reduction in harvest cell count in the TAOK1 overexpressing group after two to three days of induction (**Figure 5A, C**). Cell viability has also significantly reduced as seen in the CCK-8 assay (**Figure 5E**). Taken together, the data suggest that TAOK1 overexpression in our endogenous TAOK1 overexpression SH-SY5Y neuronal cell model is sufficient to promote neuronal death.

doi:10.6342/NTU202402516

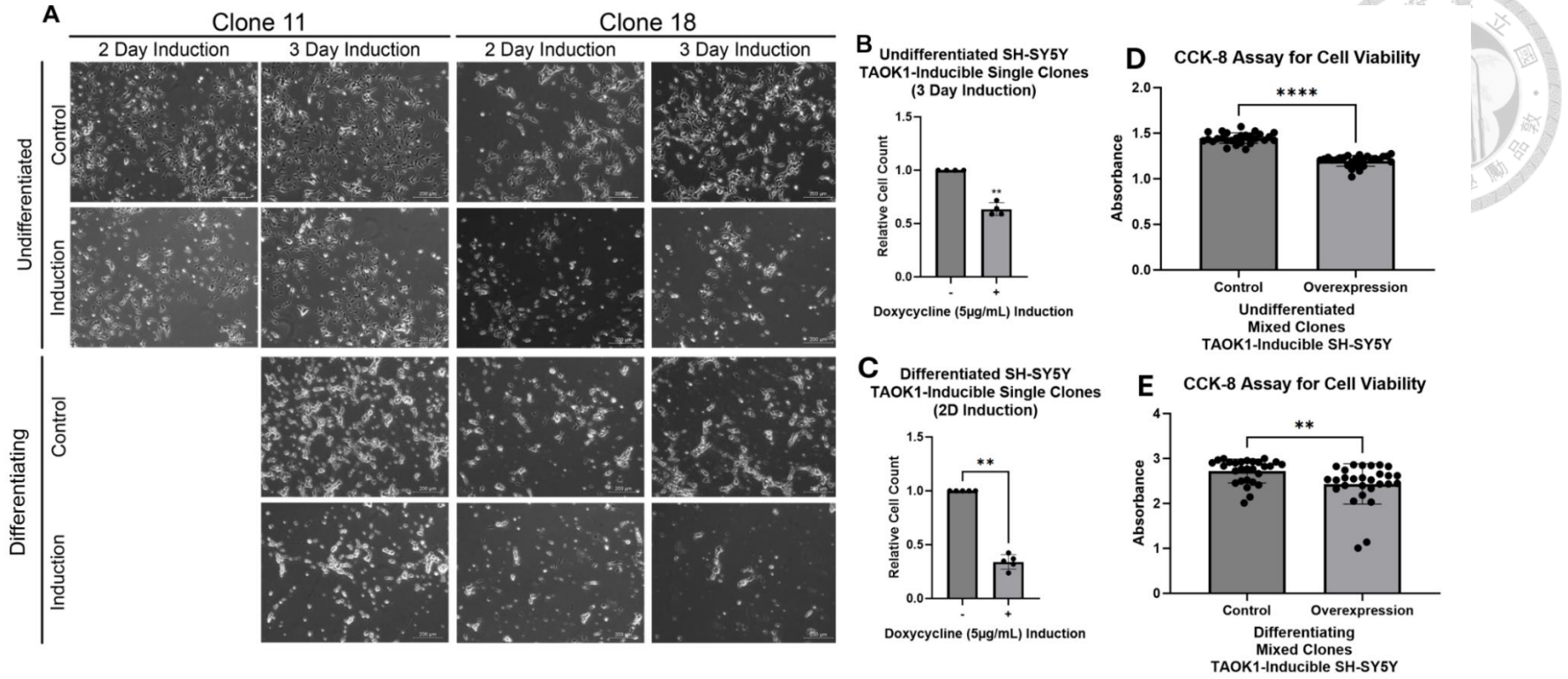

Figure 5. TAOK1 overexpression promotes cell death in both undifferentiated and differentiating SH-SY5Y. **(A)** Brightfield imaging shows a marked reduction in confluency in TAOK1 overexpressing cell populations regardless of differentiation status. **(B)** Harvest cell count was also significantly reduced in TAOK1 overexpressing groups of undifferentiated SH-SY5Y 3 days of doxycycline induction, and in **(C)** differentiating SH-SY5Y 2 days after induction. **(D, E)** CCK-8 Cell viability assay performed on undifferentiated and differentiating mixed clones reflects reduced absorbance, indicating lowered cell viability after TAOK1 overexpression.

doi:10.6342/NTU202402516

3.3. TAOK1 Overexpression Promotes Cell Death via Programmed Cell Death

While earlier results clearly demonstrate that TAOK1 overexpression induces neuronal loss, we aimed to accurately determine the mechanism of cell death to better characterize our cell model. Given the known involvement of TAOK1 in Caspase-3 signalling and its role in inducing apoptotic cell death, we first sought to verify if this pathway is activated in our model.

Through RT-qPCR, we observed an increase in the relative gene expression of Caspase-3 in both undifferentiated and differentiating cells with TAOK1 overexpression (**Figure 6D, E**). Western blot analysis also showed an increase in pro-Caspase-3 protein levels (**Figure 6C**). However, we were unable to identify cleaved Caspase-3, the active form of Caspase-3 in the western blot analysis. Thus, a TUNEL assay was conducted to stain for double-stranded breaks (DSBs) that are characteristic of apoptotic cell death. TUNEL assay results reflect a significant increase in apoptosis in our differentiating TAOK1-overexpressing cells compared to controls (**Figure 6A, B**).

As a preliminary study to elucidate the mechanisms behind this apoptotic cell death, we proceeded to assess the changes in gene expression of BCL-2 pathway proteins using RNA-seq analysis. These included the pro-apoptotic members, BAX, BAK and BOK, and anti-apoptotic BCL-2. In both undifferentiated and differentiating cells, RNA-seq analysis revealed a downregulation in *BAX*, *BAK1* and *BOK* expression, and an upregulation of *BCL2* (**Figure 7A, B**). BAX, BAK and BOK are pro-apoptotic proteins, while BCL-2 is considered an anti-apoptotic regulator of the pathway. Taken together, there is a shift towards cell survival mechanisms through this pathway.

While this is inconsistent with the observation of increased cell death in TAOK1 overexpressing cells, we considered the possibility of TAOK1 regulation through cellular

doi:10.6342/NTU202402516

pathways that governs cellular survival, and the activation of other pro-apoptotic pathways. Amongst which is the MAPK-Mef2 signalling. The expression of Mef2 transcription factors were assessed through RNA-seq analysis. The Mef2 family of transcription factors function downstream of p38-MAPK signalling and play crucial roles in regulating gene expression related to cellular survival and apoptosis (Lisek, et al. 2023).

In undifferentiated cells, the expression of *MEF2A, MEF2B* and *MEF2C* were upregulated, while *MEF2D* was downregulated (**Figure 8A**). This expression profile was consistent in that of differentiating SH-SY5Y clone 18 overexpressing TAOK1 (**Figure 8B)**. Mef2 family of transcription factors are known to be pro-apoptotic in circumstances of high cellular stress, hence, potentially contributing to the apoptotic events in this study. Further RNA-seq analysis of selected Mef2a and Mef2b target genes such as *CASP3*, *BCLAF1* and *DNAJB4*, genes whose upregulation is associated with increased apoptosis, were upregulated in TAOK1 overexpressing cells (**Figure 8D**). This trend of *MEF2A*, *MEF2B*, and *MEF2C* upregulation and *MEF2D* downregulation with TAOK1 overexpression, may reflect a TAOK1-associated pathway that is gradually shifting the cells towards apoptosis.

Overall, TAOK1 overexpressing cells undergo an increase in apoptosis, as evidenced by elevated Caspase-3 activity, reduced cell reduced confluency, cell viability observed in trypan blue and CCK-8 assays, and the increase in TUNEL-positive cells following TAOK1 overexpression. In preliminary RNA-seq analysis, the potential pro-survival signalling as seen in BCL-2 associated gene expression accompanied by the upregulation of several Mef2s and that of several pro-apoptotic target genes suggests a nuanced relationship between cell survival and cell death.

doi:10.6342/NTU202402516

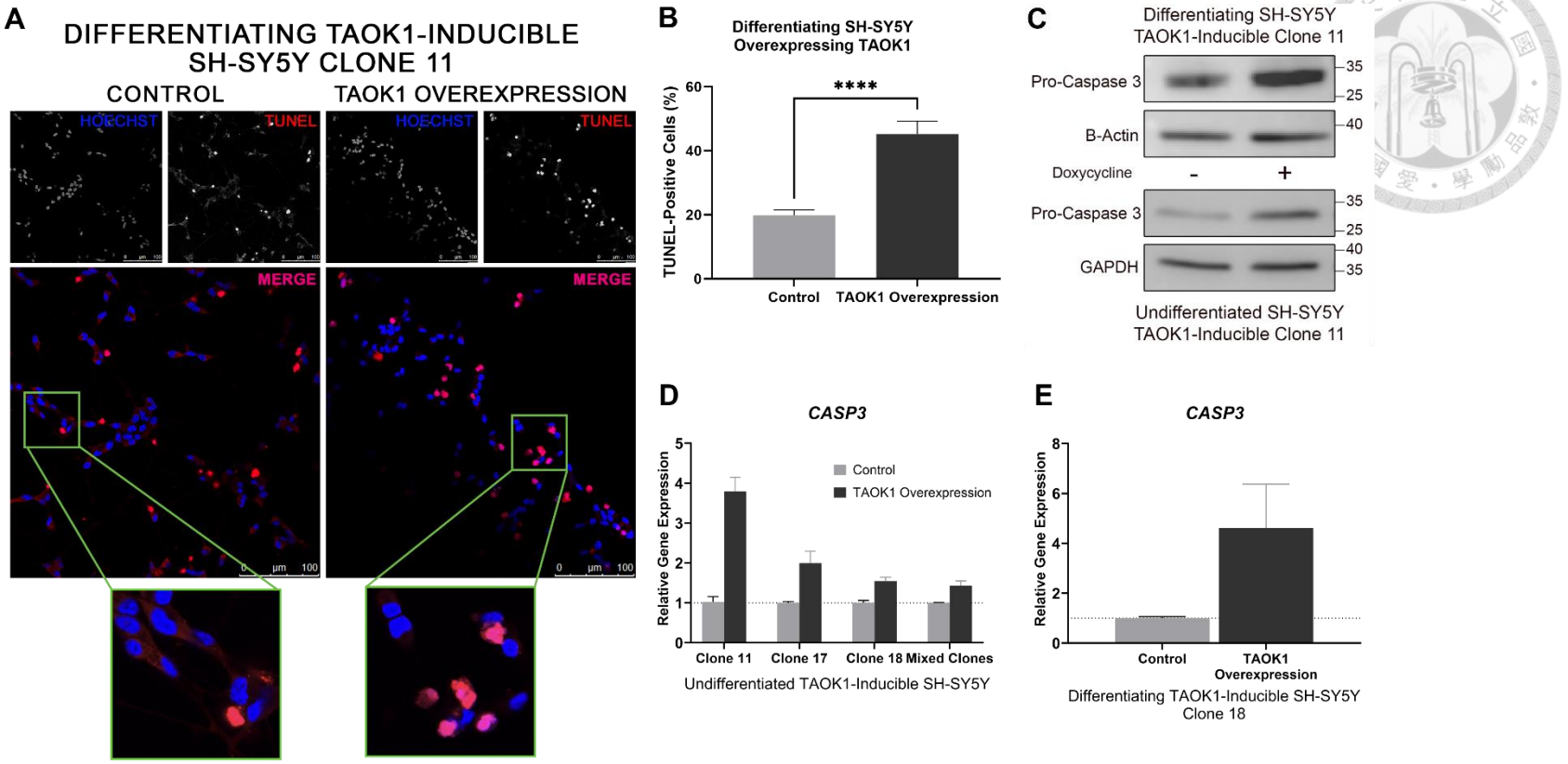

Figure 6. TAOK1 overexpression promotes apoptotic cell death in both undifferentiated and differentiating SH-SY5Y. (A, B) Immunofluorescence image of TUNEL-stained differentiating cells shows increase in TUNEL-positive cells (white arrows) with TAOK1 overexpression. **(C)** Western blots show upregulation pro-Caspase-3 with TAOK1 overexpression in both undifferentiated and differentiating SH-SY5Y. **(D)** *CASP3* was also upregulated in undifferentiated and **(E)** differentiating cells overexpressing TAOK1. (Scale Bar: 50μm)

doi:10.6342/NTU202402516

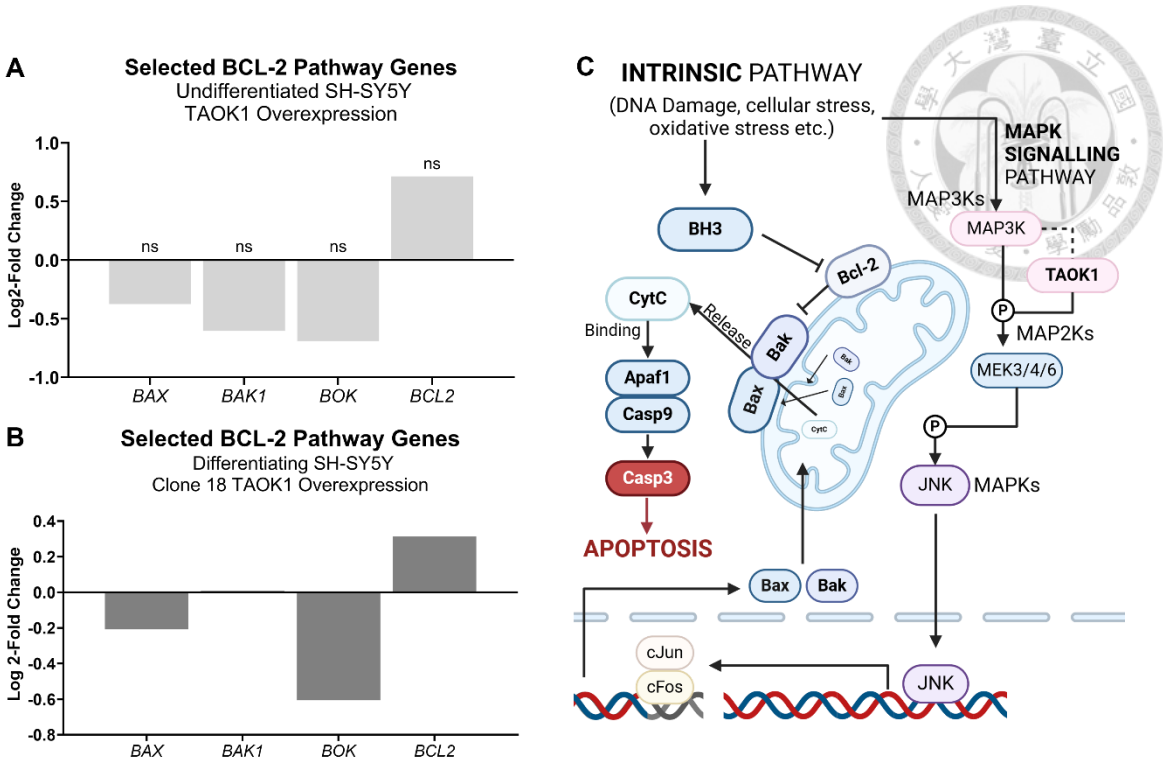

Figure 7. RNA sequencing analysis reveals potential downregulation of BCL-2 pathway of cell death. **(A)** Log 2-Fold Change from DeSeq2 analysis of multiple undifferentiated clones overexpressing TAOK1 shows that expression of pro-apoptotic proteins *BAX*, *BAK1* and *BOK* were decreased while *BCL2* increased. **(B)** Log 2-Fold Change from EdgeR analysis of differentiating single clone 18 overexpressing TAOK1 shows that *BAX* and *BOK* expression were decreased while *BAK1* was unchanged and *BCL2* expression was upregulated. **(C)** Schematic illustrating the BCL-2 apoptotic pathway (Created with BioRender.com). (ns $p > 0.05$)

doi:10.6342/NTU202402516

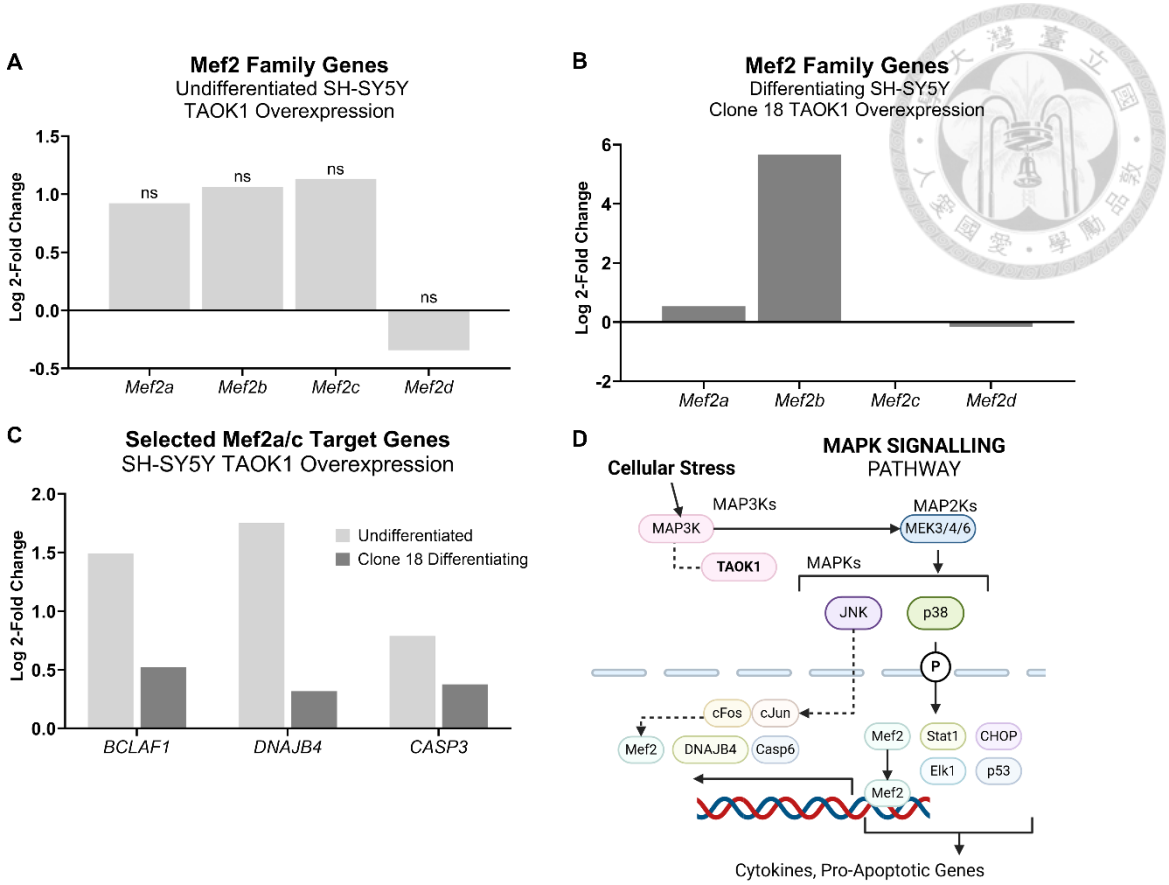

Figure 8. RNA sequencing analysis suggests potential dysregulation of apoptosis and cytoskeletal integrity regulators, Mef2 transcription factor family genes. (A) Log 2-Fold Change from DeSeq2 analysis of multiple undifferentiated clones overexpressing TAOK1 shows that *MEF2A, MEF2B* and *MEF2C* were upregulated while *MEF2D* was downregulated non-significantly. **(B)** Log 2-Fold Change from EdgeR analysis of differentiating single clone 18 overexpressing TAOK1 Expression of *MEF2A* and *MEF2B* were increased, while *MEF2C* and *MEF2D* were decreased. **(C)** TAOK1 overexpression was accompanied by upregulation of genes encoding pro-apoptotic proteins BCLAF1, DNAJB4 and CASP4 targeted by Mef2a and Mef2c transcription factors. **(D)** Schematic illustrating the Mef2 signalling pathway (Created with BioRender). (ns $p > 0.05$)

doi:10.6342/NTU202402516

3.4. TAOK1 Overexpression Drives Neurite Loss in Differentiating SH-SY5Y after branch formation

Besides neuronal loss, synapse loss is also a major hallmark of neurodegenerative diseases that is critical to healthy neuronal function. This is associated with microtubule instability which can lead neurite loss. While studies in neurodevelopment have shown that TAOK1 mutants can restrict neurite branching in developing neurons, little is known about branch loss in mature neurons. Given that TAOK1 overexpression increases Tau phosphorylation, we proceeded to assess its effects on neurite maintenance in our model.

TAOK1 overexpression was induced in differentiating cells that has visibly established neurite branching, specified in this study at 7 days after the start of differentiation. Changes in neurite length in differentiating cells was identified through immunofluorescence staining of β-Tubulin III (TUBB3), a differentiation marker that stains the β-tubulin subunit, and α-Tubulin of microtubules. Immunofluorescence imaging revealed shortened neurites in TAOK1 overexpressing cells compared to the control (**Figure 9A, B**). Neurites that were maintained in both populations prior to induction in the TAOK1 overexpressing group, became visibly reduced in the TAOK1 overexpressing group (**Figure 9C – E**). This shows that TAOK1 overexpression can drive neurite breakdown after TAOK1 induction, suggesting deficits in neurite maintenance.

doi:10.6342/NTU202402516

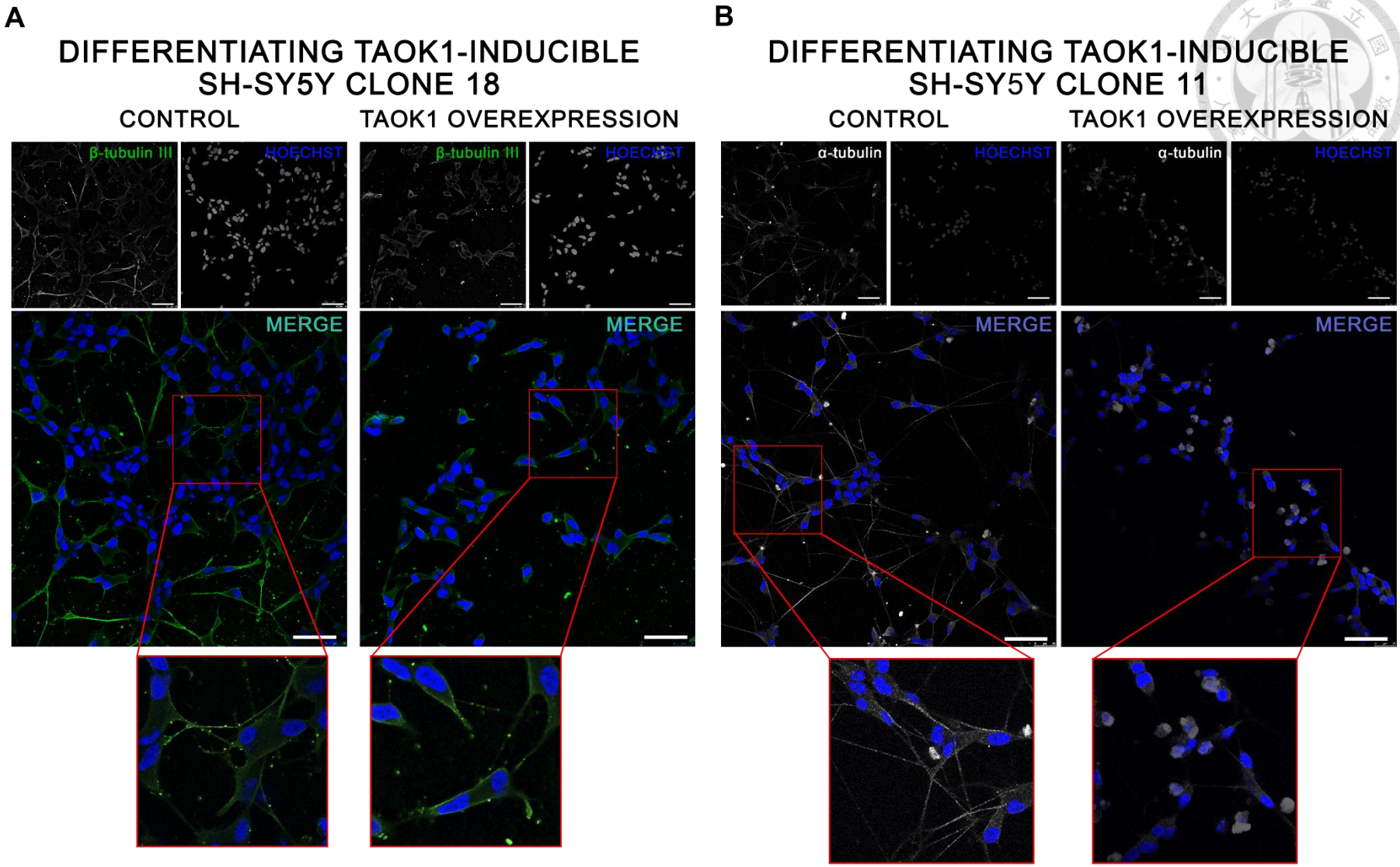

doi:10.6342/NTU202402516

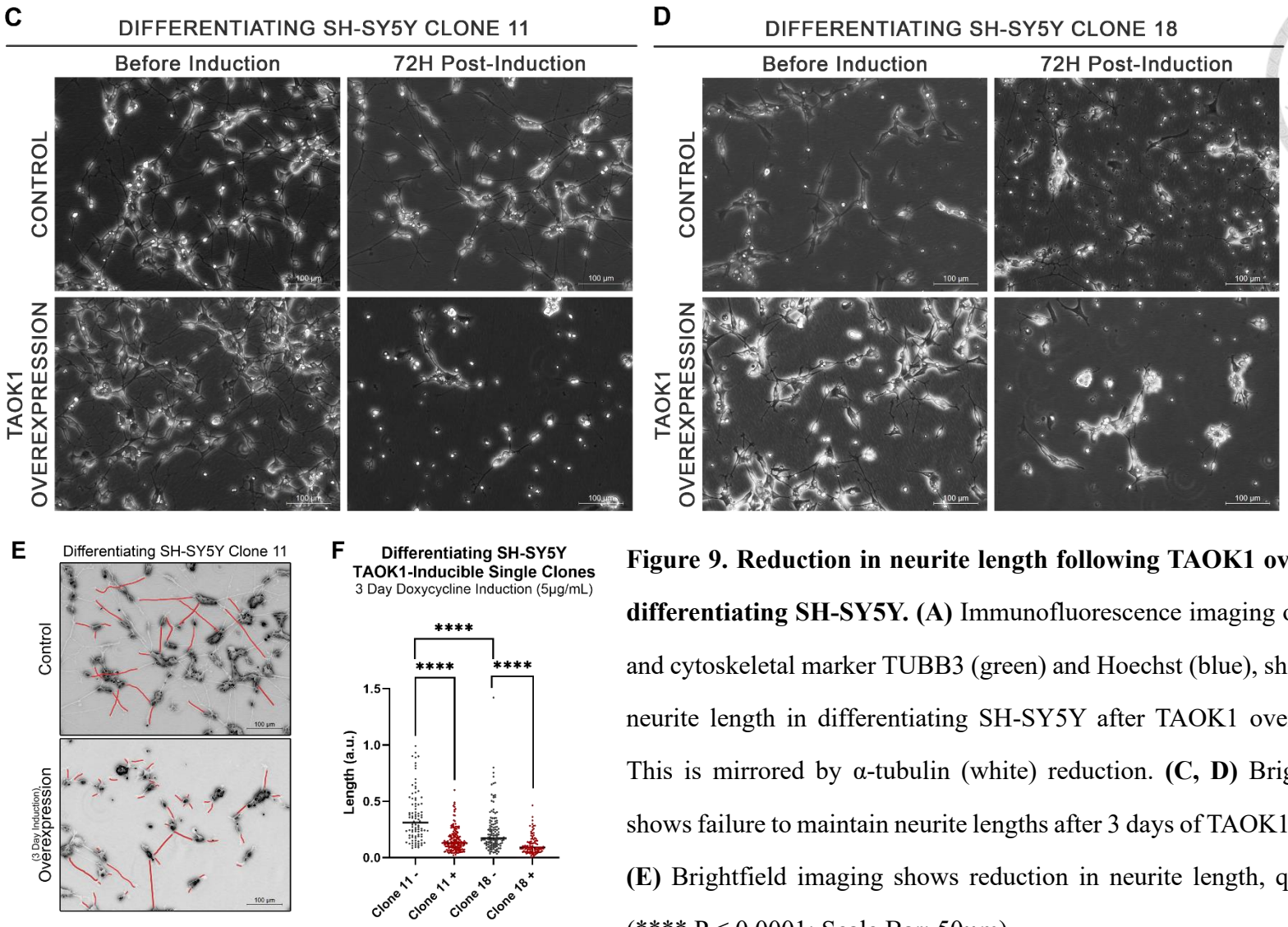

Figure 9. Reduction in neurite length following TAOK1 overexpression in differentiating SH-SY5Y. (A) Immunofluorescence imaging of differentiation and cytoskeletal marker TUBB3 (green) and Hoechst (blue), shows reduction in neurite length in differentiating SH-SY5Y after TAOK1 overexpression. **(B)** This is mirrored by α-tubulin (white) reduction. **(C, D)** Brightfield imaging shows failure to maintain neurite lengths after 3 days of TAOK1 overexpression. **(E)** Brightfield imaging shows reduction in neurite length, quantified in (F). (**** $P \leq 0.0001$; Scale Bar: 50µm)

doi:10.6342/NTU202402516

3.4.1. TAOK1 Overexpression Increases Tau Phosphorylation

TAOK1 is known to promote Tau hyperphosphorylation, and that Tau binding is heavily associated with neuronal branching in neurodevelopment. Hence, we hypothesise that in this model, TAOK1 increases Tau phosphorylation, and these hyperphosphorylated Tau may dissociate from microtubules, resulting in increased microtubule instability and subsequent neurite breakdown.

Phosphorylated Tau was quantified through western blot analysis, specifically targeting the phosphorylated Tau at Serine 262, a TAOK1 phosphorylation site that known to inhibit microtubule binding. The results revealed that TAOK1 overexpression significantly increases Tau phosphorylation specific to the TAOK1 phosphorylation site at serine 262 (**Figure 10**).

This supports the hypothesis that TAOK1-induced Tau hyperphosphorylation may be contributing towards microtubule dissociation and cytoskeletal stability to cause neurite breakdown in differentiating neurons.

doi:10.6342/NTU202402516

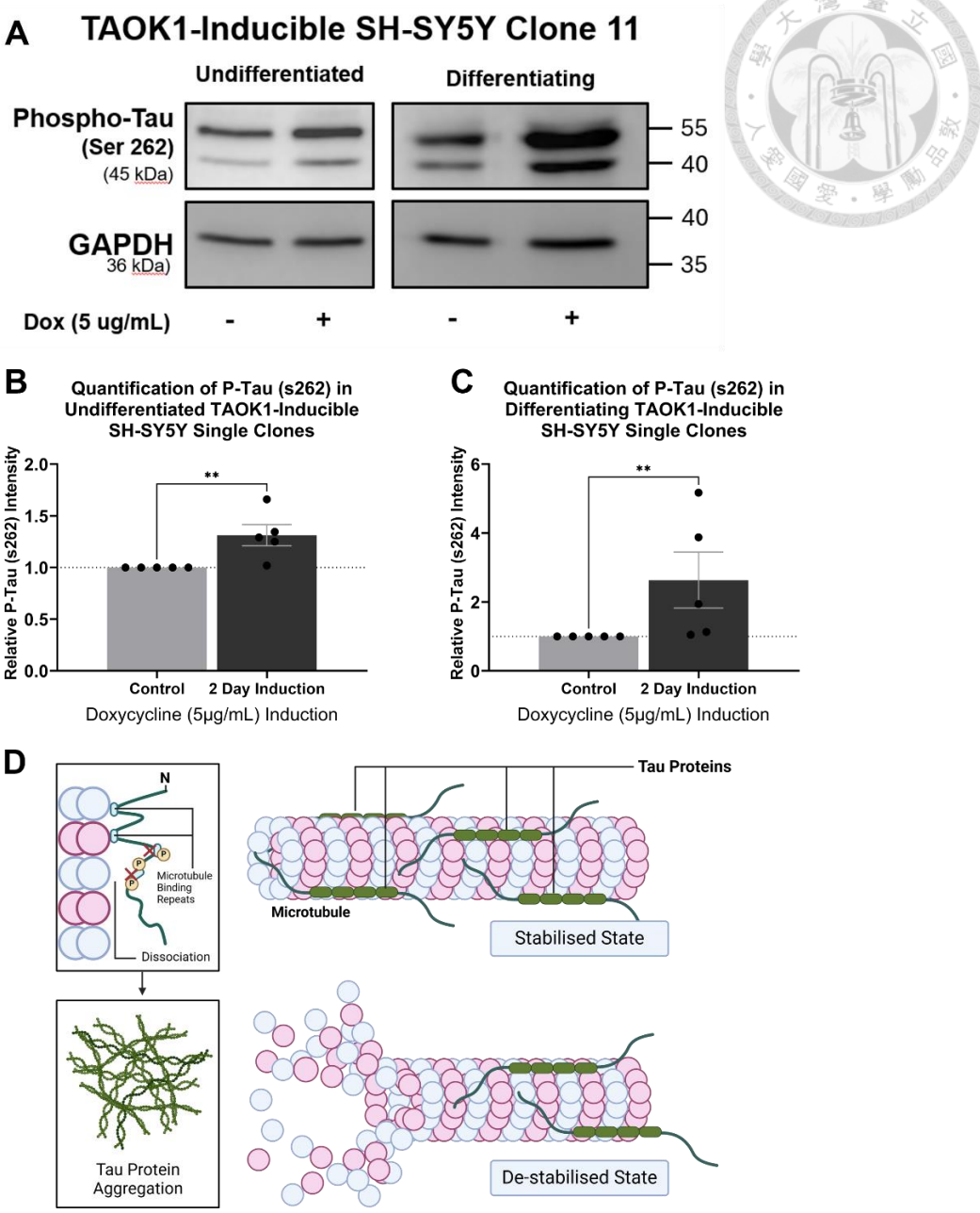

Figure 10. Tau phosphorylation was increased in both undifferentiated and differentiating SH-SY5Y following TAOK1 overexpression. (A) Western blot shows increase in phosphorylated Tau (Ser 262) in undifferentiated and differentiating cells after 2 days of doxycycline induction to overexpress TAOK1. **(B, C)** Densitometric quantification of relative intensity of western blot bands in multiple single clones. **(D)** Illustration of how Tau hyperphosphorylation can lead to microtubule destabilisation (Created with BioRender) (* $p \leq 0.05$)

doi:10.6342/NTU202402516

3.4.2. Neurofilament expression may be upregulated to counteract microtubule destabilisation in TAOK1-overexpressing cells

Next, we also wanted to further identify the consequential changes in cytoskeletal stability. Besides microtubules, neurofilaments are part of the neuronal cytoskeleton that provides structural support for neurites, specifically in axons. A preliminary RNA-seq analysis revealed an upregulation of the genes encoding neurofilament light and heavy chains, *NEFL* and *NEFM*, while the heavy chain (*NEFH*) was downregulated in the differentiating cells overexpressing TAOK1 (**Figure 11**). This hints at a potential compensatory mechanism to counteract microtubule destabilisation in differentiating cells overexpressing TAOK1.

doi:10.6342/NTU202402516

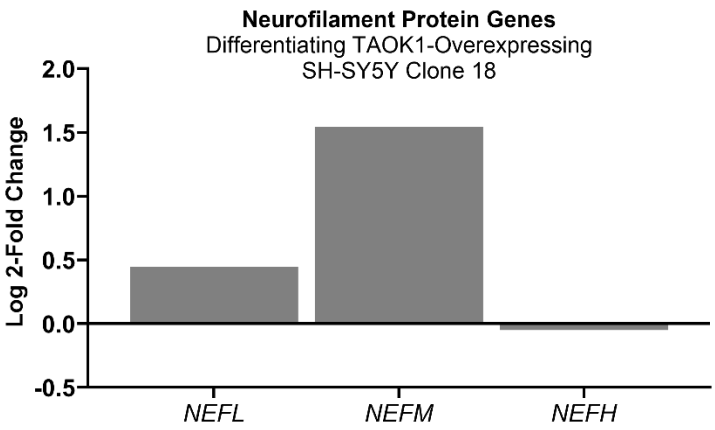

Figure 11. RNA sequencing analysis shows that TAOK1 overexpression promotes neurofilament subunit genes *NEFL, NEFM* upregulation and minimal *NEFH* downregulation in differentiating SH-SY5Y. Log 2-Fold Change from EdgeR analysis of differentiating single clone 18 overexpressing TAOK1 shows that genes encoding neurofilament subunits *NEFM* and *NEFL* were upregulated, while *NEFH* coincided with a smaller degree of downregulation in differentiating cells which have already shown significant neurite outgrowth.

doi:10.6342/NTU202402516

3.4.3. Synaptic activity may be dysregulated through microtubule-associated synaptic proteins in TAOK1-overexpressing cells

While SH-SY5Y are unable to form mature synaptic connections, we wanted to assess possible influences in synaptic activity, through the expression of microtubule-synapse proteins, and TAOK1 targets. These included Septin 7 (*SEPTIN7*), a known TAOK1 phosphorylation target associated with synaptic cytoskeleton, *GRIA2*, encodes for the GluR2 subunit for the AMPA receptor involved in synaptic transmission through calcium signalling, and Syntabulin (*SYBU*) a protein associated with microtubular transport and mitochondria tethering to microtubules. *SEPTIN7* along with *GRIA2* were upregulated in TAOK1 overexpressing cells. On the other hand, the expression of *SYBU* was found to be downregulated (**Figure 12A**). This gene expression profile was mirrored in undifferentiated cells as well.

Taken together, TAOK1 overexpression may lead to changes in the expression of several proteins associated with synaptic activity and microtubule dynamics. Given the close relationship between microtubules and neurofilaments in the growth and maintenance of neurites, changes in the expression of genes encoding neurofilament proteins is heavily reflective of alterations to the cytoskeleton. Overall, TAOK1 overexpression results in significant alterations to the gene expression profile of these cytoskeletal and synaptic proteins. This may either reflect or drive the observed neurite loss in differentiating cells.

doi:10.6342/NTU202402516

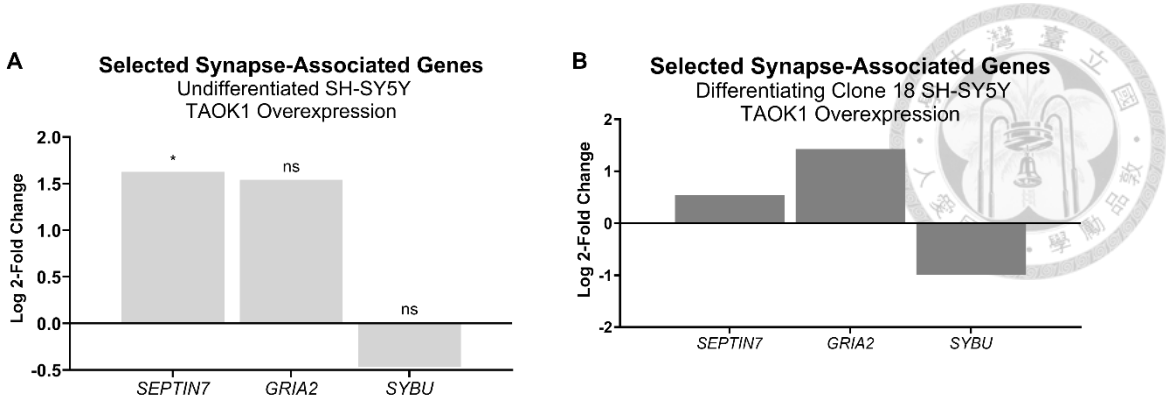

Figure 12. RNA sequencing analysis of genes encoding cytoskeletal protein SEPTIN7, glutamate receptor GluA2 (*GRIA2*) and microtubular transport protein Syntabulin (*SYBU*) shows variable expression patterns while consistent upregulation and downregulation are observed in differentiating SH-SY5Y. **(A)** Log 2-Fold Change from EdgeR analysis of differentiating clone 18 cells, shows that *SEPT7* and *GRIA2* were upregulated, while *SYBU* was downregulated with TAOK1 overexpression. **(B)** Log 2-Fold Change from DeSeq2 analysis of multiple undifferentiated clones shows that TAOK1 overexpression led to upregulation of *SEPTIN7* and *GRIA2* but downregulation in *SYBU*. **(**ns: $p > 0.05$; * $p \leq 0.05$)

doi:10.6342/NTU202402516

3.4.4. TAOK1 Overexpression Increases ROS levels

The increase in neuron death is often accompanied by, and contributed to by, increased cellular stress. Given that we have observed a reduction in ATP production in preliminary studies, we suspect that TAOK1 may be causing some degree of mitochondrial dysfunction in neurons. To investigate this, we measured ROS levels in our cells to determine if TAOK1 overexpression is sufficient to increase oxidative stress by measuring ROS levels in our cells.

Quantification of ROS levels through dihydroethidium (DHE) staining revealed an increase in superoxide and hydrogen peroxide in undifferentiated and differentiating TAOK1-overexpressing cells compared to the control (**Figure 13**). This increase was observed across multiple single clones and mixed clone populations. These findings suggest that TAOK1 overexpression is sufficient to induce oxidative stress in neurons.

doi:10.6342/NTU202402516

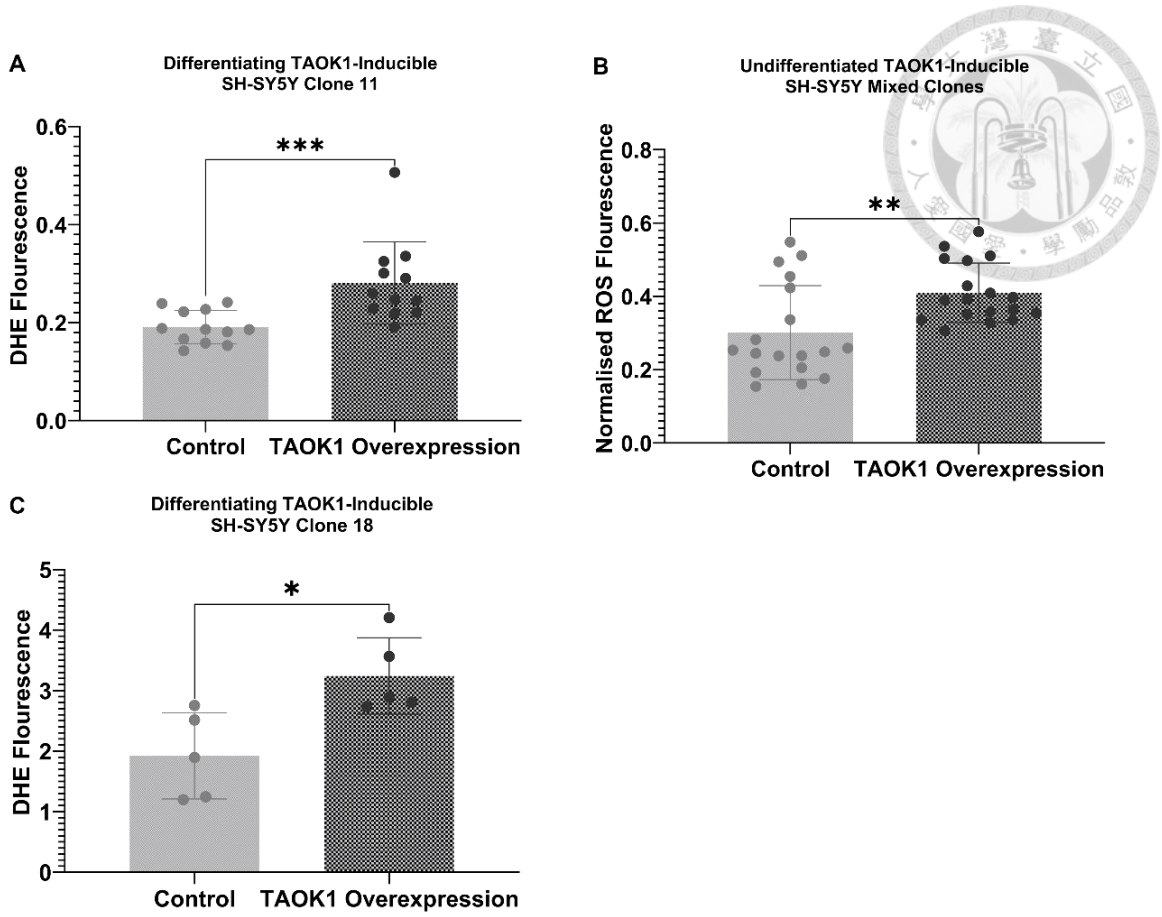

Figure 13. Quantification of ROS through DHE staining of live SH-SY5Y show increased ROS levels in TAOK1 overexpressing cells compared to control. (A) DHE fluorescence increased after TAOK1 overexpression of undifferentiated mixed clones normalised against CCK-8 Cell count. **(B)** DHE fluorescence of differentiating clone 11 and **(C)** clone 18 were both increased significantly after TAOK1 overexpression. (* $p \leq 0.05$; ** $p \leq 0.01$; *** $p \leq 0.001$)

doi:10.6342/NTU202402516

3.4.5. Increased ROS levels has limited effects on Nrf2 Signalling

To further elucidate the mechanisms behind the increased ROS levels in TAOK1 overexpressing SH-SY5Y cells, we analysed the expression of several proteins associated with mitochondrial function and redox homeostasis. RNA-seq analysis showed an upregulation of the gene encoding major antioxidant pathway transcription factor Nrf2 *(NFE2L2)*. Nrf2 activity is known to be upregulated by high ROS levels to activate downstream antioxidant activity against oxidative stress and is regulated as part of MAPK signalling pathways (Kobayashi, et al. 2006; Hammad, et al. 2023).

Under high oxidative stress, Nrf2 signalling will upregulate the expression of various antioxidants. Analysis of its target genes that encode antioxidants showed an upregulation of Catalase (*CAT*) and Superoxide Dismutase 1 (*SOD1*) in undifferentiated cells, but only Catalase was upregulated in differentiating cells overexpressing TAOK1. However, both antioxidant genes *GPX1*, and *GPX4,* which are also Nrf2 targets, were downregulated in both undifferentiated and differentiating populations (**Figure 14**).

doi:10.6342/NTU202402516

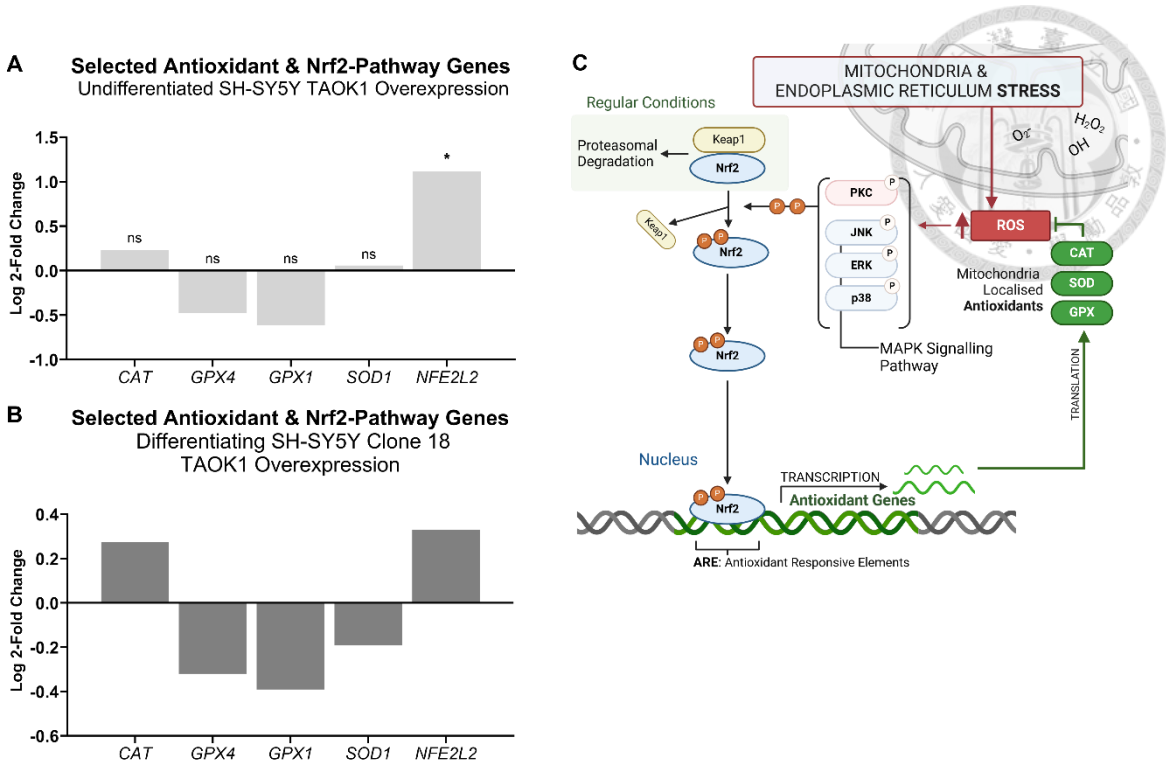

Figure 14. RNA sequencing analysis shows that TAOK1 overexpression upregulates *NFE2L2* gene encoding antioxidant regulator Nrf2 and targeted antioxidants genes *CAT* and *SOD1*, but a downregulation of *GPX4* and *GPX1*. (A) From the log 2-Fold Change from DeSeq2 analysis of multiple undifferentiated clones overexpressing, *NFE2L2* was upregulated together with its targeted *SOD1* and *CAT*. However, *GPX1* and *GPX4* were downregulated. **(B)** Log 2-Fold Change from EdgeR analysis of differentiating clone 18, only *CAT* was upregulated with *NFE2L2*, but *GPX1*, *GPX4* and *SOD* were downregulated with TAOK1 overexpression. **(C)** Schematic illustrating Nrf2 antioxidant pathway (Created with BioRender). (ns: $p > 0.05$; * $p \leqslant 0.05$)

doi:10.6342/NTU202402516

3.4.6. Increased ROS levels in TAOK1 overexpressing cells coincides with potential mitochondrial dysfunction

As redox homeostasis requires a balance between antioxidants activity and ROS production, we hypothesised that this dysregulation may also be caused by mitochondria dysfunction. In the earlier preliminary studies, ATP production was found to be reduced, but we also wanted to observe the expression of mitochondrial protein-coding genes. Out of the 13 known protein coding genes, RNA-seq analysis revealed a downregulation in the expression of 12 of these genes in undifferentiated cells (**Figure 15A**), and 4 in differentiating cells overexpressing TAOK1 (**Figure 15B**). This suggests a potential impairment in mitochondria dysfunction associated with cellular toxicity and dysregulation of redox homeostasis.

doi:10.6342/NTU202402516

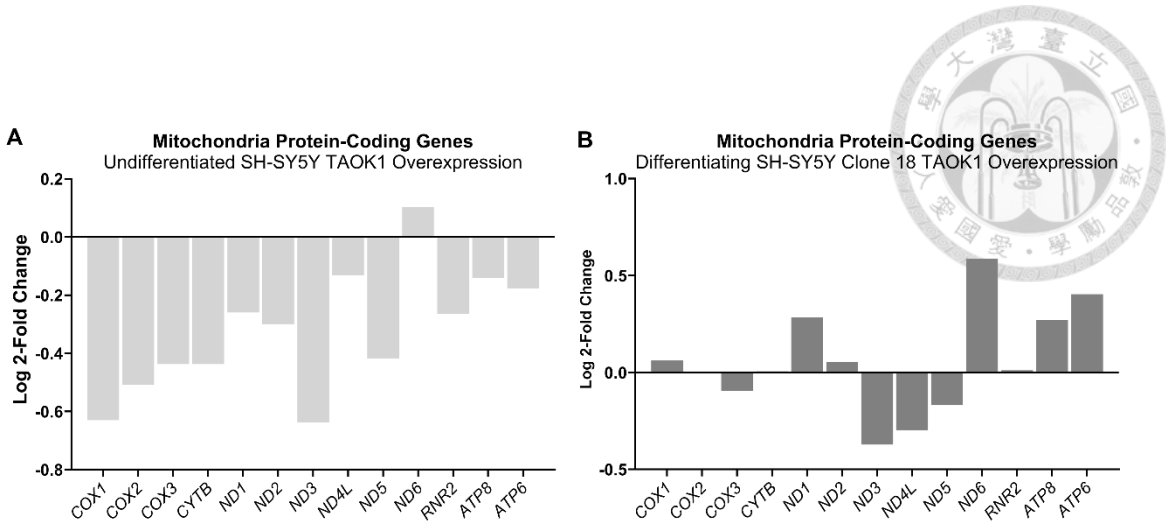

Figure 15. RNA Sequencing analysis of mitochondrial protein-coding genes suggests mitochondria dysfunction in TAOK1-overexpressing cells. (A) Log 2-Fold Change from DeSeq2 analysis of multiple undifferentiated clones overexpressing TAOK1 shows a downregulation in the expression of 12 out of 13 known protein-coding genes. **(B)** On the other hand, 4 were found to be downregulated, while 6 had minimal change from baseline, as seen from the log 2-Fold Change from EdgeR analysis of differentiating single clone 18 overexpressing TAOK1.

doi:10.6342/NTU202402516

3.4.7. Increased ROS levels in TAOK1 overexpressing cells may be associated with increased ER stress caused by abnormal protein aggregation

To identify sources where TAOK1 may be promoting this increase in ROS, we look back into Tau. Abnormal Tau hyperphosphorylation and neurofibrillary tangle formation is known to contribute towards ER stress through the unfolded protein response (UPR), increasing ROS production and driving apoptosis (Salminen, et al. 2009; Ajoolabady, et al. 2022). To identify the ER stress responses, we look into the expression of genes that are upregulated during ER stress.

RNA-seq analysis revealed the upregulation of genes encoding ER chaperone proteins Clusterin (*CLU)* and ER degradation enhancing alpha-mannosidase 3 (*EDEM3*) in differentiating cells overexpressing TAOK1 (**Figure 16B**). However, only *EDEM3* was upregulated whilst *CLU* was downregulated in undifferentiated cells (**Figure 16A**). These are known proteins that are upregulated by ER stress caused by increase in misfolded proteins (Satapathy, et al. 2023). *CREBRF*, a negative regulator of the UPR was also upregulated. Together, this gene expression profile suggests a potential increase in ER stress responses, potentially consequential of increased sensing of misfolded proteins in the cytoplasm. However, the increase in *CREBRF* expression also presents a possibility of the cell's shift towards recovery mechanisms during cellular stress.

doi:10.6342/NTU202402516

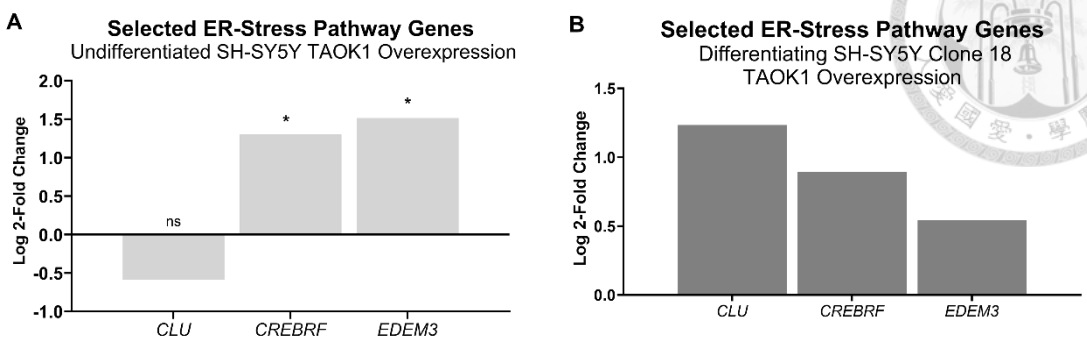

Figure 16. RNA sequencing analysis shows that TAOK1 overexpression promotes the expression of ER stress pathway genes *CLU, CREBRF* and *EDEM3* in SH-SY5Y. **(A)** Log 2-Fold Change from DeSeq2 analysis of multiple undifferentiated clones overexpressing TAOK1 shows that *EDEM3* and *CREBRF* were upregulated, but *CLU* was downregulated. **(B)** Expression of *CLU*, *CREBRF* and *EDEM3* increased with TAOK1 overexpression in differentiating SH-SY5Y overexpressing TAOK1 as seen from the log 2-Fold Change from EdgeR analysis of differentiating single clone 18. (ns: $p > 0.05$; * $p \leq 0.05$)

doi:10.6342/NTU202402516

3.5. TAOK1 Overexpression Drives Transposable Element De-Repression

Given the known contributions of Tau phosphorylation and ROS in driving aberrant TE de-repression, we hypothesized that TAOK1 overexpression might contribute to TE de-repression. By analysing TE expression through RT-qPCR, we aimed to determine if TAOK1 overexpression correlates with increased TE activity.

Through RT-qPCR analysis, we observed an increase in the transcripts of HERVs, Alu, and LINE-1 family members in both undifferentiated and differentiating cells with TAOK1 overexpression (**Figure 17A – D**). However, these families were downregulated in single clone 11, contrary to the other clone groups in this study (**Figure 17E**).

The observed TE de-repression indicates a potential mechanism by which TAOK1 contributes to genomic instability and neuronal dysfunction. Given earlier observations of increased Tau phosphorylation and ROS levels, TAOK1 may induce this increase in TE motility through Tau-mediated mechanisms or the activation of the MAPK signalling pathways.

doi:10.6342/NTU202402516

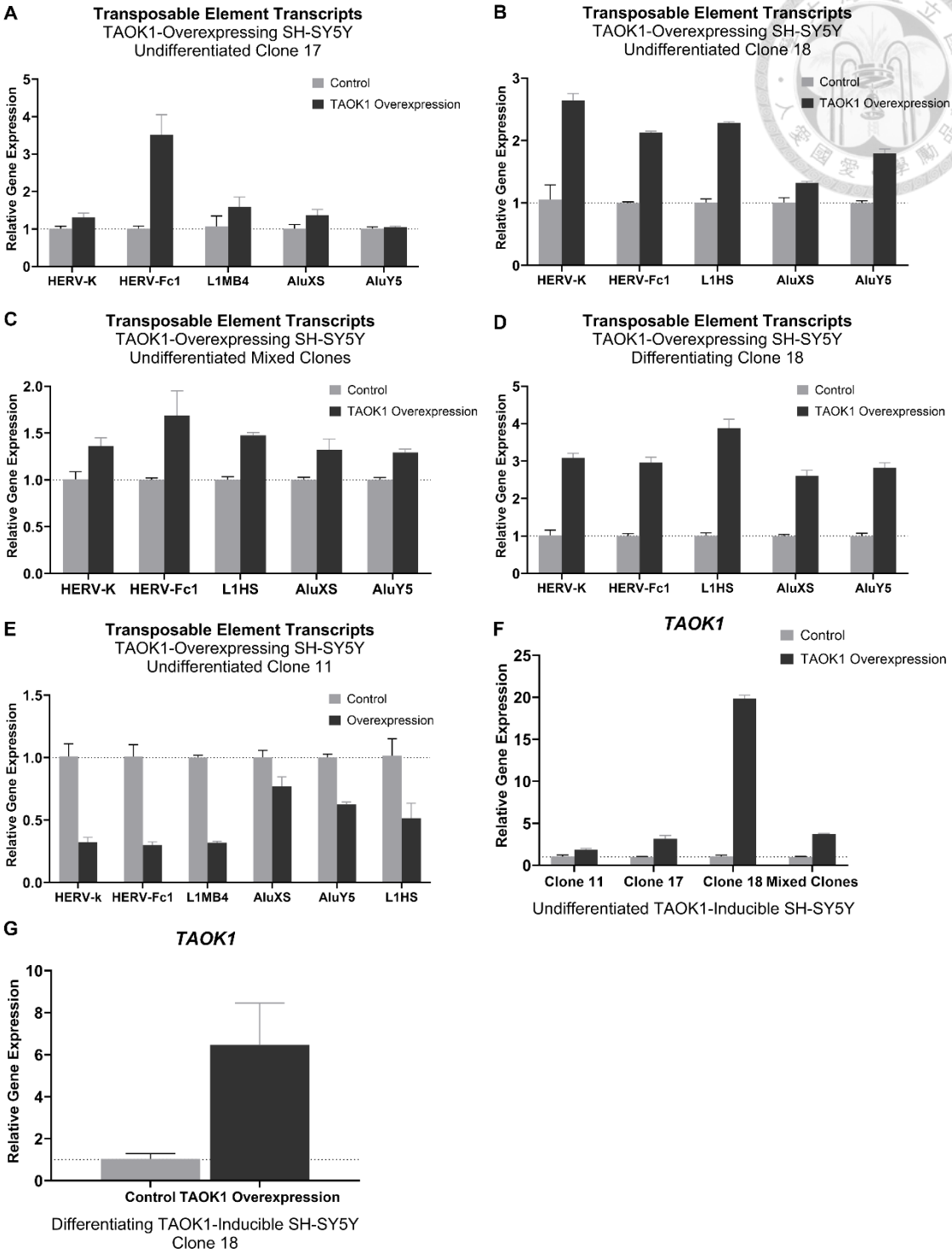

Figure 17. TAOK1 Overexpression resulted in de-repression in several transposable element families across most single clones. RT-qPCR shows increase in relative gene expression of TE transcripts of HERV-k-gag, HERV-FC1, L1HS/L1MB4, AluSX and AluYC5 in **(A – C)** undifferentiated mixed clones, 17 and 18 and mixed clones. **(D)** This

doi:10.6342/NTU202402516

upregulation was also found in differentiating clone 18 overexpressing TAOK1. **(E)** However, in the undifferentiated clone 11, TAOK1 overexpression had led to the downregulation of the same TE transcripts. **(F, G)** Relative gene expression of TAOK1 in undifferentiated mixed clones, 11, 17 and 18, and differentiating clone 18.

doi:10.6342/NTU202402516

3.5.1. TAOK1 Overexpression may influence cGAS-STING Pathway activity

To understand the potential neurotoxic pathways associated with aberrant TE de-repression, we examined the cGAS-STING signalling pathway, which is known to be activated by cytoplasmic DNA. The cGAS-STING pathway detects cytosolic DNA, which can arise from various sources, including aberrant TE de-repression. Upon sensing DNA, cyclic GMP-AMP synthase (cGAS) catalyses the formation of cyclic GMP-AMP (cGAMP), which binds to and activates the stimulator of interferon genes (STING). This activation triggers a cascade of downstream signalling events, leading to the production of type I interferons and other pro-inflammatory cytokines.

Our analysis revealed an increase in the relative mRNA levels of STING in both differentiating and undifferentiated cells with TAOK1 overexpression (**Figure 18A, B**). Additionally, analysis of RNA-seq data also shows an upregulation of *TBK1*, a target of STING activity that can phosphorylate interferon regulatory transcription factors (IRFs) to promote IFN-I responses (**Figure 19A, B**). However, *IFI6* and *IFIT1*, which are downstream of IFN-I signaling were downregulated in differentiating SH-SY5Y clone 18 overexpressing TAOK1, but *IFIT1* was upregulated in the undifferentiated single clones (**Figure 19A, B**). Together, the upregulation of *STING* and *TBK1* suggests the activation of the cGAS-STING pathway in response to TAOK1 overexpression. This may be due to the presence of TE-derived cytoplasmic DNA. The activation of this pathway indicates a link between TE de-repression and the induction of neuroinflammatory responses.

doi:10.6342/NTU202402516

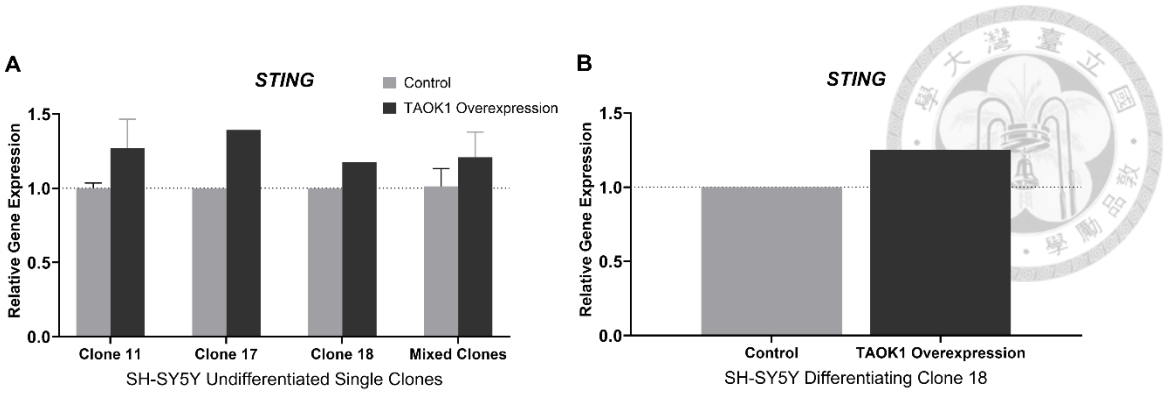

Figure 18. TAOK1 overexpression promotes STING expression in undifferentiated and differentiating SH-SY5Y. RT-qPCR reveals increase in relative gene expression of *STING* in **(A)** undifferentiated and **(B)** differentiating SH-SY5Y overexpressing TAOK1.

doi:10.6342/NTU202402516

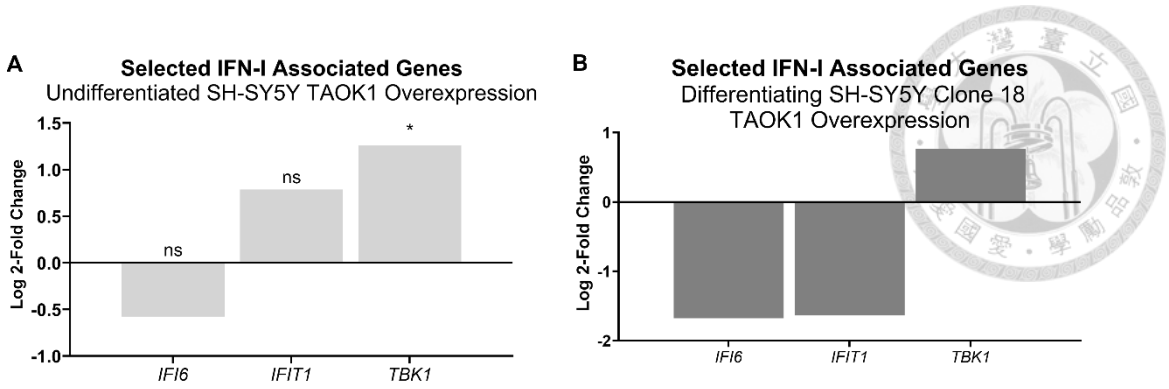

Figure 19. RNA sequencing analysis shows limited promotion of IFN-I response with downregulation interferon-stimulated genes *IFI6* and *IFIT1* and upregulation of interferon regulator *TBK1*. (A) Log 2-Fold Change from DeSeq2 analysis of multiple undifferentiated clones overexpressing TAOK1 shows that there was a non-significant downregulation of *IFI6* and upregulation of *IFIT1*. However, the expression of STING target, interferon regulator *TBK1* was upregulated. **(C)** Log 2-Fold Change from EdgeR analysis of differentiating single clone 18 overexpressing TAOK1 shows that *IFI6* and *IFIT1* were both downregulated but an upregulation in TBK1 expression. (ns: $p > 0.05$; * $p \leq 0.05$)

doi:10.6342/NTU202402516

3.5.2. TAOK1 Overexpression has limited effects on PIWI-piRNA Pathway

To understand the significance of TE activation and its potential neurotoxic effects, it is important to explore the regulatory mechanisms that normally suppress TE activity, such as the PIWI-piRNA pathway. This pathway plays a crucial role in maintaining genomic stability by silencing TEs, and its disruption could contribute to the neurotoxicity observed in our model. To further investigate the regulatory mechanisms behind TE activation, we examined the expression of key components of the PIWI-piRNA pathway, specifically PIWIL1 and PIWIL4, through western blot analysis. However, our results show that the levels of PIWIL1 and PIWIL4 do not increase in response to TAOK1 overexpression (**Supplementary Figure 2**).

doi:10.6342/NTU202402516

3.6. TAOK1 Overexpression has limited influence on NLRP3 Inflammasome Signalling

Given the activation of the cGAS-STING pathway observed with TAOK1 overexpression, we next investigated neuroinflammatory processes known to be downstream of this pathway, specifically focusing on the NLRP3 inflammasome signalling. Additionally, inflammasome signalling can be upregulated by increased ROS levels and is known to be activated by TEs like Alu, both of which have been associated observed in our model.

To assess the involvement of NLRP3 inflammasome signalling in our model, we examined the expression levels of various components of the inflammasome pathway, including caspase-1, NLRP3, and IL-1β. We hypothesized that the activation of the cGAS-STING pathway, triggered by TE de-repression and subsequent cytoplasmic DNA accumulation, along with elevated ROS levels, could lead to the activation of the NLRP3 inflammasome. This activation would contribute to neuroinflammation and neurotoxicity in TAOK1-overexpressing cells. Western blot analysis revealed no significant difference in the levels of pro-caspase-1, and NLRP3 between TAOK1-overexpressing cells and controls (**Supplementary Figure 3**). Quantification of IL-1β in the culture medium of TAOK1 overexpressing cells also found no significant difference (**Supplementary Figure 3**). Despite the increase in ROS levels and TE activity associated with TAOK1 overexpression, these findings indicate that TAOK1 overexpression is unlikely to activate canonical inflammasome signalling to increase pro-inflammatory cytokine release and pyroptosis.

doi:10.6342/NTU202402516

4. Discussion

4.1. Regulation of TAOK1 expression is crucial for Neuron Survival

Our study reveals that overexpression of TAOK1 in SH-SY5Y cells results in a significant decrease in cell confluency and harvest cell count (**Figure 5**). This reduction in cell viability was further confirmed by CCK-8 assays, which consistently demonstrated lower viability in TAOK1-overexpressing cells (**Figure 5**). These findings led us to investigate the mechanisms underlying this decrease in neuron survival. In a previous study, TAOK1 expression has been associated with increased apoptotic cell death via Caspase-3, prompting us to kickstart this investigation from apoptotic cell death (Wu & Wang, 2008).

Western blot analysis and RT-qPCR revealed an upregulation of the gene encoding Caspase-3, a protein involved in the execution of apoptosis (**Figure 6C – E**). This upregulation was accompanied by a notable increase in markers of apoptotic cell death. While we were unable to identify cleaved Capase-3 in the western blot analysis, we observed a higher percentage of TUNEL-positive cells, indicative of DNA fragmentation, a hallmark of apoptosis, in TAOK1-overexpressing cells (**Figure 6A, B**).

Our results suggest that TAOK1 overexpression activates apoptotic pathways, contributing to increased neuronal death. The marked increase in Caspase-3 expression and TUNEL positive cells supports the role of TAOK1 in promoting apoptosis. These findings provide insights into the cellular mechanisms by which TAOK1 influences neuron survival and the potential of targeting TAOK1 in therapeutic strategies aimed at reducing neuronal loss in neurodegenerative diseases. Further research is necessary to

doi:10.6342/NTU202402516

elucidate the precise molecular interactions between TAOK1 and apoptotic signalling pathways.

4.1.1. BCL-2 Signalling is unlikely to promote TAOK1-mediated cell death

Given the increased cell death observed, along with the potential for mitochondrial dysfunction indicated by elevated ROS levels, and reduced ATP production in preliminary studies, we examined the expression of proteins associated with the BCL-2 signalling pathway (**Figure 7**). This pathway involves various pro-apoptotic and anti-apoptotic proteins localised to the mitochondrial outer membrane, which regulate mitochondrial-associated apoptotic responses (Moldoveanu and Czabotar, 2020). Pro-apoptotic members such as Bax, Bak, and Bok are localised to the mitochondrial outer membrane and induce apoptosis via the activation of caspase-9 and caspase-3. The translocation and co-localisation of Bax and Bak to the mitochondrial membrane drive mitochondrial membrane permeabilization, leading to the release of cytochrome C into the cytosol. Cytochrome C then binds to and activates Apaf1-Caspase-9, which in turn activates caspase-3, resulting in apoptosis (Wolf, Shoeniger, and Edlich, 2022). Our investigation into the BCL-2 signalling pathway aims to elucidate the mechanisms underlying the observed increase in cell death and to understand the role of mitochondrial dysfunction in this process.

The expression of *Bax, Bak1* and *Bok* were found to be downregulated with TAOK1 overexpression, while *BCL2* was upregulated. This reflects an anti-apoptotic response from the BCL-2 signalling pathway to temper apoptosis. More experiments should be conducted with higher replicate count to obtain significance for this finding. The downregulation of *Bax, Bak* and *Bok* reflects a shift towards cellular survival. This is corroborated by the upregulation of anti-apoptotic protein *BCL2*, indicating a cellular

doi:10.6342/NTU202402516

response to temper apoptosis and promoting cell survival. In other studies, Bax and Bak have been implicated to modulate cell survival when experiencing increased oxidative stress and ER stress (Seervi, et al. 2018; White, et al. 2020). The gene expression profile may be reflective of a pro-survival response upon cellular stress through BCL-2 signalling.

However, these gene expression are only preliminary, and is not fully reflective of cellular status. It is necessary to observe the changes in protein expression through western blot analysis, and protein localisation of Bax and Bak through immunofluorescence staining and imaging. Additionally, the release of cytochrome C from the mitochondria into the cytoplasm is a characteristic of Bax/Bak pro-apoptotic signalling. Hence, by observing the changes in localisation of cytochrome in TAOK1 overexpression versus a control, will provide insights into this pathway.

doi:10.6342/NTU202402516

4.1.2. TAOK1 may mediate cell survival through Mef2-MAPK signalling

To explore other pathways whereby changes in TAOK1 expression may affect neuronal survival, we look into the MAPK pathway. TAOK1 activity functions upstream of the p38 MAPK signalling pathways to promote the activation of various transcription factors involved in cellular functions. Amongst which is the family of Mef2s, a group of transcription factors that can become upregulated with the activation of the p38-MAPK signalling pathway. Mef2s are known to regulate neuronal survival through apoptosis and can regulate synaptic activity through the scaffolding protein PSD95 (Lisek, et al. 2023). In terms of neuronal survival, the Mef2-p38 pathway is recognised to be pro-apoptotic in mature neurons when faced with high cellular stress, but anti-apoptotic during development (Kawasaki, et al. 1997; Akhtar, et al. 2012; Okamoto, et al. 2000). Furthermore, dysregulation in Mef2s have also been associated with AD and PD pathology (Yin, et al. 2012; Ren, et al. 2022).

In RNA-seq analysis, the expression of *MEF2A, MEF2B* and *MEF2C* were found to be upregulated, and *MEF2D* downregulated in both undifferentiated and differentiating clones TAOK1 overexpressing SH-SY5Y (**Figure 8A, B**).

The expression of *MEF2A* has been identified as a possible risk factor in AD development influencing neuroinflammation and cell death, and its silencing has been explored as a therapy to improve neuronal survival (González, et al. 2007; Welsbie, et al. 2017; Natarajaseenivasan, et al. 2020). Though, the roles that Mef2s play in neuronal survival is complicated and can be neurotoxic or neuroprotective in different contexts. Mef2A has been implicated in AD pathology where it was suggested to be associated with increased risk of late-onset AD (LOAD), that is commonly attributed to impaired amyloid-β clearance (González, et al. 2007; Dong, et al. 2017). It was also implicated in

doi:10.6342/NTU202402516

neuroinflammatory, where p38-induced Mef2A activation was found to promote the particularly interesting new cysteine histidine-rich (PINCH) protein expression in neurons and can disrupt actin cytoskeleton and mitochondria mis-localisation to cause toxicity (Natarajaseenivasan, et al. 2020). Meanwhile Mef2C can regulate a wide range of genes that is associated with various neurological defects in diseases, majority of which, are associated with deficits in synaptic activity and dendritic branching (Lisek, et al. 2023). A recent study has also demonstrated that IFN-I response through tau activation of cGAS-STING downregulates Mef2C to reduce cognitive resilience and promote synapse loss. Therefore, proposing that Mef2C is essential for cognitive resilience against tau pathology (Udeochu, et al. 2023). While Mef2B's role in neuronal cells are not as well studied as the other members of the Mef2 transcription factor family, studies have suggested that it plays a similar role to other members.

As Mef2 family of proteins are transcriptional factors, we also identified some pro-apoptotic genes whose promoters are targeted by Mef2a and Mef2b. We not only found the upregulation of *CASP3,* but also *BCLAF1* and *DNAJB4* in TAOK1 overexpressing cells (**Figure 8D**). BCLAF1 is a BCL-2 associated transcription factor that is known to promote apoptosis, while DNAJB4 is a heat shock protein that is associated with Hsp70.

While we did not see an upregulation in the pro-apoptotic members of the BCL-2 signalling family, we may wish to consider that the BCL-2 associated pro-apoptotic response may have yet to be triggered, or that it is suppressed in another way. Alternatively, we may also wish to observe the protein expression of BCLAF1 through western blot analysis and changes in its nuclear localisation through immunofluorescence imaging to determine its relevance. On the other hand, DNAJB4 is a co-chaperone of

doi:10.6342/NTU202402516

Hsp70, a major heat shock protein that is responsible for promoting protein refolding and degradation as part of the heat shock response (Mayer & Gierasch, 2019). An upregulation in various heat shock proteins is known to occur downstream of increased cellular stress due to protein aggregation (Collier & Benesch, 2020). This suggests that there is increased cellular stress in the cell, during TAOK1 overexpression, potentially through increased protein aggregation.

This upregulation of *MEF2A*, *MEF2B* and *MEF2C* may reflect an increased neurotoxic in the cell that can affect cellular survivability. Whilst preliminary, the upregulation in several of its gene targets associated with cell survival and cellular stress hints at a TAOK1-associated mediation of cell survival responses.

Overall, as a serine/threonine kinase, TAOK1 is known for many regulatory roles in various cellular pathways like MAPK, which is associated with cell survival and maintenance, making its dysregulation a critical factor in neuronal cell death. In this study, we have observed increased apoptotic cell death, but a conclusive pathway where TAOK1 activity can consistently promote apoptosis remains elusive. More work is necessary to elucidate these pathways whereby TAOK1 may be regulating cellular survival.

doi:10.6342/NTU202402516

4.2. TAOK1 Expression is critical to Neurite Maintenance in Differentiating Neurons

Neurons possess protoplasmic processes known as axons and dendrites that extend from the cell body that are responsible for transmitting or receiving electrical impulses, respectively. A neuron possess a single axon and multiple dendrites, and the establishment of neuronal polarity is critical for synaptic transmission. Neuronal polarisation is a tightly regulated process and is highly affected by changes in microtubule dynamics, where microtubule polymerisation and depolymerisation must be properly maintained to ensure proper cell function (Baas, et al. 2016; Conde and Cáceres 2009). Amongst the most important factors that regulates microtubule stability are microtubule-associated proteins (MAPs), which includes Tau (Barbier, et al. 2019). Tau phosphorylation by TAOK1 to regulate axonal and dendritic growth and branch has been extensively studied in the context of neurodevelopment. Tau binding to microtubules are regulated through phosphorylation to mediate microtubule dynamics, and TAOK1 can promote phosphorylation of residues located at microtubule binding domains and its adjacent sites (Tavares, et al. 2013). Consequentially, spine and synapse formation and activity in dendrites have been found to be highly dependent on TAOK1-mediated phosphorylation of Tau either directly, or through MARK and PAR-1 (Biernat, et al. 2002; Timm, et al. 2003; Liu, et al. 2010).

However, little is known about the precise mechanisms underlying TAOK1-mediated kinase activity in the maintenance of neurites and synapses in neurodegenerative diseases. Most hypotheses stem from indirect and speculative relationships through tau phosphorylation and known synaptic protein targets like Septin 7 (Byeon, et al. 2022). The maintenance of axon and dendrite branches is critical for

doi:10.6342/NTU202402516

ensuring synaptic plasticity and normal brain function. Failure to maintain these connections can result in diminished neuronal function, and the progressive loss of cognitive abilities in patients suffering from neurodegenerative diseases (Lin and Koleske 2010; Gcwensa, et al. 2021). This study aims to not only establish a distinction in neurite dynamics in this neurodegenerative context, but to uncover the molecular mechanisms behind this event.

To investigate the effects of TAOK1 overexpression on neurite maintenance in differentiating neurons, we induced TAOK1 overexpression after the cells had already exhibited significant neurite growth. This was standardised across our experiments at 7 days of culture in differentiation media. Observations using brightfield imaging revealed a reduction in the length of neuronal processes in differentiating neurons following TAOK1 overexpression. Neurite establishment in these cells was confirmed through immunofluorescence staining of class III β-tubulin (TUBB3) and α-tubulin. α- and β-tubulins are essential components of microtubules that heterodimerize and assemble into microtubules (Binarová and Tuszynski 2019). TUBB3 in particular, expressing predominantly in neurons, is often used as a marker for neuronal differentiation (Duly, et al. 2022). The reduction in neurite length was evident following TAOK1 overexpression in differentiating cells, in stark contrast to the control population, which maintained their neurites over the same culture duration (**Figure 9**). This finding demonstrates that TAOK1 overexpression specifically disrupts neurite stability and maintenance after neurite outgrowth. Neurites are critical for neuronal connectivity and communication through the formation of synapses. The observed reduction in neurite length has significant implications for the maintenance of neuronal connectivity and synaptic plasticity, highlighting the potential role of TAOK1 in neurodegenerative processes.

doi:10.6342/NTU202402516

We hypothesize that the abnormal hyperphosphorylation of Tau by increased TAOK1 activity could increase the susceptibility of the cell to form protein aggregates. This could disrupt axonal and dendritic transport, and with the destabilisation of microtubules. neurite breakdown will be promoted (Combs, et al. 2019). TAOK1's phosphorylation of Tau and other targets, which promotes neurite extension and synapse formation during development, can, when dysregulated later in life, result in neurite loss and synaptic breakdown, thereby promoting neurodegeneration.

4.2.1. TAOK1-mediated Tau Hyperphosphorylation may disrupt neurite maintenance in differentiating SH-SY5Y via microtubule destabilisation

Over the past three decades, pathological tau hyperphosphorylation has been increasingly implicated to drive synaptic dysfunction in neurodegenerative diseases. Tau has been known to promote the loss of synaptic proteins, cause microtubule destabilisation to disrupt mitochondrial transport and impair synapse activity (Callahan and Coleman 1995; Wu, et al. 2021). Interestingly, increased TAOK1 activity has also been observed in brain regions most vulnerable to AD-associated degeneration and abnormal tau hyperphosphorylation (Caušević, et al. 2010; Tavares, et al. 2013). Hence, we hypothesize that neurite breakdown in TAOK1 overexpressing cells is through pathological tau hyperphosphorylation and may contribute to neuron and function loss.

To further investigate the relationship between TAOK1 and tau in causing neurite instability, we first wanted to identify if TAOK1 overexpression can increase tau phosphorylation in our model. Using western blot analysis, we identified and increase in phosphorylated serine 262 (ser262), a known target of TAOK1 activity (**Figure 10**). Amongst the known TAOK1 phosphorylation sites, ser262 is known to affect tau ability to bind to microtubules (Gong and Iqbal 2008). Thus, supporting that hypothesis that the

doi:10.6342/NTU202402516

reduction in neurite length observed in this study may be through increased Tau phosphorylation, inhibiting its ability to bind to and stabilise microtubules.

To further validate TAOK1's direct role in Tau detachment from microtubules from hyperphosphorylation, we may investigate other phosphorylation sites targeted by TAOK1, especially those located at or adjacent to microtubule binding sites. Known phosphorylation sites like Ser356 and Thr231, are critical for Tau's binding affinity to microtubules and dysregulate (Yang, et al. 2014). Assessing the phosphorylation status of these sites through western blotting and mass spectrometry can help determine if TAOK1 overexpression inhibits Tau binding to microtubules. Verification that phosphorylation at or adjacent to microtubule binding sites will strengthen the hypothesis that TAOK1 overexpression promotes microtubule destabilisation and cause neurite breakdown through tau hyperphosphorylation.

4.2.2. Compensatory upregulation of neurofilament proteins may occur in response to Neurite instability caused by TAOK1-mediated tau hyperphosphorylation

Neurofilaments are major cytoskeletal components of neurons and are essential to the growth and maintenance of neurites, particularly axons (Yuan, et al. 2012). Dysregulation in neurofilament proteins could reflect neurite health and stability and shed light into the mechanisms behind the neurite loss in differentiating cells overexpressing TAOK1. Neurofilaments are composed of three proteins, neurofilament light chain, heavy chain, and medium chain. Through RNA seq analysis, we found the upregulation of the gene encoding the neurofilament medium and light chains (*NEFM* & *NEFL*) with TAOK1 overexpression (**Figure 11**). This upregulation of *NEFM* and *NEFL* may represents a compensatory mechanism to stabilise the neuronal cytoskeleton in response

doi:10.6342/NTU202402516

to microtubular instability induced by TAOK1 overexpression. Neurofilaments, play a critical role in providing structural support for the neuron. However, the gene encoding the heavy chain, *NEFH* did not see the same degree of upregulation as the other two subunits, and instead was mildly downregulated. The specific upregulation of *NEFL* and *NEFM* without a corresponding increase in *NEFH* might suggest that the cells are attempting to rapidly assemble neurofilaments to counteract the destabilising effects of Tau hyperphosphorylation. However, the lack of *NEFH* upregulation could have implications on the proper formation of neurofilaments. The specific upregulation of NEFL and NEFM, but not NEFH, might be related to their distinct roles within the neurofilament network.

During neurofilament assembly, NEFL self assembles to form the core structural backbone, before NEFM comes in to elongate and stabilise the filaments by interacting with NEFL, and NEFH is the last to be incorporated (Shea, et al. 1997; Laser-Azogui, et al. 2015; Uchida, Peng and Brown, 2023). The upregulation in *NEFL* and *NEFM* may be indicative of rapid assembly of neurofilaments in response to cellular stress. The lack of *NEFH* upregulation in the face of increased *NEFL* and *NEFM* expression suggests an early stage where the cells are beginning to assemble more neurofilaments to counteract the destabilising effects of tau hyperphosphorylation. This compensatory response highlights the cell's attempt to maintain cytoskeletal stability during neurotoxic conditions caused by TAOK1 overexpression.

4.2.3. TAOK1-mediated tau hyperphosphorylation may dysregulate synaptic activity through microtubule-associated synaptic proteins

SH-SY5Y cells are a useful model for investigating neuronal differentiation and the consequences of TAOK1 overexpression, but there are certain limitations. One major

doi:10.6342/NTU202402516

drawback is that they cannot establish mature synaptic connections, which makes it challenging to directly examine if the reduction of neurites observed in this model is linked to synaptic loss. However, we can still observe other molecular mechanisms associated with neurite loss. One possible alternative to explore potential synaptic dysfunction through altered synaptic protein activity.

Alongside tubulins and neurofilaments, septins are regarded as another filament protein that is heavily associated with the synapse cytoskeleton scaffold. Septin 7 in particular is a cytoskeletal GTP-binding protein that is crucial to dendritic growth and the maintenance of synaptic plasticity and activity (Marttinen, et al. 2015). It is also a known target of TAOK1 phosphorylation at Thr426 (Werner and Yadav 2022). Its phosphorylation drives its translocation from the base of dendritic protrusions to dendritic spine heads, promoting spine and synapse maturation through the stabilization of PSD-95 (Byeon, et al. 2022). Reduction or dysregulation in the expression and activity synaptic proteins and changes in their phosphorylation status will indicate synaptic dysfunction, even in the absence of actual synaptic activity in this cell model. The gene expression of these proteins were assessed through the analysis of RNA-seq data. Septin 7 was found to be upregulated in both undifferentiated and differentiating SH-SY5Y overexpressing TAOK1 (**Figure 12**). This upregulation of may be a compensatory response to maintain synaptic stability given the breakdown of the main tubulin cytoskeletal structure resultant of TAOK1 overexpression.

Next, we have also discovered the downregulation of Syntabulin (*SYBU*) expression (**Figure 12**). Syntabulin is a microtubule-associated protein that plays an important role in neuronal excitation and inhibition by facilitating mitochondrial transport on microtubules. Syntabulin is responsible for the binding of Syntaxin-1B (STX1B) to

doi:10.6342/NTU202402516

microtubules for transport to synapses to form the SNARE complex essential to synaptic vesicle fusion and neurotransmitter release at the synapse (Ke, et al. 2023). This downregulation in *SYBU* may reflect impaired microtubular trafficking and contribute to impaired synaptic function that may be associated with increased microtubular instability.

When looking at other synaptic proteins, we have also discovered an upregulation in *GRIA2*, the gene encoding the GluA2 subunit of the AMPA receptor (**Figure 12**). AMPA receptors are critical for synaptic transmission by facilitating the influx of cations like Na^+ to promote rapid synaptic depolarisation in response to glutamate binding. The GluA2 subunit is particularly responsible for regulating Ca^{2+} permeability of the AMPA receptor, and its dysregulation could impair neurotransmission and affect Ca^{2+} permeability. Therefore, if the upregulation in *GRIA2* expression is accompanied by an equivalent GluA2 protein upregulation, it may contribute towards increased Ca^{2+} permeability and accumulation in the cell, presenting another source of cellular stress and toxicity (Cerella, Diederich and Ghibelli, 2010). Through PICK1 interaction, GluA2 also plays an important role in the regulation of AMPA receptor endocytosis to manage long-term depression. Their dysregulation have also been associated with the pathogenesis of several neurological diseases associated with dysregulation in neural excitability such as Epilepsy and Autism Spectrum Disorder (ASD), highlight their importance in neuronal function (Salpietro, et al. 2019; Ke, et al. 2023). An upregulation in GluA2 may be a compensatory response to plausible synaptic dysfunction. In the event of neurite loss or reduction in synaptic activity, the upregulation of GluA2 in addition to Septin 7 may compensate for the destabilisation of synaptic structures.

Future experiments may observe other microtubule-associated synaptic proteins to assess possible dysregulations resultant of TAOK1-associated pathological conditions.

doi:10.6342/NTU202402516

For example, PSD-95, a scaffold protein involved in postsynaptic signalling and synaptic plasticity. Its degradation is known to be promoted by Mef2s, which is regulated through TAOK1-associated p38-MAPK signalling (Tsai, et al. 2012). Also, synaptophysin (*SYP*) is a pre-synaptic protein whose synthesis is associated with tau hyperphosphorylation and p38-MAPK signalling (Li, et al. 2003). Their gene and protein expression and phosphorylation statuses may be assessed through RT-qPCR and western blotting. While SH-SY5Y are unable to form mature synaptic connections, observing the statuses of synaptic proteins may be able to give insights into plausible implications on synaptic activity due to TAOK1 overexpression.

The downregulation of Septin 7, Syntabulin and GluR2 reflects a disruption in synaptic activity. Meanwhile, the upregulation of *NEFL* and *NEFM* may be indicative of a compensatory mechanism to maintain neurite integrity during cellular stress. Although SH-SY5Y cannot form mature synaptic connections, changes in the expression of synaptic proteins and components associated with neurite cytoskeletal structure can reflect the detrimental effects of TAOK1 overexpression on neuronal health. Our current data have demonstrated that TAOK1 overexpression in differentiating neurons leads to a reduction in neurite length. This is likely due to microtubule instability caused by aberrant tau hyperphosphorylation at microtubule binding sites such as Ser262. The gene expression profile of that encoding the neurofilament subunits, *SEPTIN7*, *GRIA2* and *SYBU* are also reflective of compensatory mechanisms and deficits in synaptic activity in differentiating neurons due to TAOK1 overexpression.

doi:10.6342/NTU202402516

4.3. TAOK1 Overexpression Dysregulates Redox Homeostasis

Intracellular ROS levels have also been known to influence MAPK signalling through oxidative modifications of MAPK pathway members, and associated proteins like dual-specificity phosphatases (DUSPs) (Son, et al. 2011; Takata, et al. 2020). As a member of this pathway, TAOK1 has also been implicated in redox homeostasis, where oxidative stress-activated MAPK phosphorylation was found to coincide with increased TAOK1 protein levels in human hepatocytes (Yin, et al. 2016). However, the directionality of TAOK1 expression and ROS levels is unclear beyond this limited context.

In this study, TAOK1 overexpression has led to abnormal tau hyperphosphorylation, which is known to lead to protein aggregation. The formation of protein aggregates are known to increase mitochondrial and ER stress, and this can be reflected in the cell as mitochondrial dysfunction, impairing ATP production and increasing ROS levels. As preliminary studies had demonstrated a reduction in ATP production, we questioned if TAOK1-mediated toxicity could affect mitochondrial function and perpetuate neurotoxicity by dysregulating redox homeostasis.

Cellular ROS levels was measured using a DHE staining of ROS such as intracellular superoxide anions and hydrogen peroxide. A significant increase in ROS levels was found in both undifferentiated and differentiating cells compared to the control when TAOK1 overexpression was induced (**Figure 13**).

As redox homeostasis relies on an intricate balance between ROS production and ROS scavenging by antioxidants, cellular stressors that disrupts mitochondria function, such as protein aggregates can promote ROS production and tip this balance. Hence, a detectable increase in ROS levels is representative of dysregulated redox homeostasis, and can have drastic consequences on cellular activity, including genomic instability and

doi:10.6342/NTU202402516

inflammation. With this, we hypothesise that TAOK1-mediated Tau hyperphosphorylation may cause mitochondrial dysfunction and promote neurotoxicity by promoting ROS production.

4.3.1. Mitochondria impairment is associated with increased ROS levels in TAOK1-overexpressing cells

As the major site for intracellular ROS production, dysfunction in the mitochondria can be a major source of increased ROS in the cell (Palma, et al. 2024). To elucidate this, we looked into the expression of mitochondrial protein-coding genes as a readout of mitochondrial function. Through RNA-seq analysis, we have discovered the downregulation of various mitochondrial protein-coding genes. Out of the 13, 10 of the mitochondrial protein-coding genes were downregulated in undifferentiated cells and 4 in differentiating cells overexpressing TAOK1 (**Figure 15**).

The alteration of mitochondrial gene expression suggests a possibility mitochondria DNA damage. Most importantly, these genes encode subunits of the complexes found in the electron transport chain that is responsible for ATP production in the mitochondria (Zhai, et al. 2023). Deficiencies in ATP production and its depletion can promote cellular death and has drastic consequences on neurons which have high energy demands (Eguchi & Tsujimoto, 1997; Kushnareva & Newmeyer, 2010; Fricker, et al. 2018). While we cannot yet determine the directionality of ROS production and mitochondria dysfunction, these results presents a possibility of a vicious cycle whereby increased oxidative stress can cause mitochondria damage, and further promote oxidative stress. However, it is highly likely that mitochondria dysfunction has occurred downstream of TAOK1 overexpression and possesses a high potential for promoting neurotoxicity through increased oxidative stress.

doi:10.6342/NTU202402516

Nevertheless, more experiments will be required to assess the degree mitochondria dysfunction. This may be done through the measurement of ATP levels to determine mitochondrial function. Additionally, one may also look at mitochondrial membrane potential using fluorescent dyes such as JC-1 and TMRE, which can reveal disruptions in mitochondrial integrity. A decrease in mitochondrial potential will reflect mitochondrial dysfunction. In addition, Also, to obtain significance for the RNA sequencing data, future experiments with more biological replicates should be conducted.

4.3.2. Nrf2 antioxidant pathway activity may be potentiated by TAOK1 overexpression, but insufficient to alleviate oxidative stress

The accumulation of oxidative stress causing cellular toxicity is often dependent on whether endogenous antioxidative pathways can handle the increased oxidative load. Given our current hypothesis that mitochondrial dysfunction increases ROS production, we also wanted to investigate the integrity of endogenous antioxidants and regulatory pathways that may be activated during oxidative stress. One of the most common antioxidant pathways is the Nrf2 signalling pathway, regulated by p38/JNK/ERK-MAPK signalling to maintain redox homeostasis in the cell (Pan, et al. 2016). During oxidative stress, the activity and expression of nuclear factor erythroid 2 p45-related factor 2 (Nrf2) is known to be upregulated (Kasai, et al. 2020). Nrf2 is a transcription factor that serves as a major antioxidant pathway regulator that promotes the transcription of various antioxidants such as SODs, CAT and GPXs to counteract high cellular oxidative stress (Hammad, et al. 2023). In normal conditions, Keap1, an Nrf2 inhibitor, will binds and tag Nrf2 for proteasomal degradation. However, under oxidative stress, Keap1 loses its ubiquitination activity and can lead to the release of Nrf2 to translocate into the nucleus to promote antioxidant gene expression (Kobayashi, et al. 2005).

doi:10.6342/NTU202402516

To investigate if this pathway can become activated, we used RNA-seq analysis to observe the expression of the gene encoding Nrf2, *NFE2L2*, and that of several of its downstream targets. In both undifferentiated and differentiating cells, *NFE2L2* was found to be upregulated in TAOK1 overexpressing cells compared to the control (**Figure 14**). However, when observing the expression of its downstream antioxidant gene targets, we only found a mild upregulation in its downstream targets antioxidants, Catalase (*CAT)* and *SOD1* in TAOK1 overexpressing undifferentiated cells, and only *CAT* was upregulated in differentiating cells.

While an upregulation in *NFE2L2* gene expression can be taken to signify increased sensing of intracellular oxidative stress, the lack of consistent upregulation across Nrf2-targeted antioxidant genes may represent a disconnection in this pathway. It is likely that the initial increase in oxidative stress may be due to TAOK1-mediated Tau hyperphosphorylation. This increased oxidative stress may then activate Nrf2 signalling as represented by the upregulation in *NFE2L2* expression, potentiated by TAOK1 through the MAPK signalling pathway.

It is necessary to further characterise this pathway and identify if there is an impairment in Nrf2 pathway activity that can disrupt the activation of antioxidants. This may occur during Nrf2 nuclear translocation, interaction with target genes, or impairment in Keap1 activity. Protein expression of Nrf2, and its target antioxidants such as the aforementioned GPXs, SODs and CAT, should be assessed through western blot analysis. Visualising Keap1-Nrf2 co-localisation and Nrf2 localisation through immunofluorescence microscopy will also provide insights into the integrity of Nrf2 function in response to oxidative stress in the cell.

doi:10.6342/NTU202402516

Overall, this study has shown that TAOK1 overexpression can increase ROS levels in SH-SY5Y, and trigger antioxidant pathways like Nrf2 to restore redox homeostasis. However, the downregulation of various antioxidant genes despite high ROS levels leaves the cells at a vulnerable state where the persistent oxidative stress can damage cellular components including the mitochondria itself, creating a vicious cycle of increased oxidative stress and mitochondria damage. Eventually, not only impairing cell function but also cause cell death.

More experiments would be necessary to properly validate the mitochondria damage downstream of TAOK1 overexpression, how intracellular antioxidant pathways are affected, and the possible neurotoxicity to the cell.

doi:10.6342/NTU202402516

4.3.3. Oxidative Stress in TAOK1 Overexpression may be associated with ER Stress Response Mechanisms

To identify how TAOK1 overexpression can drive mitochondrial dysfunction and aberrant ROS production, we looked further into how TAOK1-mediated Tau hyperphosphorylation may contribute to this event. The accumulation of misfolded proteins and aggregates including Tau can increase endoplasmic reticulum (ER) stress and upregulate stress responses like the unfolded protein response (UPR). This period of prolonged stress promotes mitochondria stress and dysfunction, and increased ROS through the mitochondria-associated membrane (MAM) between the mitochondria and ER (Cao & Kaufman, 2014; Zeeshan, et al. 2016).

To identify ER stress responses, we looked into genes that encode proteins that are known to be upregulated during ER stress. Through RNA-seq analysis, *CLU*, *CREBRF* and *EDEM3* were found to be upregulated following TAOK1 overexpression in differentiating cells (**Figure 16B**). While *CREBRF* and *EDEM3* were upregulated, but *CLU* downregulated in undifferentiated cells overexpressing TAOK1 (**Figure 16A**).

Clusterin (CLU) is an ER chaperone protein that directs misfolded proteins for degradation. *CLU* expression is known to be upregulated by increased ER stress induced by increased detection of misfolded proteins in the cytosol. *CLU* is also a major genetic risk factor for LOAD by its role in Aβ aggregation and clearance (Moon, Herring & Zhao, 2021; Foster, et al. 2019). An upregulation in *CLU* expression is an indicator of increased ER stress due to misfolded proteins to avoid pathological accumulation that can cause neuronal dysfunction. Additionally, EDEM3 is another ER protein that promotes ER-associated degradation (ERAD), a pathway that targets misfolded proteins for ER

doi:10.6342/NTU202402516

degradation, hence indicating increased sensing of misfolded proteins in the cell (Hirao, et al. 2006).

CREB3 regulatory factor (CREBRF) regulates the ER's UPR by negatively regulating CREB3 during UPR. CREB3 is a transcription factor that is upregulated by ER stress to activate the UPR to reduce ER stress or promote cell death through karyoptosis (Lee, et al. 2024). CREBRF functions by suppressing CREB3 activity and promoting its degradation by binding and sequestering it into discrete nuclear foci (Wong, et al. 2018). Hence, an upregulation in *CREBRF* is an indication of increased ER stress and the need to suppress the cytotoxic UPR. Together, this gene expression profile reflects increased ER stress caused by misfolded proteins, and an upregulation of cellular activity to suppress UPR. Together, the upregulation in *EDEM3*, *CLU* and *CREBRF* expression highlights the toxicity posed by TAOK1-mediated tau phosphorylation, and potential for pathological consequences when current UPR responses may be insufficient.

However, to fully understand how TAOK1 overexpression may drive ER stress and if UPR is neurotoxic in this context, more experiments are necessary. The expression of various endoplasmic stress response element (ERSE) containing genes, which are upregulated by ER stress, and can induce cytotoxic responses like apoptosis may be assessed. These includes c-Jun, c-FOS, which forms the Activator Protein 1 (AP-1), that can drive downstream responses like inflammation and apoptosis. Additionally, validation of the protein expression of CLU, EDEM3 and CREBRF through western blot analysis and localisation in immunofluorescence microscopy can verify their activity and relevance to our study.

Overall, TAOK1 overexpression increases oxidative stress, likely due to mitochondrial dysfunction and a dysregulation of redox homeostasis. This may be

doi:10.6342/NTU202402516

exacerbated by TAOK1-mediated Tau hyperphosphorylation, which promotes mitochondrial and ER stress through UPR, overwhelming the cell's stress responses. However, more experiments are necessary to elucidate mitochondria and ER dysfunction, and the contributions of increased oxidative stress on deteriorating neuronal health.

doi:10.6342/NTU202402516

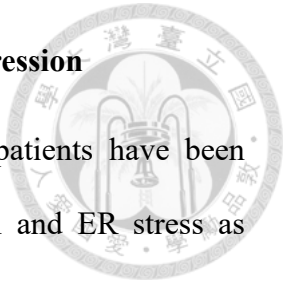

4.4. TAOK1 Expression drives Transposable Element De-Repression

Tau-mediated toxicity in animal models and in dementia patients have been attributed to a variety of pathways such as causing mitochondrial and ER stress as explored in the previous section. When it comes to aging, genomic instability have been proposed as a source of pathological consequence from pathological Tau hyperphosphorylation (Colnaghi, et al. 2020). With literature over the years demonstrating the potential of Tau-mediated activation of TEs in both animal models in AD patients. Besides contributing to mitochondrial stress, increased neurofibrillary tangle burden from abnormal tau hyperphosphorylation is also a source of increased TE de-repression (Guo, et al. 2018). Given the observations of increased Tau phosphorylation due to TAOK1 overexpression, it is plausible that the upregulation of TE transcripts may be caused by Tau hyperphosphorylation as well. Hence, we looked to see if this neurotoxicity may be replicated in our cellular model

The expression of several TE families, namely HERV, LINE-1 and Alu, were investigated for their known dysregulation by pathological protein aggregation and increased oxidative stress that has been observed in our study, in various neurological contexts (Giorgi, Marcantonio and Del Re 2011; Guo, et al. 2018; de Oliveira, et al. 2021). The harmful consequences of dysregulated TEs in neurodegenerative disorders have been increasingly studied over the years. While increased TE transposition is known for driving DNA damage and genomic instability, inflammation and neurotoxicity have also been promoted by abnormal TE de-repression (Jönsson, et al. 2020; Chesnokova, Beletskiy and Kolosov, 2022; Singh, Borkar and Bhatt 2024).

Analysis of gene expression of RT-qPCR data reveals an increase in expression of TE transcripts in TAOK1 overexpressing neurons regardless of differentiation status in

doi:10.6342/NTU202402516

most clones, suggesting that TAOK1 overexpression contributes to TE de-repression (**Figure 17**). TEs, which are typically silenced in the genome, can become reactivated under conditions of cellular stress, contributing to genomic instability and inflammation. The observed de-repression of TEs in our model aligns with findings from tauopathy models, where abnormal Tau phosphorylation and aggregation are associated with TE activation.

Overall, this increase in TE de-repression may most likely be due to the abnormal Tau hyperphosphorylation driven by increased TAOK1 activity from its overexpression.

4.4.1. Perspectives: TAOK1-induced Oxidative Stress may promote TE De-repression by inducing genomic instability

Earlier in this study, we have demonstrated increased ROS levels in TAOK1 overexpressing cells. Oxidative stress is another known activator of TEs, and the elevated ROS levels observed in our model may further exacerbate TE de-repression. This creates a vicious cycle where TE activation leads to increased genomic instability and cellular stress, perpetuating neuronal damage. To further investigate the relation between oxidative stress and dysregulated TEs, treatment of cell groups using antioxidants to mitigate oxidative stress may be conducted to observe its effects on TE activity.

This may be conducted by adding ascorbic acid (vitamin C), a potent antioxidant, into the culture medium of TAOK1 overexpressing cells. If antioxidant treatment with ascorbic acid effectively reduces ROS levels and leads to a corresponding decrease in TE transcripts, it would provide strong evidence that oxidative stress is a key driver of TE activation in TAOK1 overexpressing cells. This also highlights the importance of oxidative stress in genomic stability and the reduction of oxidative stress could be a potential therapy to mitigate TE-mediated toxicity in neurodegenerative diseases.

doi:10.6342/NTU202402516

4.4.2. Perspectives: Relevance of the PIWI-piRNA Pathway

In this study, an increase in TE transcripts from RT-qPCR was observed after TAOK1 induction, driving the question to the mechanism behind this de-repression event. As mentioned in the earlier sections, TE de-repression may occur

The PIWI-piRNA pathway is one of the most well-conserved mechanisms across eukaryotes involved in the suppression of abnormal transposable element (TE) expression through transcriptional and post-transcriptional gene silencing (TGS and PTGS).

TE de-repression can indicate a compromised TE silencing pathway. PIWI proteins encode for a heavily conserved subfamily of proteins that bind to Piwi-interacting RNAs (piRNAs), which mainly target TEs for degradation. PIWIL1, PIWIL2, and PIWIL4 are known to be expressed in the human brain and are involved in neuronal differentiation and axon regeneration. In a recent study, the expression of PIWIL1 and piRNA transcripts has also been observed to increase in AD models, possibly due to heterochromatin decondensation mediated by pathological tau hyperphosphorylation (Sato, Takayama and Inoue, 2023).

However, in both western blot analysis and RNA-sequencing data, we were unable to observe any significant changes in the expression of the PIWI proteins PIWIL1, 2, and 4 at both the RNA and protein levels (**Supplementary Figure 2**). This lack of change suggests that the PIWI-piRNA pathway may not be the primary mechanism of TE regulation in this model, or it may indicate that the pathway's activity is regulated post-transcriptionally or post-translationally in a manner not detectable by these methods.

Small RNA sequencing to observe the changes in piRNA populations, including looking for piRNA cluster activity, or increase in piRNA transcripts. By comparing the

doi:10.6342/NTU202402516

abundance of piRNA transcripts between TAOK1 overexpression and control, we may identify the presence of increased PIWI-piRNA pathway activity through PTGS.

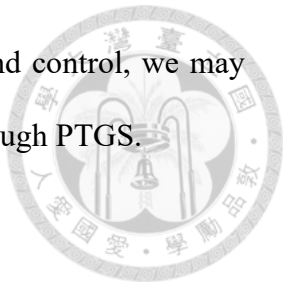

doi:10.6342/NTU202402516

5. Future Work & Perspectives

5.1. Pro-Inflammatory Consequences of TAOK1 Overexpression

5.1.1. TAOK1-induced TE De-repression may promote inflammation through Interferon responses via the cGAS-STING pathway

The increase in TE transcripts observed in TAOK1 overexpressing SH-SY5Y cells has other implications for inflammation, through the accumulation of cytosolic DNA. Amongst the various pathological effects of TE de-repression is the generation of nucleic acids through retrotranposition. Class I TEs, also known as retrotransposons, are known for their able to undergo reverse transcription to convert their RNA transcripts into DNA om the cytoplasm and integrate themselves back into the organism genome (Bourque, et al. 2018). When silenced retrotransposons become de-repressed, such as in the case of pathological tau hyperphosphorylation, their activity increases, and inevitably results in the accumulation of cytosolic DNA in the cytoplasm (Miller, et al. 2021). These transcripts may be misidentified by antiviral pathways due to their structural similarities to viral nucleic acids and activate innate immune response pathways. Over the years, various studies have implicated pathological retrotransposon activation to be capable of activating innate immune response pathways through increased cytosolic nucleic acid sensing (Gazquez-Gutierrez, et al. 2021; Russ & Iordanskiy, 2023;). Interestingly, this study had identified several retrotransposon families, including HERVs, LINE-1 and Alu TEs to be upregulated in TAOK1 overexpressing SH-SY5Y regardless of differentiation status. Hence, we wished to explore the possibility of aberrant TE de-repression driving inflammation through antiviral defences in this cell model.

The IFN-I response is amongst the best activated innate immune responses from increased sensing of cytosolic nucleic acids. One of the better characterised dsDNA

doi:10.6342/NTU202402516

sensors, is the cyclic GMP-AMP synthase (cGAS). cGAS-STING pathway activation by LINE-1, HERV and Alu have been observed to trigger IFN-I response and drive inflammation in various cell types (Li, et al. 2022; Li, et al. 2023; Mathavarajah & Dellaire, 2024). Additionally, the cGAS-STING pathway has been increasingly implicated in inflammation to promote neurodegeneration in several aging-associated diseases (Paul, Snyder & Bohr, 2021; Gulen, et al. 2023). To explore this possibility, we next analysed the expression of STING in TAOK1 overexpressing cells. Increased mRNA expression of STING was discovered through RT-qPCR, suggesting the potential upregulation of the cGAS-STING pathway activity (**Figure 18**). The activation of the cGAS-STING pathway is known to trigger the production of IFN-Is and other pro-inflammatory cytokines, initiating an inflammatory response that can exacerbate neuronal damage. Thus, we proceeded to observe the downstream effectors of the cGAS-STING pathway affected by IFN-I activity.

Through RNA-seq analysis, we have identified differentially expressed genes that are known to be interferon-stimulated genes (ISGs). These include IFIT1 and *IFI6*. In differentiating cells overexpressing TAOK1, *IFIT1* and *IFI6* were discovered to be downregulated (**Figure 19B**). On the other hand, *IFIT1* was found to be upregulated and *IFI6* downregulated in the undifferentiated population overexpressing TAOK1 (**Figure 19A**). The gene encoding TBK1, which is a target of STING, was found to be upregulated in both undifferentiated and differentiating SH-SY5Y overexpressing TAOK1.

Interferon-induced protein with tetratricopeptide repeats 1 (IFIT6) is a well-known ISG that are induced by the IFN-Is IFN-α and IFN-β. They can inhibit viral replication by recognising viral-like mRNA patterns and binding to these mRNA, and by binding to eukaryotic translation initiation factors (Diamond & Farzan, 2013; Franco, Chattopadhyay & Pan, 2023). In other studies, upregulated IFITs have also been identified

doi:10.6342/NTU202402516

to coincide with increased TE activity (Kuriyama, et al. 2021). The upregulation of *IFIT1* could indicate an anti-viral response in the cell due to TE de-repression causing increased cytosolic nucleic acids. Meanwhile, Interferon Alpha-Inducible protein 6 (IFI6) is another ISG that can be induced by IFN-α and has been observed in studies to coincide with cGAS-STING pathway activation (Sajid, et al. 2021; Frittoli, et al. 2022). IFI6 is a protein localised to the mitochondria that is upregulated during viral infections to serve an anti-apoptotic function through Bcl-2/Bax regulation (Qi, et al. 2015). This can be a protective mechanism to allow other immune responses to act against the infection. In other studies, IFI6 upregulation has been found to accompany TE dysregulation in lung cells even in the absence of viral infections, (Rostami & Bradic, 2021). However, the lack of *IFI6* upregulation and inconsistent upregulation of *IFIT6* suggests that it is unlikely that there is a sustainable IFN-I response via this pathway.

On the other hand, TANK binding kinase 1 (TBK1) is a key player of the IFN-I pathway and is activated by STING to phosphorylate downstream interferon regulatory factors (IRF) to activate them (Yum, et al. 2021). Heightened TBK1 activity can be an indicator of IFN-I response through IRF3 and NF-κB pathways to mediate immune responses within the cell. Together with the lack of consistent ISG upregulation, this may be indicative of early IFN-I pathway activation.

In future experiments, we may also quantify the levels of various IFN-Is such as IFN-α and IFN-βs, and other pro-inflammatory cytokines in the culture media of TAOK1 overexpressing cells. It is also crucial to assess the phosphorylation statuses of TBK1 targets like IRF3 and IRF7 through western blot analysis or immunocytochemistry can provide further evidence of cGAS-STING pathway activation. This can be achieved through ELISA or multiplex cytokine assays. Together, they can help determine the pro-inflammatory effects of TAOK1 mediated TE-derepression.

doi:10.6342/NTU202402516

Additionally, to investigate the activation of not only cGAS-STING, but other nucleic acid sensor pathways like AIM2, from increased cytosolic nucleic acids due to TE activity, we may also measure their levels in the cytoplasm. This may be done through immunostaining using commercially available antibodies against dsDNA.

Overall, in this study, our findings reveal an increase in TE transcripts from HERV, LINE-1 and Alu families, in both undifferentiated and differentiating cells overexpressing TAOK1. This upregulation suggests a disruption in the cellular mechanisms responsible for maintaining TE silencing. The increased TE activity observed may be a consequence of heightened cellular stress, including oxidative stress and ER stress, both of which are known to activate TEs. This is supported by the upregulation of ROS and the potential involvement of the cGAS-STING pathway, which could link TE activity to inflammatory responses. Future experiments should focus on understanding the exact mechanisms by which TAOK1 overexpression leads to TE activation. Understanding these mechanisms will provide deeper insights into the cellular responses to TAOK1 overexpression and its implications in neurodegenerative diseases

5.1.2. Limited Effects on NLRP3 Inflammasome Signalling

The canonical inflammasome pathway is the NLRP3 inflammasome signalling pathway. The NLRP3 inflammasome is known to be activated by the TE family Alu, and by IFN-I signalling via STAT1 (Kopitar-Jerala 2017; Lee, et al. 2022). In our experiments, we have observed Alu to be amongst the upregulated TEs by TAOK1 overexpression in both undifferentiated and differentiating cells. Furthermore, ROS is also known to be able to promote NLRP3 inflammasome activation. With these observations, we hypothesised if TAOK1 overexpression may promote inflammation through the NLRP3 inflammasome signalling pathway.

doi:10.6342/NTU202402516

To answer these, we looked into the expression of various key NLRP3 inflammasome pathway proteins, and the secretion of pro-inflammatory cytokine IL-1B. However, western blot analysis did not observe any significant increase in pro-caspase-1, NLRP3 or IL-1β protein levels (**Supplementary Figure 3**). Quantification of IL-1β secreted into the culture medium was also unable to reveal any meaningful differences in TAOK1 overexpressing cells.

While our results did not show significant activation of the NLRP3 inflammasome pathway, it is important to consider the potential for TAOK1 to mediate inflammasome priming. Inflammasome activation requires both priming and activation signals. Although no significant increase in pro-caspase-1, NLRP3, or IL-1β protein levels was observed, the increase in ROS and TE activity suggests a potential for priming. Priming involves the upregulation of inflammasome components without their immediate activation, regulating the NLRP3 inflammasome activation (Kelley, et al. 2019). This suggests that TAOK1 may sensitize neurons to inflammatory stimuli, potentially contributing to a heightened state of neuroinflammatory readiness that could exacerbate neurodegenerative processes under certain conditions.

As with other pathways, the activity of the NLRP3 inflammasome is not just limited to activation by triggering signals, but also subject to regulation from associated pathways. One of which, is through Nrf2 signalling. Earlier in this study, we have found a significant upregulation of the gene encoding Nrf2, *NFE2L2* in TAOK1-overexpressing cells. As discussed earlier, Nrf2 is a major antioxidant regulator that can mediate anti-inflammatory responses during oxidating stress. During oxidative stress, Nrf2 is able to prevent the expression of various pro-inflammatory cytokines to modulate inflammation (Ahmed, et al. 2017). Amongst which is IL-1β, one of the characteristic cytokines that is upregulated as part of the NLRP3 inflammasome pathway. Additionally, in macrophages,

doi:10.6342/NTU202402516

Nrf2 can further inhibit ROS activated NLRP3 inflammasome activity by inducing NQO1 expression to inhibit the cleavage of pro-caspase 1 and IL-1β transcription (Liu, et al. 2017). However, analysis of *NQO1* expression from RNA-seq data showed a non-significant and mild increase in undifferentiated cells and decrease in differentiating cells even with *NFE2L2* upregulation (**Supplementary Figure 4**). Hence, it may be necessary to conduct more experiments with increased samples, and through other methods such as RT-qPCR and western blot analysis to verify if Nrf2-mediated NQO1 activity may inhibit NLRP3 inflammasome activity.

Additionally, it may also be relevant to investigate non-canonical inflammasome signalling pathways such as the caspase-4 inflammasome signalling pathway. Localised to the ER, multiple studies have also suggested that caspase-4 may be activated by through UPR with chronic ER stress (Hitomi, et al. 2004). Scientists using the SH-SY5Y cell line has demonstrated that under ER stress, caspase-4 can become activated and contribute towards neuronal apoptosis through caspase-9 (Yamamuro, et al. 2010). This is in alignment with the hypothesis that TAOK1-mediated tau hyperphosphorylation may increase ER stress to cause neurotoxicity. Caspase-4 is also known to be involved in non-canonical inflammasome signalling pathway, most commonly in response to microbial lipopolysaccharides (LPS) in the cytoplasm (Martinon and Tschopp 2007; Al Mamun, et al. 2021). In the non-canonical inflammasome pathway, caspase-4 activation recognised to promote pyroptosis through gasdermin D (GSDMD) cleavage, to generate the pore-forming complex independently of NLRP3 activity (Schmid-Burgk, et al. 2015). Taken the known caspase-4 pathways, it is plausible that ER stress mediated caspase-4 activation may be promoting pyroptosis instead of apoptosis. And this ER stress could be mediated by TAOK1-induced tau phosphorylation. However, more experiments are necessary to verify the validity of a non-canonical inflammasome signalling pathway.

doi:10.6342/NTU202402516

Additionally, identification of GSDMD cleavage, through western blot analysis, and ASC speck formation through flow cytometry and immunofluorescence microscopy will also reveal more information on this pathway.

doi:10.6342/NTU202402516

5.2. Dose-Dependent effects of TAOK1-Associated Neurotoxicity

The discovery of TAOK1 as a protein biomarker emerged due to its accumulation in the plasma extracellular vesicles of PDD and AD-MCI patients. This led us to consider the possibility that TAOK1 levels correlate with the degree of neurotoxicity in the neuronal population. In this study, we utilised several TAOK1-inducible single clones to investigate the neurotoxic effects on our cell model. As outlined in the materials and methods section, the generation of these stable, TAOK1-inducible single clones, and their expression of *TAOK1*, depends on the insertion of the TAOK1-containing construct into their genome. Insertion sites near regulatory regions or within highly active genomic loci may lead to higher expression levels of *TAOK1*, while insertion in less active regions may result in lower expression. Secondly, clonal differences in the cellular machinery and intrinsic genetic variability can also contribute to differential gene expression. These inherent differences between clones can affect how each cell line responds to TAOK1 induction, leading to variability in downstream effects. As such, the effects of TAOK1 expression can vary between different single clones.

Using selected single clones increases replicability between batches of cell cultures and allows us to pool them together to avoid clonal biases while maintaining a high degree of control. Whoever, another advantage is the ability to study the potential dose-dependent correlation between TAOK1 and neurotoxic effects in a neuronal cell model.

In earlier results, we observed a difference in the degree of cell death through confluency changes, over the same period of TAOK1 induction in both undifferentiated and differentiating cells (**Figure 5A**). Similarly, we observed differences in relative gene expression for each single clone's matched non-induction controls, such as in genes like

doi:10.6342/NTU202402516

CASP3 (**Figure 6D**). This was especially noticiable in the relative gene expression of TE transcripts, where undifferentiated clone 11 showed a decrease in relative gene expression compared to other clones like 18, which showed an increase (**Figure 17B, E**). To better understand this phenomenon, we conducted RNA sequencing analysis on individual undifferentiated single clones using EdgeR to observe differential gene expression visualised through log 2-fold values of selected genes in the pathways observed throughout this study (**Supplementary Figure 5**). This analysis differed from the previous analyses done for the undifferentiated cells, which used RNA sequencing raw values of each individual clone as biological replicates during analysis, employing DeSeq2 to examine differential gene expression.

We identified observable variability in the differential gene expression between individual undifferentiated single clones 11, 17, and 18. In undifferentiated clone 11, 16 out of 40 of the differentially expressed genes selected for analysis showed the greatest degree of variation among the three clones. Conversely, in clone 18, exhibited the smallest degree of variation in 20 of the 40 genes. This prompted us to examine the variability of TAOK1 expression from the same set of RNA sequencing results (**Supplementary Figure 5H**).

Interestingly, we found that the highest upregulation of TAOK1, compared to its control, was in single clone 18, followed by clones 17 and 11 (**Supplementary Figure 5H**). Despite this, clone 11 exhibits the most significant changes in the expression of genes in various pathways, suggesting that even moderate increases in TAOK1 can profoundly affect cellular functions. Based on these results, it is unlikely that there is a direct inverse relationship between TAOK1 expression and gene expression changes in the selected pathways, where increased *TAOK1* expression would equate to a greater degree of differential gene expression. However, the fact that clone 18 has the highest

doi:10.6342/NTU202402516

TAOK1 expression but shows less variability in gene expression changes suggests that high levels of TAOK1 might lead to cellular mechanisms that dampen the response to avoid excessive stress.

We can conclude that there are inherent differences between different single clones, which may be associated with differences in *TAOK1* expression. However, more experiments may be conducted to analyse the relation between TAOK1 dosage and the progression of neurotoxicity in neurons with higher statistical relevance.

doi:10.6342/NTU202402516

5.3. Repressing TAOK1 Expression to Suppress Neurodegeneration

In our study, we have demonstrated that TAOK1 overexpression drives neurotoxicity and neurite loss, suggesting that TAOK1 could be a viable target for therapeutic intervention in neurodegenerative diseases, aimed at mitigating neuronal damage and promoting neuronal health. However, reckless inhibition of TAOK1 expression is not a solution for controlling neurodegenerative processes driven by its overexpression. TAOK1 plays a critical role in various cellular functions, and its normal expression is essential for maintaining cellular homeostasis. Deficits in TAOK1 expression have been linked to neurodevelopmental disorders, indicating that an optimal level of TAOK1 is crucial for regular cell activity and neuronal development (Byeon and Yadav, 2024). To develop effective therapies, it is important to consider the balance required in regulating TAOK1 expression. Complete inhibition of TAOK1 such as genetic ablation could lead to adverse effects on neurodevelopment and other cellular processes, while partial repression like pharmaceutical treatment might be sufficient to mitigate the neurotoxic effects observed in neurodegenerative conditions without disrupting its essential functions.

As a starting point, future experiments may be conducted using our cell model, but with dosage treatment of selective TAOK kinase inhibitors such as compound-43 (CP-43, CAS No. 850467-66-2), on TAOK1 overexpressing cells (Giacomini, et al. 2018). A rescue of the morphological or molecular changes closer to the control levels could be indicative of a possibility of using TAOK1 inhibitors as a form of treatment in early neurodegeneration.

doi:10.6342/NTU202402516

6. Conclusion

Neurodegeneration involves numerous pathological disruptions in regular cellular pathways. A single dysregulated gene can trigger a cascade of toxic effects within a cell, which, when accumulated, can lead to disease. In this study, we observed that TAOK1 overexpression promotes increased neuronal death through apoptosis. This effect is potentially mediated by various interrelated pathways, such as MAPK signalling, which involves TAOK1 and can upregulate transcription factors associated with cell survival, inflammation, and stress responses. The inability to maintain neurites in differentiating cells following TAOK1 overexpression may be due to TAOK1-dependent tau phosphorylation, which causes microtubule destabilisation. Additionally, increased cellular toxicity may result from potential tau aggregation, contributing to mitochondrial dysfunction and ER stress. This is visualised through the increase in ROS levels, downregulation of mitochondrial protein-coding genes, and upregulation of ER stress genes following TAOK1 overexpression. TAOK1 overexpression also led to the increase in TE transcripts, which may not only cause DNA damage and genetic instability, but also carries the potential to promote inflammation through cGAS-STING pathway activation. Overall, TAOK1 overexpression can promote neuronal and functional loss through various neurotoxic pathways by increasing tau phosphorylation, promoting neurite loss, inducing cellular stress, and causing TE de-repression. These individual pathways may also be regulated by TAOK1 through MAPK signalling (**Figure 20**).

While many plausible pathways associated with neurotoxicity and inflammation have been uncovered, these findings remain preliminary. Further studies are necessary to establish their significance. Over time, these findings set the foundation for understanding the precise mechanisms by which TAOK1 modulates neurotoxic pathways and assist in the development of targeted interventions for neurodegenerative diseases.

doi:10.6342/NTU202402516

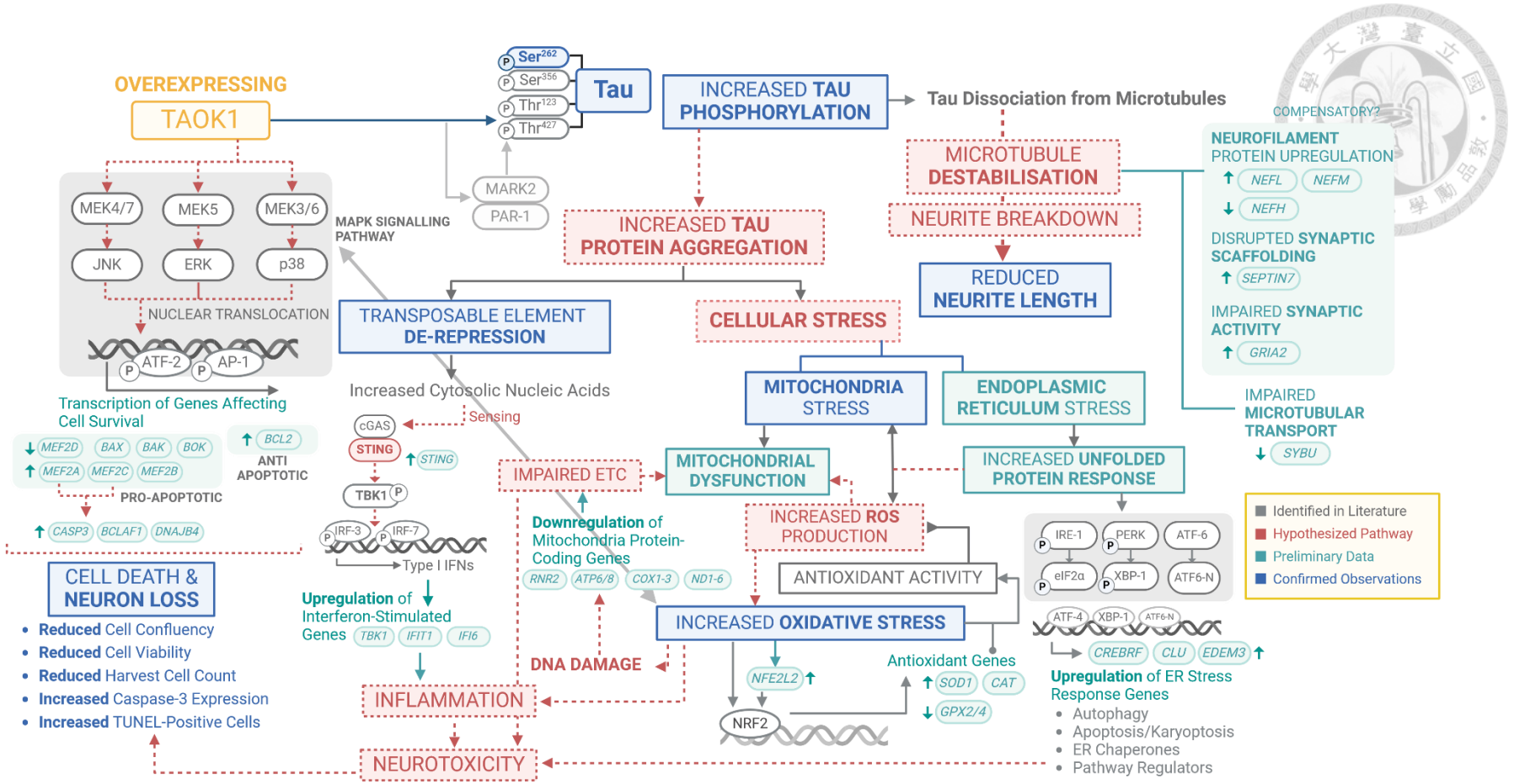

Figure 20. Schematic diagram of neurotoxic mechanisms mediated by TAOK1 Overexpression. TAOK1 overexpression is able to affect MAPK signalling pathways, tau phosphorylation to destabilise microtubules and cause neurite loss, TE de-repression, oxidative and ER stress. These interconnected pathways highlight how dysregulated TAOK1 can drive neurotoxicity and neurodegeneration. (Created with BioRender.com)

doi:10.6342/NTU202402516

7. References

1. Abramov, A. Y., Potapova, E. V., Dremin, V. V., & Dunaev, A. V. (2020). Interaction of Oxidative Stress and Misfolded Proteins in the Mechanism of Neurodegeneration. *Life (Basel, Switzerland)*, *10*(7), 101. https://doi.org/10.3390/life10070101

2. Ahmed, S. M., Luo, L., Namani, A., Wang, X. J., & Tang, X. (2017). Nrf2 signaling pathway: Pivotal roles in inflammation. *Biochimica et biophysica acta. Molecular basis of disease*, *1863*(2), 585–597. https://doi.org/10.1016/j.bbadis.2016.11.005

3. Ajoolabady, A., Lindholm, D., Ren, J., & Pratico, D. (2022). ER stress and UPR in Alzheimer's disease: mechanisms, pathogenesis, treatments. *Cell death & disease*, *13*(8), 706. https://doi.org/10.1038/s41419-022-05153-5

4. Akhtar, M. W., Kim, M. S., Adachi, M., Morris, M. J., Qi, X., Richardson, J. A., Bassel-Duby, R., Olson, E. N., Kavalali, E. T., & Monteggia, L. M. (2012). In vivo analysis of MEF2 transcription factors in synapse regulation and neuronal survival. *PloS one*, *7*(4), e34863. https://doi.org/10.1371/journal.pone.0034863

5. Al Mamun, A., Ara Mimi, A., Wu, Y., Zaeem, M., Abdul Aziz, M., Aktar Suchi, S., Alyafeai, E., Munir, F., & Xiao, J. (2021). Pyroptosis in diabetic nephropathy. *Clinica chimica acta; international journal of clinical chemistry*, *523*, 131–143. https://doi.org/10.1016/j.cca.2021.09.003

6. American Psychiatric Association. (2022). Diagnostic and statistical manual of mental disorders (5th ed., text rev.) https://doi.org/10.1176/appi.books.9780890425787

doi:10.6342/NTU202402516

7. Baas, P. W., Rao, A. N., Matamoros, A. J., & Leo, L. (2016). Stability properties of neuronal microtubules. *Cytoskeleton (Hoboken, N.J.)*, *73*(9), 442–460. https://doi.org/10.1002/cm.21286

8. Banks, W. A., & Rhea, E. M. (2021). The Blood-Brain Barrier, Oxidative Stress, and Insulin Resistance. *Antioxidants (Basel, Switzerland)*, *10*(11), 1695. https://doi.org/10.3390/antiox10111695

9. Barbier, P., Zejneli, O., Martinho, M., Lasorsa, A., Belle, V., Smet-Nocca, C., Tsvetkov, P. O., Devred, F., & Landrieu, I. (2019). Role of Tau as a Microtubule-Associated Protein: Structural and Functional Aspects. *Frontiers in aging neuroscience*, *11*, 204. https://doi.org/10.3389/fnagi.2019.00204

10. Beeman, N., Sapre, T., Ong, S. E., & Yadav, S. (2023). Neurodevelopmental disorder-associated mutations in TAOK1 reveal its function as a plasma membrane remodeling kinase. *Science signaling*, *16*(766), eadd3269. https://doi.org/10.1126/scisignal.add3269

11. Beeman, N., Sapre, T., Ong, S. E., & Yadav, S. (2023). Neurodevelopmental disorder-associated mutations in TAOK1 reveal its function as a plasma membrane remodeling kinase. *Science signaling*, *16*(766), eadd3269. https://doi.org/10.1126/scisignal.add3269

12. Biedler, J. L., Roffler-Tarlov, S., Schachner, M., & Freedman, L. S. (1978). Multiple neurotransmitter synthesis by human neuroblastoma cell lines and clones. *Cancer research*, *38*(11 Pt 1), 3751–3757.

13. Biernat, J., Wu, Y. Z., Timm, T., Zheng-Fischhöfer, Q., Mandelkow, E., Meijer, L., & Mandelkow, E. M. (2002). Protein kinase MARK/PAR-1 is required for neurite

doi:10.6342/NTU202402516

outgrowth and establishment of neuronal polarity. *Molecular biology of the cell*, *13*(11), 4013–4028. https://doi.org/10.1091/mbc.02-03-0046

14. Binarová, P., & Tuszynski, J. (2019). Tubulin: Structure, Functions and Roles in Disease. *Cells*, *8*(10), 1294. https://doi.org/10.3390/cells8101294

15. Bivona, G., Iemmolo, M., Piccoli, T., Agnello, L., Lo Sasso, B., Ciaccio, M., & Ghersi, G. (2022). High Cerebrospinal Fluid CX3CL1 Levels in Alzheimer's Disease Patients but Not in Non-Alzheimer's Disease Dementia. *Journal of clinical medicine*, *11*(19), 5498. https://doi.org/10.3390/jcm11195498

16. Bourque, G., Burns, K. H., Gehring, M., Gorbunova, V., Seluanov, A., Hammell, M., Imbeault, M., Izsvák, Z., Levin, H. L., Macfarlan, T. S., Mager, D. L., & Feschotte, C. (2018). Ten things you should know about transposable elements. *Genome biology*, *19*(1), 199. https://doi.org/10.1186/s13059-018-1577-z

17. Bravo, J. I., Nozownik, S., Danthi, P. S., & Benayoun, B. A. (2020). Transposable elements, circular RNAs and mitochondrial transcription in age-related genomic regulation. *Development (Cambridge, England)*, *147*(11), dev175786. https://doi.org/10.1242/dev.175786

18. Bright, F., Chan, G., van Hummel, A., Ittner, L. M., & Ke, Y. D. (2021). TDP-43 and Inflammation: Implications for Amyotrophic Lateral Sclerosis and Frontotemporal Dementia. *International journal of molecular sciences*, *22*(15), 7781. https://doi.org/10.3390/ijms22157781

19. Byeon, S., & Yadav, S. (2024). Pleiotropic functions of TAO kinases and their dysregulation in neurological disorders. *Science signaling*, *17*(817), eadg0876. https://doi.org/10.1126/scisignal.adg0876

doi:10.6342/NTU202402516

20. Byeon, S., Werner, B., Falter, R., Davidsen, K., Snyder, C., Ong, S. E., & Yadav, S. (2022). Proteomic Identification of Phosphorylation-Dependent Septin 7 Interactors that Drive Dendritic Spine Formation. *Frontiers in cell and developmental biology*, *10*, 836746. https://doi.org/10.3389/fcell.2022.836746

21. Callahan, L. M., & Coleman, P. D. (1995). Neurons bearing neurofibrillary tangles are responsible for selected synaptic deficits in Alzheimer's disease. *Neurobiology of aging*, *16*(3), 311–314. https://doi.org/10.1016/0197-4580(95)00035-d

22. Canovas, B., & Nebreda, A. R. (2021). Diversity and versatility of p38 kinase signalling in health and disease. *Nature reviews. Molecular cell biology*, *22*(5), 346–366. https://doi.org/10.1038/s41580-020-00322-w

23. Cao, S. S., & Kaufman, R. J. (2014). Endoplasmic reticulum stress and oxidative stress in cell fate decision and human disease. *Antioxidants & redox signaling*, *21*(3), 396–413. https://doi.org/10.1089/ars.2014.5851

24. Caušević, M., Farooq, U., Lovestone, S., & Killick, R. (2010). β-Amyloid precursor protein and tau protein levels are differently regulated in human cerebellum compared to brain regions vulnerable to Alzheimer's type neurodegeneration. *Neuroscience letters*, *485*(3), 162–166. https://doi.org/10.1016/j.neulet.2010.08.088

25. Cerella, C., Diederich, M., & Ghibelli, L. (2010). The dual role of calcium as messenger and stressor in cell damage, death, and survival. *International journal of cell biology*, *2010*, 546163. https://doi.org/10.1155/2010/546163

26. Chaphalkar, R. M., Stankowska, D. L., He, S., Kodati, B., Phillips, N., Prah, J., Yang, S., & Krishnamoorthy, R. R. (2020). Endothelin-1 Mediated Decrease in Mitochondrial Gene Expression and Bioenergetics Contribute to Neurodegeneration

doi:10.6342/NTU202402516

of Retinal Ganglion Cells. *Scientific reports*, *10*(1), 3571. https://doi.org/10.1038/s41598-020-60558-6

27. Chesnokova, E., Beletskiy, A., & Kolosov, P. (2022). The Role of Transposable Elements of the Human Genome in Neuronal Function and Pathology. *International journal of molecular sciences*, *23*(10), 5847. https://doi.org/10.3390/ijms23105847
28. Collier, M. P., & Benesch, J. L. P. (2020). Small heat-shock proteins and their role in mechanical stress. *Cell stress & chaperones*, *25*(4), 601–613. https://doi.org/10.1007/s12192-020-01095-z
29. Colnaghi, L., Rondelli, D., Muzi-Falconi, M., & Sertic, S. (2020). Tau and DNA Damage in Neurodegeneration. *Brain sciences*, *10*(12), 946. https://doi.org/10.3390/brainsci10120946
30. Combs, B., Mueller, R. L., Morfini, G., Brady, S. T., & Kanaan, N. M. (2019). Tau and Axonal Transport Misregulation in Tauopathies. *Advances in experimental medicine and biology*, *1184*, 81–95. https://doi.org/10.1007/978-981-32-9358-8_7
31. Conde, C., & Cáceres, A. (2009). Microtubule assembly, organization and dynamics in axons and dendrites. *Nature reviews. Neuroscience*, *10*(5), 319–332. https://doi.org/10.1038/nrn2631
32. Corder, E. H., Saunders, A. M., Strittmatter, W. J., Schmechel, D. E., Gaskell, P. C., Small, G. W., Roses, A. D., Haines, J. L., & Pericak-Vance, M. A. (1993). Gene dose of apolipoprotein E type 4 allele and the risk of Alzheimer's disease in late onset families. *Science (New York, N.Y.)*, *261*(5123), 921–923. https://doi.org/10.1126/science.8346443
33. da Costa, L. S., Outlioua, A., Anginot, A., Akarid, K., & Arnoult, D. (2019). RNA viruses promote activation of the NLRP3 inflammasome through cytopathogenic

doi:10.6342/NTU202402516

effect-induced potassium efflux. *Cell death & disease*, *10*(5), 346. https://doi.org/10.1038/s41419-019-1579-0

34. Damier, P., Hirsch, E. C., Agid, Y., & Graybiel, A. M. (1999). The substantia nigra of the human brain. II. Patterns of loss of dopamine-containing neurons in Parkinson's disease. *Brain: a journal of neurology*, *122 (Pt 8)*, 1437–1448. https://doi.org/10.1093/brain/122.8.1437

35. De Marinis, E., Fiocchetti, M., Acconcia, F., Ascenzi, P., & Marino, M. (2013). Neuroglobin upregulation induced by 17β-estradiol sequesters cytocrome c in the mitochondria preventing H2O2-induced apoptosis of neuroblastoma cells. *Cell death & disease*, *4*(2), e508. https://doi.org/10.1038/cddis.2013.30

36. de Oliveira, D. S., Rosa, M. T., Vieira, C., & Loreto, E. L. S. (2021). Oxidative and radiation stress induces transposable element transcription in Drosophila melanogaster. *Journal of evolutionary biology*, *34*(4), 628–638. https://doi.org/10.1111/jeb.13762

37. Diamond, M. S., & Farzan, M. (2013). The broad-spectrum antiviral functions of IFIT and IFITM proteins. *Nature reviews. Immunology*, *13*(1), 46–57. https://doi.org/10.1038/nri3344

38. DiSabato, D. J., Quan, N., & Godbout, J. P. (2016). Neuroinflammation: the devil is in the details. *Journal of neurochemistry*, *139 Suppl 2*(Suppl 2), 136–153. https://doi.org/10.1111/jnc.13607

39. Domizio, J. D., Gulen, M. F., Saidoune, F., Thacker, V. V., Yatim, A., Sharma, K., Nass, T., Guenova, E., Schaller, M., Conrad, C., Goepfert, C., de Leval, L., Garnier, C. V., Berezowska, S., Dubois, A., Gilliet, M., & Ablasser, A. (2022). The cGAS-

doi:10.6342/NTU202402516

STING pathway drives type I IFN immunopathology in COVID-19. *Nature*, *603*(7899), 145–151. https://doi.org/10.1038/s41586-022-04421-w

40. Dong, F., Zhang, X., Wold, L. E., Ren, Q., Zhang, Z., & Ren, J. (2005). Endothelin-1 enhances oxidative stress, cell proliferation and reduces apoptosis in human umbilical vein endothelial cells: role of ETB receptor, NADPH oxidase and caveolin-1. *British journal of pharmacology*, *145*(3), 323–333. https://doi.org/10.1038/sj.bjp.0706193

41. Dong, H. K., Gim, J. A., Yeo, S. H., & Kim, H. S. (2017). Integrated late onset Alzheimer's disease (LOAD) susceptibility genes: Cholesterol metabolism and trafficking perspectives. *Gene*, *597*, 10–16. https://doi.org/10.1016/j.gene.2016.10.022

42. Duc Nguyen, H., Hee Jo, W., Hong Minh Hoang, N., & Kim, M. S. (2022). Anti-inflammatory effects of B vitamins protect against tau hyperphosphorylation and cognitive impairment induced by 1,2 diacetyl benzene: An in vitro and in silico study. *International immunopharmacology*, *108*, 108736. https://doi.org/10.1016/j.intimp.2022.108736

43. Dulovic-Mahlow, M., Trinh, J., Kandaswamy, K. K., Braathen, G. J., Di Donato, N., Rahikkala, E., Beblo, S., Werber, M., Krajka, V., Busk, Ø. L., Baumann, H., Al-Sannaa, N. A., Hinrichs, F., Affan, R., Navot, N., Al Balwi, M. A., Oprea, G., Holla, Ø. L., Weiss, M. E. R., Jamra, R. A., … Lohmann, K. (2019). De Novo Variants in TAOK1 Cause Neurodevelopmental Disorders. *American journal of human genetics*, *105*(1), 213–220. https://doi.org/10.1016/j.ajhg.2019.05.005

doi:10.6342/NTU202402516

44. Duly, A. M. P., Kao, F. C. L., Teo, W. S., & Kavallaris, M. (2022). βIII-Tubulin Gene Regulation in Health and Disease. *Frontiers in cell and developmental biology*, *10*, 851542. https://doi.org/10.3389/fcell.2022.851542

45. Eguchi, Y., Shimizu, S., & Tsujimoto, Y. (1997). Intracellular ATP levels determine cell death fate by apoptosis or necrosis. *Cancer research*, *57*(10), 1835–1840.

46. Encinas, M., Iglesias, M., Liu, Y., Wang, H., Muhaisen, A., Ceña, V., Gallego, C., & Comella, J. X. (2000). Sequential treatment of SH-SY5Y cells with retinoic acid and brain-derived neurotrophic factor gives rise to fully differentiated, neurotrophic factor-dependent, human neuron-like cells. *Journal of neurochemistry*, *75*(3), 991–1003. https://doi.org/10.1046/j.1471-4159.2000.0750991.x

47. Fan Zhai, Xinyi Ma, Liying Yan, Jie Qiao. (2023). Chapter 6 - The molecular genetics of oogenesis. *Human Reproductive and Prenatal Genetics (Second Edition), Academic Press.* 145-163. ISBN 9780323913805. https://doi.org/10.1016/B978-0-323-91380-5.00011-3.

48. Fang, C. Y., Lai, T. C., Hsiao, M., & Chang, Y. C. (2020). The Diverse Roles of TAO Kinases in Health and Diseases. *International journal of molecular sciences*, *21*(20), 7463. https://doi.org/10.3390/ijms21207463

49. Fjell, A. M., McEvoy, L., Holland, D., Dale, A. M., Walhovd, K. B., & Alzheimer's Disease Neuroimaging Initiative (2014). What is normal in normal aging? Effects of aging, amyloid and Alzheimer's disease on the cerebral cortex and the hippocampus. *Progress in neurobiology*, *117*, 20–40. https://doi.org/10.1016/j.pneurobio.2014.02.004

50. Foster, E. M., Dangla-Valls, A., Lovestone, S., Ribe, E. M., & Buckley, N. J. (2019). Clusterin in Alzheimer's Disease: Mechanisms, Genetics, and Lessons From Other

doi:10.6342/NTU202402516

Pathologies. *Frontiers in neuroscience*, *13*, 164. https://doi.org/10.3389/fnins.2019.00164

51. Fricker, M., Tolkovsky, A. M., Borutaite, V., Coleman, M., & Brown, G. C. (2018). Neuronal Cell Death. *Physiological reviews*, *98*(2), 813–880. https://doi.org/10.1152/physrev.00011.2017

52. Frittoli, E., Palamidessi, A., Iannelli, F., Zanardi, F., Villa, S., Barzaghi, L., Abdo, H., Cancila, V., Beznoussenko, G. V., Della Chiara, G., Pagani, M., Malinverno, C., Bhattacharya, D., Pisati, F., Yu, W., Galimberti, V., Bonizzi, G., Martini, E., Mironov, A. A., Gioia, U., … Scita, G. (2023). Tissue fluidification promotes a cGAS-STING cytosolic DNA response in invasive breast cancer. *Nature materials*, *22*(5), 644–655. https://doi.org/10.1038/s41563-022-01431-x

53. Garg, R., Koo, C. Y., Infante, E., Giacomini, C., Ridley, A. J., & Morris, J. D. H. (2020). Rnd3 interacts with TAO kinases and contributes to mitotic cell rounding and spindle positioning. *Journal of cell science*, *133*(6), jcs235895. https://doi.org/10.1242/jcs.235895

54. Gazquez-Gutierrez, A., Witteveldt, J., R Heras, S., & Macias, S. (2021). Sensing of transposable elements by the antiviral innate immune system. *RNA (New York, N.Y.)*, *27*(7), 735–752. Advance online publication. https://doi.org/10.1261/rna.078721.121

55. GBD 2021 Nervous System Disorders Collaborators (2024). Global, regional, and national burden of disorders affecting the nervous system, 1990-2021: a systematic analysis for the Global Burden of Disease Study 2021. *The Lancet. Neurology*, *23*(4), 344–381. https://doi.org/10.1016/S1474-4422(24)00038-3

56. GBD 2021 Forecasting Collaborators (2024). Burden of disease scenarios for 204 countries and territories, 2022-2050: a forecasting analysis for the Global Burden of

doi:10.6342/NTU202402516

Disease Study 2021. *Lancet (London, England)*, *403*(10440), 2204–2256. https://doi.org/10.1016/S0140-6736(24)00685-8

57. Gcwensa, N. Z., Russell, D. L., Cowell, R. M., & Volpicelli-Daley, L. A. (2021). Molecular Mechanisms Underlying Synaptic and Axon Degeneration in Parkinson's Disease. *Frontiers in cellular neuroscience*, *15*, 626128. https://doi.org/10.3389/fncel.2021.626128

58. Giacomini, C., Koo, C. Y., Yankova, N., Tavares, I. A., Wray, S., Noble, W., Hanger, D. P., & Morris, J. D. H. (2018). A new TAO kinase inhibitor reduces tau phosphorylation at sites associated with neurodegeneration in human tauopathies. *Acta neuropathologica communications*, *6*(1), 37. https://doi.org/10.1186/s40478-018-0539-8

59. Giorgi, G., Marcantonio, P., & Del Re, B. (2011). LINE-1 retrotransposition in human neuroblastoma cells is affected by oxidative stress. *Cell and tissue research*, *346*(3), 383–391. https://doi.org/10.1007/s00441-011-1289-0

60. Gong, C. X., & Iqbal, K. (2008). Hyperphosphorylation of microtubule-associated protein tau: a promising therapeutic target for Alzheimer disease. *Current medicinal chemistry*, *15*(23), 2321–2328. https://doi.org/10.2174/092986708785909111

61. González, P., Alvarez, V., Menéndez, M., Lahoz, C. H., Martínez, C., Corao, A. I., Calatayud, M. T., Peña, J., García-Castro, M., & Coto, E. (2007). Myocyte enhancing factor-2A in Alzheimer's disease: genetic analysis and association with MEF2A-polymorphisms. *Neuroscience letters*, *411*(1), 47–51. https://doi.org/10.1016/j.neulet.2006.09.055

62. González, P., Alvarez, V., Menéndez, M., Lahoz, C. H., Martínez, C., Corao, A. I., Calatayud, M. T., Peña, J., García-Castro, M., & Coto, E. (2007). Myocyte enhancing

doi:10.6342/NTU202402516

factor-2A in Alzheimer's disease: genetic analysis and association with MEF2A-polymorphisms. *Neuroscience letters*, *411*(1), 47–51. https://doi.org/10.1016/j.neulet.2006.09.055

63. Gritsenko, A., Yu, S., Martin-Sanchez, F., Diaz-Del-Olmo, I., Nichols, E. M., Davis, D. M., Brough, D., & Lopez-Castejon, G. (2020). Priming Is Dispensable for NLRP3 Inflammasome Activation in Human Monocytes *In Vitro*. *Frontiers in immunology*, *11*, 565924. https://doi.org/10.3389/fimmu.2020.565924

64. Gulen, M. F., Samson, N., Keller, A., Schwabenland, M., Liu, C., Glück, S., Thacker, V. V., Favre, L., Mangeat, B., Kroese, L. J., Krimpenfort, P., Prinz, M., & Ablasser, A. (2023). cGAS-STING drives ageing-related inflammation and neurodegeneration. *Nature*, *620*(7973), 374–380. https://doi.org/10.1038/s41586-023-06373-1

65. Guo, C., Jeong, H. H., Hsieh, Y. C., Klein, H. U., Bennett, D. A., De Jager, P. L., Liu, Z., & Shulman, J. M. (2018). Tau Activates Transposable Elements in Alzheimer's Disease. *Cell reports*, *23*(10), 2874–2880. https://doi.org/10.1016/j.celrep.2018.05.004

66. Guo, C., Jeong, H. H., Hsieh, Y. C., Klein, H. U., Bennett, D. A., De Jager, P. L., Liu, Z., & Shulman, J. M. (2018). Tau Activates Transposable Elements in Alzheimer's Disease. *Cell reports*, *23*(10), 2874–2880. https://doi.org/10.1016/j.celrep.2018.05.004

67. Halcrow, P. W., Quansah, D. N. K., Kumar, N., Steiner, J. P., Nath, A., & Geiger, J. D. (2024). HERV-K (HML-2) Envelope Protein Induces Mitochondrial Depolarization and Neurotoxicity via Endolysosome Iron Dyshomeostasis. *The Journal of neuroscience: the official journal of the Society for Neuroscience*, *44*(14), e0826232024. https://doi.org/10.1523/JNEUROSCI.0826-23.2024

doi:10.6342/NTU202402516

68. Hammad, M., Raftari, M., Cesário, R., Salma, R., Godoy, P., Emami, S. N., & Haghdoost, S. (2023). Roles of Oxidative Stress and Nrf2 Signaling in Pathogenic and Non-Pathogenic Cells: A Possible General Mechanism of Resistance to Therapy. *Antioxidants (Basel, Switzerland)*, *12*(7), 1371. https://doi.org/10.3390/antiox12071371

69. Hetz C. (2012). The unfolded protein response: controlling cell fate decisions under ER stress and beyond. *Nature reviews. Molecular cell biology*, *13*(2), 89–102. https://doi.org/10.1038/nrm3270

70. Hirao, K., Natsuka, Y., Tamura, T., Wada, I., Morito, D., Natsuka, S., Romero, P., Sleno, B., Tremblay, L. O., Herscovics, A., Nagata, K., & Hosokawa, N. (2006). EDEM3, a soluble EDEM homolog, enhances glycoprotein endoplasmic reticulum-associated degradation and mannose trimming. *The Journal of biological chemistry*, *281*(14), 9650–9658. https://doi.org/10.1074/jbc.M512191200

71. Hitomi, J., Katayama, T., Eguchi, Y., Kudo, T., Taniguchi, M., Koyama, Y., Manabe, T., Yamagishi, S., Bando, Y., Imaizumi, K., Tsujimoto, Y., & Tohyama, M. (2004). Involvement of caspase-4 in endoplasmic reticulum stress-induced apoptosis and Abeta-induced cell death. *The Journal of cell biology*, *165*(3), 347–356. https://doi.org/10.1083/jcb.200310015

72. Hong, J. T., Son, D. J., Lee, C. K., Yoon, D. Y., Lee, D. H., & Park, M. H. (2017). Interleukin 32, inflammation and cancer. *Pharmacology & therapeutics*, *174*, 127–137. https://doi.org/10.1016/j.pharmthera.2017.02.025

73. Hoyt, S. J., Storer, J. M., Hartley, G. A., Grady, P. G. S., Gershman, A., de Lima, L. G., Limouse, C., Halabian, R., Wojenski, L., Rodriguez, M., Altemose, N., Rhie, A., Core, L. J., Gerton, J. L., Makalowski, W., Olson, D., Rosen, J., Smit, A. F. A., Straight, A. F., Vollger, M. R., … O'Neill, R. J. (2022). From telomere to telomere:

doi:10.6342/NTU202402516

The transcriptional and epigenetic state of human repeat elements. *Science (New York, N.Y.)*, *376*(6588), eabk3112. https://doi.org/10.1126/science.abk3112

74. Huang, Y., Sun, X., Jiang, H., Yu, S., Robins, C., Armstrong, M. J., Li, R., Mei, Z., Shi, X., Gerasimov, E. S., De Jager, P. L., Bennett, D. A., Wingo, A. P., Jin, P., Wingo, T. S., & Qin, Z. S. (2021). A machine learning approach to brain epigenetic analysis reveals kinases associated with Alzheimer's disease. *Nature communications*, *12*(1), 4472. https://doi.org/10.1038/s41467-021-24710-8

75. Hunter, J. M., Massingham, L. J., Manickam, K., Bartholomew, D., Williamson, R. K., Schwab, J. L., Marhabaie, M., Siemon, A., de Los Reyes, E., Reshmi, S. C., Cottrell, C. E., Wilson, R. K., & Koboldt, D. C. (2022). Inherited and de novo variants extend the etiology of *TAOK1*-associated neurodevelopmental disorder. *Cold Spring Harbor molecular case studies*, *8*(2), a006180. https://doi.org/10.1101/mcs.a006180

76. Hutchison, M., Berman, K. S., & Cobb, M. H. (1998). Isolation of TAO1, a protein kinase that activates MEKs in stress-activated protein kinase cascades. *The Journal of biological chemistry*, *273*(44), 28625–28632. https://doi.org/10.1074/jbc.273.44.28625

77. Iemmolo, M., Ghersi, G., & Bivona, G. (2023). The Cytokine CX3CL1 and ADAMs/MMPs in Concerted Cross-Talk Influencing Neurodegenerative Diseases. *International journal of molecular sciences*, *24*(9), 8026. https://doi.org/10.3390/ijms24098026

78. Jo, M., Lee, S., Jeon, Y. M., Kim, S., Kwon, Y., & Kim, H. J. (2020). The role of TDP-43 propagation in neurodegenerative diseases: integrating insights from clinical

doi:10.6342/NTU202402516

and experimental studies. *Experimental & molecular medicine*, *52*(10), 1652–1662. https://doi.org/10.1038/s12276-020-00513-7

79. Jönsson, M. E., Garza, R., Johansson, P. A., & Jakobsson, J. (2020). Transposable Elements: A Common Feature of Neurodevelopmental and Neurodegenerative Disorders. *Trends in genetics: TIG*, *36*(8), 610–623. https://doi.org/10.1016/j.tig.2020.05.004

80. Kawasaki, H., Morooka, T., Shimohama, S., Kimura, J., Hirano, T., Gotoh, Y., & Nishida, E. (1997). Activation and involvement of p38 mitogen-activated protein kinase in glutamate-induced apoptosis in rat cerebellar granule cells. *The Journal of biological chemistry*, *272*(30), 18518–18521. https://doi.org/10.1074/jbc.272.30.18518

81. Ke, P., Gu, J., Liu, J., Liu, Y., Tian, X., Ma, Y., Meng, Y., & Xiao, F. (2023). Syntabulin regulates neuronal excitation/inhibition balance and epileptic seizures by transporting syntaxin 1B. *Cell death discovery*, *9*(1), 187. https://doi.org/10.1038/s41420-023-01461-7

82. Kelley, N., Jeltema, D., Duan, Y., & He, Y. (2019). The NLRP3 Inflammasome: An Overview of Mechanisms of Activation and Regulation. *International journal of molecular sciences*, *20*(13), 3328. https://doi.org/10.3390/ijms20133328

83. Keshavarz, M., Farrokhi, M. R., & Amiri, A. (2017). Caffeine Neuroprotective Mechanism Against β-Amyloid Neurotoxicity in SHSY5Y Cell Line: Involvement of Adenosine, Ryanodine, and N-Methyl-D-Aspartate Receptors. *Advanced pharmaceutical bulletin*, *7*(4), 579–584. https://doi.org/10.15171/apb.2017.069

84. Kobayashi, A., Kang, M. I., Watai, Y., Tong, K. I., Shibata, T., Uchida, K., & Yamamoto, M. (2006). Oxidative and electrophilic stresses activate Nrf2 through

doi:10.6342/NTU202402516

inhibition of ubiquitination activity of Keap1. *Molecular and cellular biology*, *26*(1), 221–229. https://doi.org/10.1128/MCB.26.1.221-229.2006

85. Komis, G., Illés, P., Beck, M., & Šamaj, J. (2011). Microtubules and mitogen-activated protein kinase signalling. *Current opinion in plant biology*, *14*(6), 650–657. https://doi.org/10.1016/j.pbi.2011.07.008

86. Kopitar-Jerala N. (2017). The Role of Interferons in Inflammation and Inflammasome Activation. *Frontiers in immunology*, *8*, 873. https://doi.org/10.3389/fimmu.2017.00873

87. Kovac, S., Angelova, P. R., Holmström, K. M., Zhang, Y., Dinkova-Kostova, A. T., & Abramov, A. Y. (2015). Nrf2 regulates ROS production by mitochondria and NADPH oxidase. *Biochimica et biophysica acta*, *1850*(4), 794–801. https://doi.org/10.1016/j.bbagen.2014.11.021

88. Krug, L., Chatterjee, N., Borges-Monroy, R., Hearn, S., Liao, W. W., Morrill, K., Prazak, L., Rozhkov, N., Theodorou, D., Hammell, M., & Dubnau, J. (2017). Retrotransposon activation contributes to neurodegeneration in a Drosophila TDP-43 model of ALS. *PLoS genetics*, *13*(3), e1006635. https://doi.org/10.1371/journal.pgen.1006635

89. Kuriyama, Y., Shimizu, A., Kanai, S., Oikawa, D., Motegi, S. I., Tokunaga, F., & Ishikawa, O. (2021). Coordination of retrotransposons and type I interferon with distinct interferon pathways in dermatomyositis, systemic lupus erythematosus and autoimmune blistering disease. *Scientific reports*, *11*(1), 23146. https://doi.org/10.1038/s41598-021-02522-6

doi:10.6342/NTU202402516

90. Kushnareva, Y., & Newmeyer, D. D. (2010). Bioenergetics and cell death. *Annals of the New York Academy of Sciences*, *1201*, 50–57. https://doi.org/10.1111/j.1749-6632.2010.05633.x

91. La Quaglia, M. P., & Manchester, K. M. (1996). A comparative analysis of neuroblastic and substrate-adherent human neuroblastoma cell lines. *Journal of pediatric surgery*, *31*(2), 315–318. https://doi.org/10.1016/s0022-3468(96)90025-1

92. Laser-Azogui, A., Kornreich, M., Malka-Gibor, E., & Beck, R. (2015). Neurofilament assembly and function during neuronal development. *Current opinion in cell biology*, *32*, 92–101. https://doi.org/10.1016/j.ceb.2015.01.003

93. Le Breton, A., Bettencourt, M. P., & Gendrel, A. V. (2024). Navigating the brain and aging: exploring the impact of transposable elements from health to disease. *Frontiers in cell and developmental biology*, *12*, 1357576. https://doi.org/10.3389/fcell.2024.1357576

94. Lee, G. E., Bang, G., Byun, J., Lee, C. J., Chen, W., Jeung, D., An, H. J., Kang, H. C., Lee, J. Y., Lee, H. S., Hong, Y. S., Kim, D. J., Keniry, M., Kim, J. Y., Choi, J. S., Fanto, M., Cho, S. J., Kim, K. D., & Cho, Y. Y. (2024). Dysregulated CREB3 cleavage at the nuclear membrane induces karyoptosis-mediated cell death. *Experimental & molecular medicine*, *56*(3), 686–699. https://doi.org/10.1038/s12276-024-01195-1

95. Lee, J., Mohammad, N., Lu, Y., Kang, K., Han, K., & Brantly, M. (2022). Alu RNA induces NLRP3 expression through TLR7 activation in α-1-antitrypsin-deficient macrophages. *JCI insight*, *7*(12), e158791. https://doi.org/10.1172/jci.insight.158791

96. Li, J., Zhang, F., Bian, W., Chen, Y., Liu, J., Liu, Z., Xiong, Y., & Wan, X. (2022). cGAS inhibition alleviates Alu RNA-induced immune responses and cytotoxicity in

doi:10.6342/NTU202402516

retinal pigmented epithelium. *Cell & bioscience*, *12*(1), 116. https://doi.org/10.1186/s13578-022-00854-y

97. Li, X., Wu, X., Li, W., Yan, Q., Zhou, P., Xia, Y., Yao, W., & Zhu, F. (2023). HERV-W ENV Induces Innate Immune Activation and Neuronal Apoptosis via linc01930/cGAS Axis in Recent-Onset Schizophrenia. *International journal of molecular sciences*, *24*(3), 3000. https://doi.org/10.3390/ijms24033000

98. Li, Y., Liu, L., Barger, S. W., & Griffin, W. S. (2003). Interleukin-1 mediates pathological effects of microglia on tau phosphorylation and on synaptophysin synthesis in cortical neurons through a p38-MAPK pathway. *The Journal of neuroscience : the official journal of the Society for Neuroscience*, *23*(5), 1605–1611. https://doi.org/10.1523/JNEUROSCI.23-05-01605.2003

99. Lin, Y. C., & Koleske, A. J. (2010). Mechanisms of synapse and dendrite maintenance and their disruption in psychiatric and neurodegenerative disorders. *Annual review of neuroscience*, *33*, 349–378. https://doi.org/10.1146/annurev-neuro-060909-153204

100. Lisek, M., Przybyszewski, O., Zylinska, L., Guo, F., & Boczek, T. (2023). The Role of MEF2 Transcription Factor Family in Neuronal Survival and Degeneration. *International journal of molecular sciences*, *24*(4), 3120. https://doi.org/10.3390/ijms24043120

101. Liu, T., Rohn, J. L., Picone, R., Kunda, P., & Baum, B. (2010). Tao-1 is a negative regulator of microtubule plus-end growth. *Journal of cell science*, *123*(Pt 16), 2708–2716. https://doi.org/10.1242/jcs.068726

102. Liu, J., Zhou, J., Luan, Y., Li, X., Meng, X., Liao, W., Tang, J., & Wang, Z. (2024). cGAS-STING, inflammasomes and pyroptosis: an overview of crosstalk mechanism

doi:10.6342/NTU202402516

of activation and regulation. *Cell communication and signaling: CCS*, *22*(1), 22. https://doi.org/10.1186/s12964-023-01466-w

103. Low, H. B., & Zhang, Y. (2016). Regulatory Roles of MAPK Phosphatases in Cancer. *Immune network*, *16*(2), 85–98. https://doi.org/10.4110/in.2016.16.2.85

104. Lue, L. F., Schmitz, C. T., Serrano, G., Sue, L. I., Beach, T. G., & Walker, D. G. (2015). TREM2 Protein Expression Changes Correlate with Alzheimer's Disease Neurodegenerative Pathologies in Post-Mortem Temporal Cortices. *Brain pathology (Zurich, Switzerland)*, *25*(4), 469–480. https://doi.org/10.1111/bpa.12190

105. Malek-Ahmadi, M., Perez, S. E., Chen, K., & Mufson, E. J. (2020). Braak Stage, Cerebral Amyloid Angiopathy, and Cognitive Decline in Early Alzheimer's Disease. *Journal of Alzheimer's disease: JAD*, *74*(1), 189–197. https://doi.org/10.3233/JAD-191151

106. Majoros, A., Platanitis, E., Kernbauer-Hölzl, E., Rosebrock, F., Müller, M., & Decker, T. (2017). Canonical and Non-Canonical Aspects of JAK-STAT Signaling: Lessons from Interferons for Cytokine Responses. *Frontiers in immunology*, *8*, 29. https://doi.org/10.3389/fimmu.2017.00029

107. Martinon, F., & Tschopp, J. (2004). Inflammatory caspases: linking an intracellular innate immune system to autoinflammatory diseases. *Cell*, *117*(5), 561–574. https://doi.org/10.1016/j.cell.2004.05.004

108. Marttinen, M., Kurkinen, K. M., Soininen, H., Haapasalo, A., & Hiltunen, M. (2015). Synaptic dysfunction and septin protein family members in neurodegenerative diseases. *Molecular neurodegeneration*, *10*, 16. https://doi.org/10.1186/s13024-015-0013-z

doi:10.6342/NTU202402516

109. Massaad, C. A., & Klann, E. (2011). Reactive oxygen species in the regulation of synaptic plasticity and memory. *Antioxidants & redox signaling*, *14*(10), 2013–2054. https://doi.org/10.1089/ars.2010.3208

110. Mathavarajah, S., & Dellaire, G. (2024). LINE-1: an emerging initiator of cGAS-STING signalling and inflammation that is dysregulated in disease. *Biochemistry and cell biology = Biochimie et biologie cellulaire*, *102*(1), 38–46. https://doi.org/10.1139/bcb-2023-0134

111. Mayer, M. P., & Gierasch, L. M. (2019). Recent advances in the structural and mechanistic aspects of Hsp70 molecular chaperones. *The Journal of biological chemistry*, *294*(6), 2085–2097. https://doi.org/10.1074/jbc.REV118.002810

112. Miller, K. N., Victorelli, S. G., Salmonowicz, H., Dasgupta, N., Liu, T., Passos, J. F., & Adams, P. D. (2021). Cytoplasmic DNA: sources, sensing, and role in aging and disease. *Cell*, *184*(22), 5506–5526. https://doi.org/10.1016/j.cell.2021.09.034

113. Mingione, A., Pivari, F., Plotegher, N., Dei Cas, M., Zulueta, A., Bocci, T., Trinchera, M., Albi, E., Maglione, V., Caretti, A., Bubacco, L., Paroni, R., Bottai, D., Ghidoni, R., & Signorelli, P. (2021). Inhibition of Ceramide Synthesis Reduces α-Synuclein Proteinopathy in a Cellular Model of Parkinson's Disease. *International journal of molecular sciences*, *22*(12), 6469. https://doi.org/10.3390/ijms22126469

114. Moens, U., Kostenko, S., & Sveinbjørnsson, B. (2013). The Role of Mitogen-Activated Protein Kinase-Activated Protein Kinases (MAPKAPKs) in Inflammation. *Genes*, *4*(2), 101–133. https://doi.org/10.3390/genes4020101

115. Moldoveanu, T., & Czabotar, P. E. (2020). BAX, BAK, and BOK: A Coming of Age for the BCL-2 Family Effector Proteins. *Cold Spring Harbor perspectives in biology*, *12*(4), a036319. https://doi.org/10.1101/cshperspect.a036319

doi:10.6342/NTU202402516

116. Moon, H. J., Herring, S. K., & Zhao, L. (2021). Clusterin: a multifaceted protein in the brain. *Neural regeneration research*, *16*(7), 1438–1439. https://doi.org/10.4103/1673-5374.301013

117. Natarajaseenivasan, K., Shanmughapriya, S., Velusamy, P., Sayre, M., Garcia, A., Gomez, N. M., & Langford, D. (2020). Inflammation-induced PINCH expression leads to actin depolymerization and mitochondrial mislocalization in neurons. *Translational neurodegeneration*, *9*(1), 32. https://doi.org/10.1186/s40035-020-00211-4

118. Natarajaseenivasan, K., Shanmughapriya, S., Velusamy, P., Sayre, M., Garcia, A., Gomez, N. M., & Langford, D. (2020). Inflammation-induced PINCH expression leads to actin depolymerization and mitochondrial mislocalization in neurons. *Translational neurodegeneration*, *9*(1), 32. https://doi.org/10.1186/s40035-020-00211-4

119. Nopparat, C., Boontor, A., Kutpruek, S., & Govitrapong, P. (2023). The role of melatonin in amyloid beta-induced inflammation mediated by inflammasome signaling in neuronal cell lines. *Scientific reports*, *13*(1), 17841. https://doi.org/10.1038/s41598-023-45220-1

120. Norden, D. M., Trojanowski, P. J., Villanueva, E., Navarro, E., & Godbout, J. P. (2016). Sequential activation of microglia and astrocyte cytokine expression precedes increased Iba-1 or GFAP immunoreactivity following systemic immune challenge. *Glia*, *64*(2), 300–316. https://doi.org/10.1002/glia.22930

121. Ochoa, E., Ramirez, P., Gonzalez, E., De Mange, J., Ray, W. J., Bieniek, K. F., & Frost, B. (2023). Pathogenic tau-induced transposable element-derived dsRNA

doi:10.6342/NTU202402516

drives neuroinflammation. *Science advances*, *9*(1), eabq5423. https://doi.org/10.1126/sciadv.abq5423

122. Okamoto, S., Krainc, D., Sherman, K., & Lipton, S. A. (2000). Antiapoptotic role of the p38 mitogen-activated protein kinase-myocyte enhancer factor 2 transcription factor pathway during neuronal differentiation. *Proceedings of the National Academy of Sciences of the United States of America*, *97*(13), 7561–7566. https://doi.org/10.1073/pnas.130502697

123. Olufunmilayo, E. O., Gerke-Duncan, M. B., & Holsinger, R. M. D. (2023). Oxidative Stress and Antioxidants in Neurodegenerative Disorders. *Antioxidants (Basel, Switzerland)*, *12*(2), 517. https://doi.org/10.3390/antiox12020517

124. Palma, F. R., Gantner, B. N., Sakiyama, M. J., Kayzuka, C., Shukla, S., Lacchini, R., Cunniff, B., & Bonini, M. G. (2024). ROS production by mitochondria: function or dysfunction?. *Oncogene*, *43*(5), 295–303. https://doi.org/10.1038/s41388-023-02907-z

125. Pan, X., Yan, D., Wang, D., Wu, X., Zhao, W., Lu, Q., & Yan, H. (2017). Mitochondrion-Mediated Apoptosis Induced by Acrylamide is Regulated by a Balance Between Nrf2 Antioxidant and MAPK Signaling Pathways in PC12 Cells. *Molecular neurobiology*, *54*(6), 4781–4794. https://doi.org/10.1007/s12035-016-0021-1

126. Paul, B. D., Snyder, S. H., & Bohr, V. A. (2021). Signaling by cGAS-STING in Neurodegeneration, Neuroinflammation, and Aging. *Trends in neurosciences*, *44*(2), 83–96. https://doi.org/10.1016/j.tins.2020.10.008

doi:10.6342/NTU202402516

127. Perea, J. R., Llorens-Martín, M., Ávila, J., & Bolós, M. (2018). The Role of Microglia in the Spread of Tau: Relevance for Tauopathies. *Frontiers in cellular neuroscience*, *12*, 172. https://doi.org/10.3389/fncel.2018.00172

128. Pizzino, G., Irrera, N., Cucinotta, M., Pallio, G., Mannino, F., Arcoraci, V., Squadrito, F., Altavilla, D., & Bitto, A. (2017). Oxidative Stress: Harms and Benefits for Human Health. *Oxidative medicine and cellular longevity*, *2017*, 8416763. https://doi.org/10.1155/2017/8416763

129. Platanias L. C. (2003). The p38 mitogen-activated protein kinase pathway and its role in interferon signaling. *Pharmacology & therapeutics*, *98*(2), 129–142. https://doi.org/10.1016/s0163-7258(03)00016-0

130. Polymeropoulos, M. H., Lavedan, C., Leroy, E., Ide, S. E., Dehejia, A., Dutra, A., Pike, B., Root, H., Rubenstein, J., Boyer, R., Stenroos, E. S., Chandrasekharappa, S., Athanassiadou, A., Papapetropoulos, T., Johnson, W. G., Lazzarini, A. M., Duvoisin, R. C., Di Iorio, G., Golbe, L. I., & Nussbaum, R. L. (1997). Mutation in the alpha-synuclein gene identified in families with Parkinson's disease. *Science (New York, N.Y.)*, *276*(5321), 2045–2047. https://doi.org/10.1126/science.276.5321.2045

131. Pothlichet, J., Meunier, I., Davis, B. K., Ting, J. P., Skamene, E., von Messling, V., & Vidal, S. M. (2013). Type I IFN triggers RIG-I/TLR3/NLRP3-dependent inflammasome activation in influenza A virus infected cells. *PLoS pathogens*, *9*(4), e1003256. https://doi.org/10.1371/journal.ppat.1003256

132. Prasad, A., Bharathi, V., Sivalingam, V., Girdhar, A., & Patel, B. K. (2019). Molecular Mechanisms of TDP-43 Misfolding and Pathology in Amyotrophic Lateral Sclerosis. *Frontiers in molecular neuroscience*, *12*, 25. https://doi.org/10.3389/fnmol.2019.00025

doi:10.6342/NTU202402516

133. Pritam, P., Deka, R., Bhardwaj, A., Srivastava, R., Kumar, D., Jha, A. K., Jha, N. K., Villa, C., & Jha, S. K. (2022). Antioxidants in Alzheimer's Disease: Current Therapeutic Significance and Future Prospects. *Biology*, *11*(2), 212. https://doi.org/10.3390/biology11020212

134. Qi, Y., Li, Y., Zhang, Y., Zhang, L., Wang, Z., Zhang, X., Gui, L., & Huang, J. (2015). IFI6 Inhibits Apoptosis via Mitochondrial-Dependent Pathway in Dengue Virus 2 Infected Vascular Endothelial Cells. *PloS one*, *10*(8), e0132743. https://doi.org/10.1371/journal.pone.0132743

135. Radzikowska, U., Eljaszewicz, A., Tan, G., Stocker, N., Heider, A., Westermann, P., Steiner, S., Dreher, A., Wawrzyniak, P., Rückert, B., Rodriguez-Coira, J., Zhakparov, D., Huang, M., Jakiela, B., Sanak, M., Moniuszko, M., O'Mahony, L., Jutel, M., Kebadze, T., Jackson, D. J., … Sokolowska, M. (2023). Rhinovirus-induced epithelial RIG-I inflammasome suppresses antiviral immunity and promotes inflammation in asthma and COVID-19. *Nature communications*, *14*(1), 2329. https://doi.org/10.1038/s41467-023-37470-4

136. Rathinam, V. A., Jiang, Z., Waggoner, S. N., Sharma, S., Cole, L. E., Waggoner, L., Vanaja, S. K., Monks, B. G., Ganesan, S., Latz, E., Hornung, V., Vogel, S. N., Szomolanyi-Tsuda, E., & Fitzgerald, K. A. (2010). The AIM2 inflammasome is essential for host defense against cytosolic bacteria and DNA viruses. *Nature immunology*, *11*(5), 395–402. https://doi.org/10.1038/ni.1864

137. Ramirez, P., Zuniga, G., Sun, W., Beckmann, A., Ochoa, E., DeVos, S. L., Hyman, B., Chiu, G., Roy, E. R., Cao, W., Orr, M., Buggia-Prevot, V., Ray, W. J., & Frost, B. (2022). Pathogenic tau accelerates aging-associated activation of transposable

doi:10.6342/NTU202402516

elements in the mouse central nervous system. *Progress in neurobiology*, *208*, 102181. https://doi.org/10.1016/j.pneurobio.2021.102181

138. Ren, J., Zhang, S., Wang, X., Deng, Y., Zhao, Y., Xiao, Y., Liu, J., Chu, L., & Qi, X. (2022). MEF2C ameliorates learning, memory, and molecular pathological changes in Alzheimer's disease in vivo and in vitro. *Acta biochimica et biophysica Sinica*, *54*(1), 77–90. https://doi.org/10.3724/abbs.2021012

139. Ren, J., Zhang, S., Wang, X., Deng, Y., Zhao, Y., Xiao, Y., Liu, J., Chu, L., & Qi, X. (2022). MEF2C ameliorates learning, memory, and molecular pathological changes in Alzheimer's disease in vivo and in vitro. *Acta biochimica et biophysica Sinica*, *54*(1), 77–90. https://doi.org/10.3724/abbs.2021012

140. Reszka, A. A., Seger, R., Diltz, C. D., Krebs, E. G., & Fischer, E. H. (1995). Association of mitogen-activated protein kinase with the microtubule cytoskeleton. *Proceedings of the National Academy of Sciences of the United States of America*, *92*(19), 8881–8885. https://doi.org/10.1073/pnas.92.19.8881

141. Rostami, M. R., & Bradic, M. (2021). The derepression of transposable elements in lung cells is associated with the inflammatory response and gene activation in idiopathic pulmonary fibrosis. *Mobile DNA*, *12*(1), 14. https://doi.org/10.1186/s13100-021-00241-3

142. Russ, E., & Iordanskiy, S. (2023). Endogenous Retroviruses as Modulators of Innate Immunity. *Pathogens (Basel, Switzerland)*, *12*(2), 162. https://doi.org/10.3390/pathogens12020162

143. Sajid, M., Ullah, H., Yan, K., He, M., Feng, J., Shereen, M. A., Hao, R., Li, Q., Guo, D., Chen, Y., & Zhou, L. (2021). The Functional and Antiviral Activity of Interferon

doi:10.6342/NTU202402516

Alpha-Inducible IFI6 Against Hepatitis B Virus Replication and Gene Expression. *Frontiers in immunology*, *12*, 634937. https://doi.org/10.3389/fimmu.2021.634937

144. Salminen, A., Kauppinen, A., Suuronen, T., Kaarniranta, K., & Ojala, J. (2009). ER stress in Alzheimer's disease: a novel neuronal trigger for inflammation and Alzheimer's pathology. *Journal of neuroinflammation*, *6*, 41. https://doi.org/10.1186/1742-2094-6-41

145. Salpietro, V., Dixon, C. L., Guo, H., Bello, O. D., Vandrovcova, J., Efthymiou, S., Maroofian, R., Heimer, G., Burglen, L., Valence, S., Torti, E., Hacke, M., Rankin, J., Tariq, H., Colin, E., Procaccio, V., Striano, P., Mankad, K., Lieb, A., Chen, S., … Houlden, H. (2019). AMPA receptor GluA2 subunit defects are a cause of neurodevelopmental disorders. *Nature communications*, *10*(1), 3094. https://doi.org/10.1038/s41467-019-10910-w

146. Satapathy, S., Walker, H., Brown, J., Gambin, Y., & Wilson, M. R. (2023). The N-end rule pathway regulates ER stress-induced clusterin release to the cytosol where it directs misfolded proteins for degradation. *Cell reports*, *42*(9), 113059. https://doi.org/10.1016/j.celrep.2023.113059

147. Schmid-Burgk, J. L., Gaidt, M. M., Schmidt, T., Ebert, T. S., Bartok, E., & Hornung, V. (2015). Caspase-4 mediates non-canonical activation of the NLRP3 inflammasome in human myeloid cells. *European journal of immunology*, *45*(10), 2911–2917. https://doi.org/10.1002/eji.201545523

148. Singh, S., Borkar, M. R., & Bhatt, L. K. (2024). Transposable Elements: Emerging Therapeutic Targets in Neurodegenerative Diseases. *Neurotoxicity research*, *42*(1), 9. https://doi.org/10.1007/s12640-024-00688-1

doi:10.6342/NTU202402516

149. Shea, T. B., Dahl, D. C., Nixon, R. A., & Fischer, I. (1997). Triton-soluble phosphovariants of the heavy neurofilament subunit in developing and mature mouse central nervous system. *Journal of neuroscience research*, *48*(6), 515–523.

150. Son, Y., Cheong, Y. K., Kim, N. H., Chung, H. T., Kang, D. G., & Pae, H. O. (2011). Mitogen-Activated Protein Kinases and Reactive Oxygen Species: How Can ROS Activate MAPK Pathways?. *Journal of signal transduction*, *2011*, 792639. https://doi.org/10.1155/2011/792639

151. Son, Y., Kim, S., Chung, H. T., & Pae, H. O. (2013). Reactive oxygen species in the activation of MAP kinases. *Methods in enzymology*, *528*, 27–48. https://doi.org/10.1016/B978-0-12-405881-1.00002-1

152. Spires-Jones, T. L., & Hyman, B. T. (2014). The intersection of amyloid beta and tau at synapses in Alzheimer's disease. *Neuron*, *82*(4), 756–771. https://doi.org/10.1016/j.neuron.2014.05.004

153. Sun, W., Samimi, H., Gamez, M., Zare, H., & Frost, B. (2018). Pathogenic tau-induced piRNA depletion promotes neuronal death through transposable element dysregulation in neurodegenerative tauopathies. *Nature neuroscience*, *21*(8), 1038–1048. https://doi.org/10.1038/s41593-018-0194-1

154. Sweeney, P., Park, H., Baumann, M., Dunlop, J., Frydman, J., Kopito, R., McCampbell, A., Leblanc, G., Venkateswaran, A., Nurmi, A., & Hodgson, R. (2017). Protein misfolding in neurodegenerative diseases: implications and strategies. *Translational neurodegeneration*, *6*, 6. https://doi.org/10.1186/s40035-017-0077-5

155. Takata, T., Araki, S., Tsuchiya, Y., & Watanabe, Y. (2020). Oxidative Stress Orchestrates MAPK and Nitric-Oxide Synthase Signal. *International journal of molecular sciences*, *21*(22), 8750. https://doi.org/10.3390/ijms21228750

doi:10.6342/NTU202402516

156. Tavares, I. A., Touma, D., Lynham, S., Troakes, C., Schober, M., Causevic, M., Garg, R., Noble, W., Killick, R., Bodi, I., Hanger, D. P., & Morris, J. D. (2013). Prostate-derived sterile 20-like kinases (PSKs/TAOKs) phosphorylate tau protein and are activated in tangle-bearing neurons in Alzheimer disease. *The Journal of biological chemistry*, *288*(21), 15418–15429. https://doi.org/10.1074/jbc.M112.448183

157. Thal, D. R., & Tomé, S. O. (2022). The central role of tau in Alzheimer's disease: From neurofibrillary tangle maturation to the induction of cell death. *Brain research bulletin*, *190*, 204–217. https://doi.org/10.1016/j.brainresbull.2022.10.006

158. Timm, T., Li, X. Y., Biernat, J., Jiao, J., Mandelkow, E., Vandekerckhove, J., & Mandelkow, E. M. (2003). MARKK, a Ste20-like kinase, activates the polarity-inducing kinase MARK/PAR-1. *The EMBO journal*, *22*(19), 5090–5101. https://doi.org/10.1093/emboj/cdg447

159. Timm, T., Li, X. Y., Biernat, J., Jiao, J., Mandelkow, E., Vandekerckhove, J., & Mandelkow, E. M. (2003). MARKK, a Ste20-like kinase, activates the polarity-inducing kinase MARK/PAR-1. *The EMBO journal*, *22*(19), 5090–5101. https://doi.org/10.1093/emboj/cdg447

160. Tsai, N. P., Wilkerson, J. R., Guo, W., Maksimova, M. A., DeMartino, G. N., Cowan, C. W., & Huber, K. M. (2012). Multiple autism-linked genes mediate synapse elimination via proteasomal degradation of a synaptic scaffold PSD-95. *Cell*, *151*(7), 1581–1594. https://doi.org/10.1016/j.cell.2012.11.040

161. Uchida, A., Peng, J., & Brown, A. (2023). Regulation of neurofilament length and transport by a dynamic cycle of phospho-dependent polymer severing and annealing. *Molecular biology of the cell*, *34*(7), ar68. https://doi.org/10.1091/mbc.E23-01-0024

doi:10.6342/NTU202402516

162. Udeochu, J. C., Amin, S., Huang, Y., Fan, L., Torres, E. R. S., Carling, G. K., Liu, B., McGurran, H., Coronas-Samano, G., Kauwe, G., Mousa, G. A., Wong, M. Y., Ye, P., Nagiri, R. K., Lo, I., Holtzman, J., Corona, C., Yarahmady, A., Gill, M. T., Raju, R. M., … Gan, L. (2023). Tau activation of microglial cGAS-IFN reduces MEF2C-mediated cognitive resilience. *Nature neuroscience*, *26*(5), 737–750. https://doi.org/10.1038/s41593-023-01315-6

163. van Woerden, G. M., Bos, M., de Konink, C., Distel, B., Avagliano Trezza, R., Shur, N. E., Barañano, K., Mahida, S., Chassevent, A., Schreiber, A., Erwin, A. L., Gripp, K. W., Rehman, F., Brulleman, S., McCormack, R., de Geus, G., Kalsner, L., Sorlin, A., Bruel, A. L., Koolen, D. A., … Kleefstra, T. (2021). TAOK1 is associated with neurodevelopmental disorder and essential for neuronal maturation and cortical development. *Human mutation*, *42*(4), 445–459. https://doi.org/10.1002/humu.24176

164. van Vliet, A. R., Verfaillie, T., & Agostinis, P. (2014). New functions of mitochondria associated membranes in cellular signaling. *Biochimica et biophysica acta*, *1843*(10), 2253–2262. https://doi.org/10.1016/j.bbamcr.2014.03.009

165. van Vliet, A. R., & Agostinis, P. (2018). Mitochondria-Associated Membranes and ER Stress. *Current topics in microbiology and immunology*, *414*, 73–102. https://doi.org/10.1007/82_2017_2

166. Vidović, M., & Rikalovic, M. G. (2022). Alpha-Synuclein Aggregation Pathway in Parkinson's Disease: Current Status and Novel Therapeutic Approaches. *Cells*, *11*(11), 1732. https://doi.org/10.3390/cells11111732

167. Villavicencio Tejo, F., & Quintanilla, R. A. (2021). Contribution of the Nrf2 Pathway on Oxidative Damage and Mitochondrial Failure in Parkinson and Alzheimer's

doi:10.6342/NTU202402516

Disease. *Antioxidants (Basel, Switzerland)*, *10*(7), 1069. https://doi.org/10.3390/antiox10071069

168. Welsbie, D. S., Mitchell, K. L., Jaskula-Ranga, V., Sluch, V. M., Yang, Z., Kim, J., Buehler, E., Patel, A., Martin, S. E., Zhang, P. W., Ge, Y., Duan, Y., Fuller, J., Kim, B. J., Hamed, E., Chamling, X., Lei, L., Fraser, I. D. C., Ronai, Z. A., Berlinicke, C. A., … Zack, D. J. (2017). Enhanced Functional Genomic Screening Identifies Novel Mediators of Dual Leucine Zipper Kinase-Dependent Injury Signaling in Neurons. *Neuron*, *94*(6), 1142–1154.e6. https://doi.org/10.1016/j.neuron.2017.06.008

169. Werner, B., & Yadav, S. (2023). Phosphoregulation of the septin cytoskeleton in neuronal development and disease. *Cytoskeleton (Hoboken, N.J.)*, *80*(7-8), 275–289. https://doi.org/10.1002/cm.21728

170. White, S. A., Zhang, L. S., Pasula, D. J., Yang, Y. H. C., & Luciani, D. S. (2020). Bax and Bak jointly control survival and dampen the early unfolded protein response in pancreatic β-cells under glucolipotoxic stress. *Scientific reports*, *10*(1), 10986. https://doi.org/10.1038/s41598-020-67755-3

171. Wilson, D. M., 3rd, Cookson, M. R., Van Den Bosch, L., Zetterberg, H., Holtzman, D. M., & Dewachter, I. (2023). Hallmarks of neurodegenerative diseases. *Cell*, *186*(4), 693–714. https://doi.org/10.1016/j.cell.2022.12.032

172. Wolf, P., Schoeniger, A., & Edlich, F. (2022). Pro-apoptotic complexes of BAX and BAK on the outer mitochondrial membrane. *Biochimica et biophysica acta. Molecular cell research*, *1869*(10), 119317. https://doi.org/10.1016/j.bbamcr.2022.119317

doi:10.6342/NTU202402516

173. Wu, M. F., & Wang, S. G. (2008). Human TAO kinase 1 induces apoptosis in SH-SY5Y cells. *Cell biology international*, *32*(1), 151–156. https://doi.org/10.1016/j.cellbi.2007.08.006

174. Wu, M., Zhang, M., Yin, X., Chen, K., Hu, Z., Zhou, Q., Cao, X., Chen, Z., & Liu, D. (2021). The role of pathological tau in synaptic dysfunction in Alzheimer's diseases. *Translational neurodegeneration*, *10*(1), 45. https://doi.org/10.1186/s40035-021-00270-1

175. Wu, Z., Lu, Z., Ou, J., Su, X., & Liu, J. (2020). Inflammatory response and oxidative stress attenuated by sulfiredoxin-1 in neuron-like cells depends on nuclear factor erythroid-2-related factor 2. *Molecular medicine reports*, *22*(6), 4734–4742. https://doi.org/10.3892/mmr.2020.11545

176. Xu, B., Lang, L. M., Lian, S., Guo, J. R., Wang, J. F., Yang, H. M., & Li, S. Z. (2019). Oxidation Stress-Mediated MAPK Signaling Pathway Activation Induces Neuronal Loss in the CA1 and CA3 Regions of the Hippocampus of Mice Following Chronic Cold Exposure. *Brain sciences*, *9*(10), 273. https://doi.org/10.3390/brainsci9100273

177. Liu, X., Zhang, X., Ding, Y., Zhou, W., Tao, L., Lu, P., Wang, Y., & Hu, R. (2017). Nuclear Factor E2-Related Factor-2 Negatively Regulates NLRP3 Inflammasome Activity by Inhibiting Reactive Oxygen Species-Induced NLRP3 Priming. *Antioxidants & redox signaling*, *26*(1), 28–43. https://doi.org/10.1089/ars.2015.6615

178. Yamamuro, A., Kishino, T., Ohshima, Y., Yoshioka, Y., Kimura, T., Kasai, A., & Maeda, S. (2011). Caspase-4 directly activates caspase-9 in endoplasmic reticulum stress-induced apoptosis in SH-SY5Y cells. *Journal of pharmacological sciences*, *115*(2), 239–243. https://doi.org/10.1254/jphs.10217sc

doi:10.6342/NTU202402516

179. Yang, C., Guo, X., Wang, G. H., Wang, H. L., Liu, Z. C., Liu, H., Zhu, Z. X., & Li, Y. (2014). Changes in tau phosphorylation levels in the hippocampus and frontal cortex following chronic stress. *Brazilian journal of medical and biological research = Revista brasileira de pesquisas medicas e biologicas*, *47*(3), 237–244. https://doi.org/10.1590/1414-431X20133275

180. Yang, Y., Wang, H., Kouadir, M., Song, H., & Shi, F. (2019). Recent advances in the mechanisms of NLRP3 inflammasome activation and its inhibitors. *Cell death & disease*, *10*(2), 128. https://doi.org/10.1038/s41419-019-1413-8

181. Yang, Q. Q., & Zhou, J. W. (2019). Neuroinflammation in the central nervous system: Symphony of glial cells. *Glia*, *67*(6), 1017–1035. https://doi.org/10.1002/glia.23571

182. Yin, R., Guo, D., Zhang, S., & Zhang, X. (2016). miR-706 inhibits the oxidative stress-induced activation of PKCα/TAOK1 in liver fibrogenesis. *Scientific reports*, *6*, 37509. https://doi.org/10.1038/srep37509

183. Yin, Y., She, H., Li, W., Yang, Q., Guo, S., & Mao, Z. (2012). Modulation of Neuronal Survival Factor MEF2 by Kinases in Parkinson's Disease. *Frontiers in physiology*, *3*, 171. https://doi.org/10.3389/fphys.2012.00171

184. Yu, Z., Poppe, J. L., & Wang, X. (2013). Mitochondrial mechanisms of neuroglobin's neuroprotection. *Oxidative medicine and cellular longevity*, *2013*, 756989. https://doi.org/10.1155/2013/756989

185. Yuan, A., Rao, M. V., Veeranna, & Nixon, R. A. (2012). Neurofilaments at a glance. *Journal of cell science*, *125*(Pt 14), 3257–3263. https://doi.org/10.1242/jcs.104729

186. Yue, J., & López, J. M. (2020). Understanding MAPK Signaling Pathways in Apoptosis. *International journal of molecular sciences*, *21*(7), 2346. https://doi.org/10.3390/ijms21072346

doi:10.6342/NTU202402516

187. Yum, S., Li, M., Fang, Y., & Chen, Z. J. (2021). TBK1 recruitment to STING activates both IRF3 and NF-κB that mediate immune defense against tumors and viral infections. *Proceedings of the National Academy of Sciences of the United States of America*, *118*(14), e2100225118. https://doi.org/10.1073/pnas.2100225118

188. Zeeshan, H. M., Lee, G. H., Kim, H. R., & Chae, H. J. (2016). Endoplasmic Reticulum Stress and Associated ROS. *International journal of molecular sciences*, *17*(3), 327. https://doi.org/10.3390/ijms17030327

189. Zhang, W., Xiao, D., Mao, Q., & Xia, H. (2023). Role of neuroinflammation in neurodegeneration development. *Signal transduction and targeted therapy*, *8*(1), 267. https://doi.org/10.1038/s41392-023-01486-5

190. Zheng, Y., & Pan, D. (2019). The Hippo Signaling Pathway in Development and Disease. *Developmental cell*, *50*(3), 264–282. https://doi.org/10.1016/j.devcel.2019.06.003

191. Zuo, X., Zhou, J., Li, Y., Wu, K., Chen, Z., Luo, Z., Zhang, X., Liang, Y., Esteban, M. A., Zhou, Y., & Fu, X. D. (2021). TDP-43 aggregation induced by oxidative stress causes global mitochondrial imbalance in ALS. *Nature structural & molecular biology*, *28*(2), 132–142. https://doi.org/10.1038/s41594-020-00537-7

doi:10.6342/NTU202402516

8. Appendix

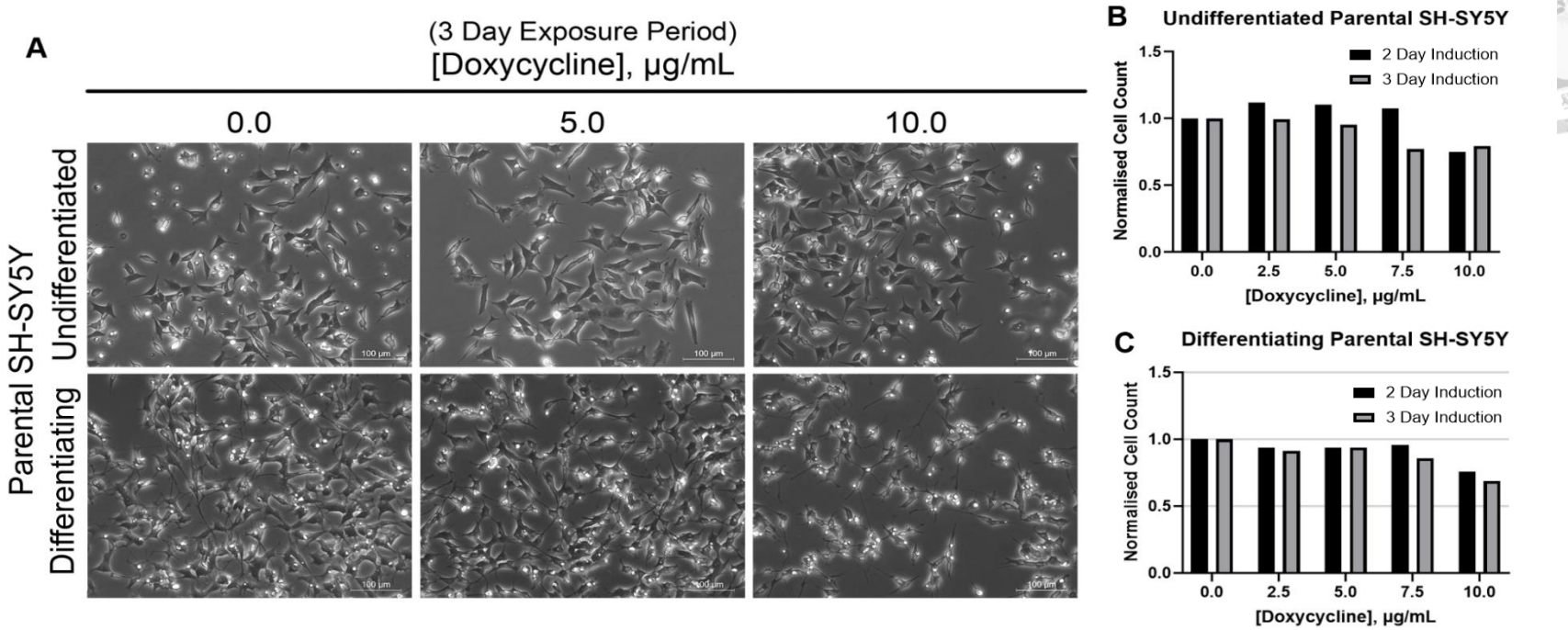

Supplementary Figure 1. Doxycycline treatment at varying concentrations shows limited effects on cell count, confluency, and morphology in undifferentiated and differentiating parental SH-SY5Y cells. (A) Three days of doxycycline exposure at concentrations from 0.0 to 10.0 µg/mL show limited changes in cell growth and morphology, with visible reduction in cell confluency at 10.0 µg/mL. **(B)** Harvest cell counts of undifferentiated SH-SY5Y cells remain consistent up to 7.5 µg/mL after 2 days before decreasing with increased exposure time and concentration. **(C)** Harvest cell counts of differentiating SH-SY5Y cells show a similar trend to the undifferentiated group.

doi:10.6342/NTU202402516

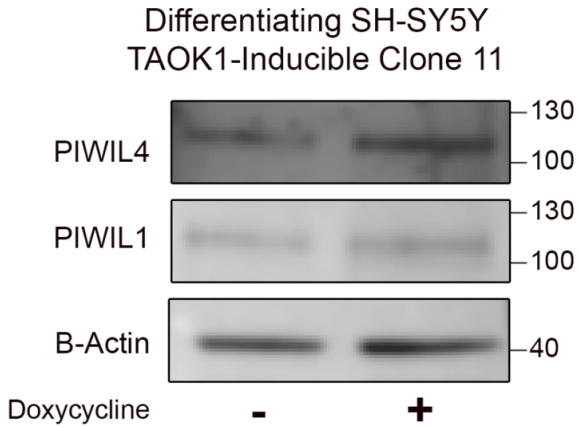

Supplementary Figure 2. Western blot analysis of PIWIL1 and PIWIL4. Protein expression levels of PIWIL1 and PIWIL4 remained unchanged with TAOK1 overexpression in differentiating SH-SY5Y cells clone 11.

doi:10.6342/NTU202402516

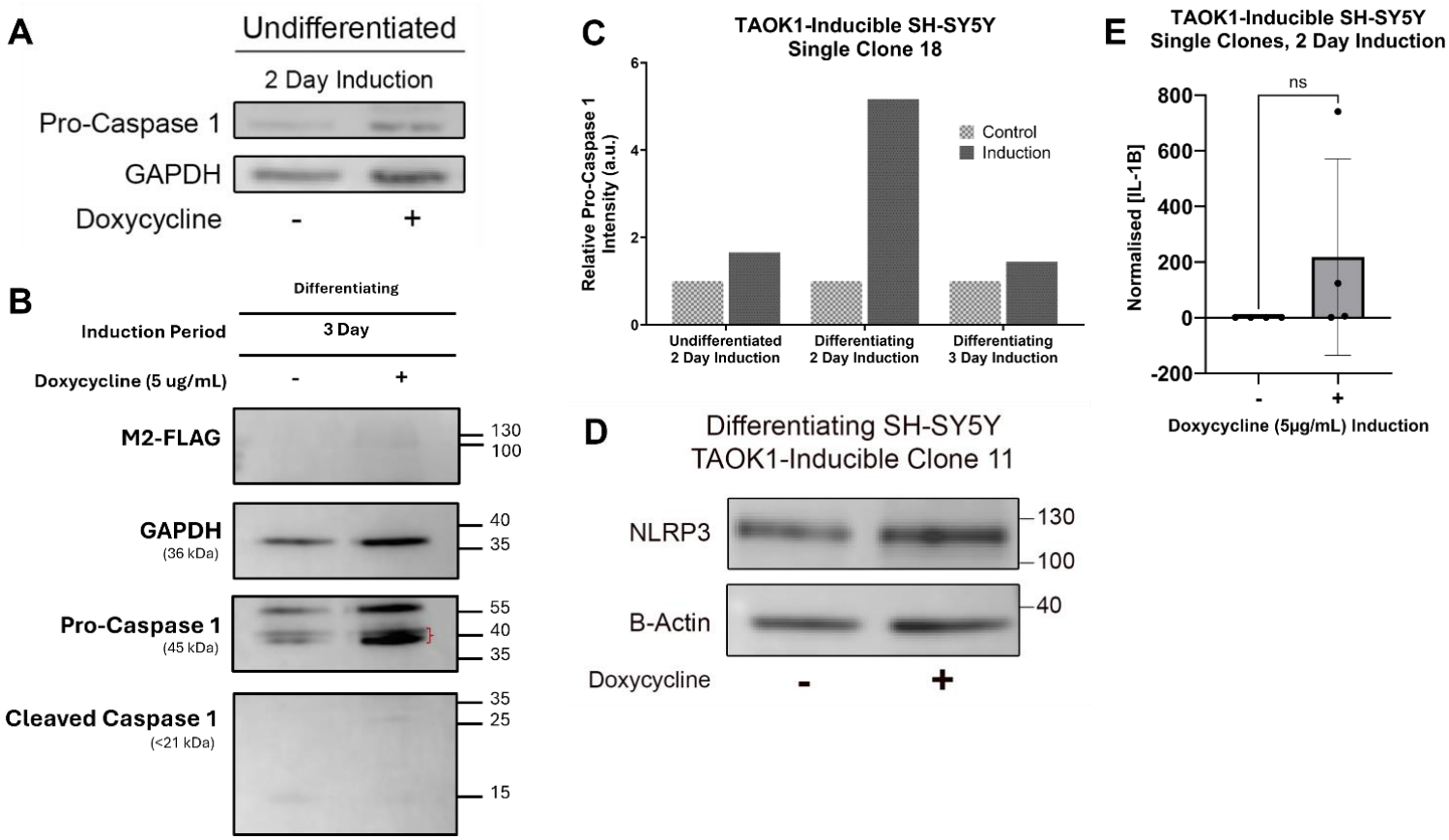

Supplementary Figure 3. The protein expression of Caspase 1 and NLRP3, and quantification of cytokine IL-1β in TAOK1 overexpressing SH-SY5Y. (A, B) Western blot analysis of Caspase 1 in undifferentiated and differentiating SH-SY5Y did not see significant change with TAOK1 overexpression. **(C)** Densitometry of Pro-Caspase 1 western blot from (A, B). **(D)** Western blot analysis of inflammasome protein NLRP3 did not see any significant change with TAOK1 overexpression in differentiating SH-SY5Y **(E)** ProQuantum Immunoassay to quantify IL-1β in culture medium after 2 days of doxycycline induction to overexpress TAOK1 in undifferentiated cells did not observe any significant changes from control.

doi:10.6342/NTU202402516

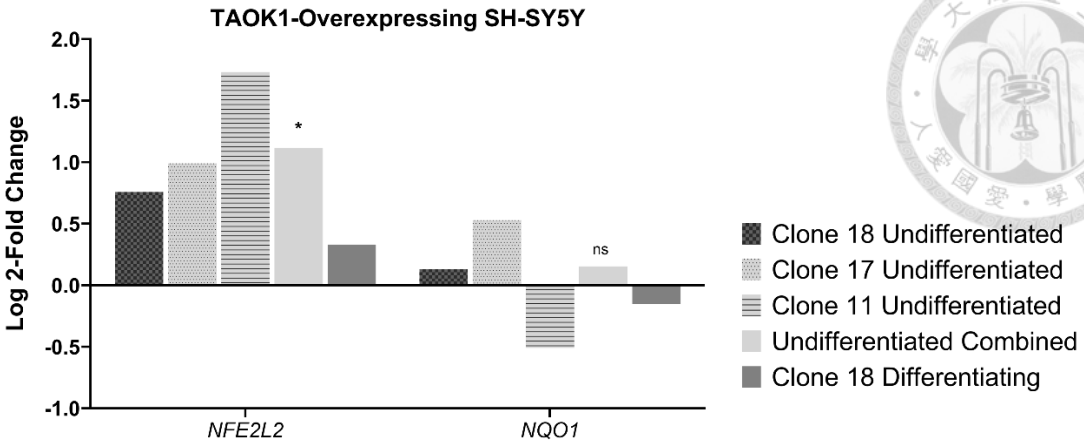

Supplementary Figure 4. ***NQO1* & *NFE2L2* Log 2-Fold Change values from RNA sequencing analysis.** Log 2-Fold change of undifferentiated and differentiating single clones were generated individually using EdgeR, while that of the undifferentiated combined group was generated separately using DeSeq2, from raw data of undifferentiated single clones.

doi:10.6342/NTU202402516

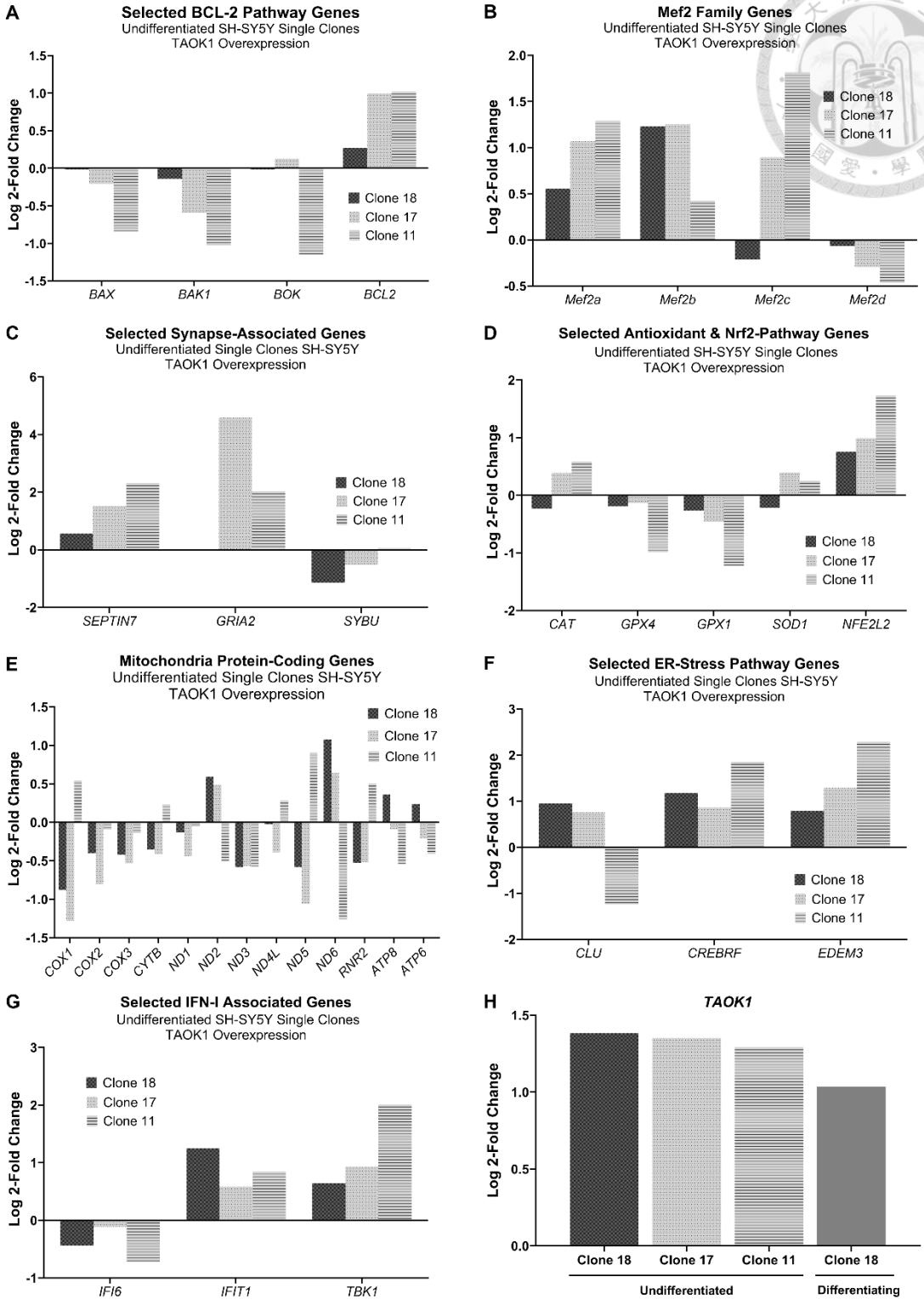

Supplementary Figure 5. RNA sequencing analysis using EdgeR to produce Log 2-Fold Change of selected genes of each observed pathway in single clones given TAOK1 overexpression. (A – G) Log 2-Fold change values of undifferentiated single clones overexpressing TAOK1. **(A)** Selected BCL2 pathway genes. **(B)** Selected Mef2

doi:10.6342/NTU202402516

transcription factor family genes. **(C)** Selected synapse-associated genes **(D)** Selected antioxidant genes upregulated by Nrf2, and Nrf2-coding gene *NFE2L2*. **(E)** Mitochondria protein-coding genes. **(F)** Selected ER-stress response pathway genes containing ERSE in their promoters. **(G)** Selected IFN-I associated genes, *IFI6* and *IFIT1* as interferon-stimulated genes, and TBK1 upstream of IFN-responses. **(H)** Log 2-Fold change values of TAOK1 in undifferentiated and differentiating single clones.

doi:10.6342/NTU202402516

Supplementary Table 1. Log 2-fold change and p-adjusted values from RNA-sequencing analysis of selected genes[1]

	Clone 18 Differentiating		Clone 18 Undifferentiated		Clone 17 Undifferentiated		Clone 11 Undifferentiated		Undifferentiated (n=3)	
Gene	**Log2FC**	**padj**	**Log2FC**	**padj**	**Log2FC**	**padj**	**Log2FC**	**padj**	**Log2FC**	**padj**
TAOK1	1.034437529	0.000398337	1.382836236	8.88135E-08	1.351792269	1.44119E-08	1.29305741	6.61549E-09	1.275157186	0.012511873
CASP3	0.375416288	0.624807495	0.362738767	1	0.180068769	0.000504138	0.754117912	1.4061E-10	-	-
BCL2	0.313422145	0.709837938	0.273543781	0.67452843	0.996316669	6.19908E-05	1.021985273	7.54784E-06	0.71316986	0.173359786
BAX	-0.207811658	0.863302894	-0.016871505	1	-0.208253666	0.566025312	-0.841594504	0.000375113	-0.37536831	0.462330424
BAK1	0.008123125	1	-0.139023089	0.917508307	-0.59372753	0.03431939	-1.021823869	1.54024E-05	-0.60343499	0.229588517
BOK	-0.606325722	0.373603011	-0.013060137	1	0.126638669	0.87400525	-1.155500436	6.75958E-06	-0.69207948	0.457579704
MEF2A	0.533735337	0.338855029	0.555951321	0.217208676	1.067090717	3.23481E-05	1.291116242	2.1634E-08	0.92242393	0.060743537
MEF2B	5.663944626	0.480946484	1.229845255	0.911358911	1.250400677	0.468069677	0.422846284	1	1.061791	-
MEF2C	-0.01399448	1	-0.215263287	0.908783128	0.894707713	0.00382366	1.814979401	1.3442E-13	1.13164595	0.231149625
MEF2D	-0.156954695	0.92303217	-0.066163507	1	-0.295625745	0.361607931	-0.465917381	0.057663311	-0.34199455	0.484699243
CASP3	0.375416	0.624807	0.075152	1	0.922632	0.000504	1.491152	1.41E-10	0.787539	0.163885
BCLAF1	0.317375	0.708854	0.338367	0.556178	1.569023	5.3E-11	2.757118	2.53E-33	1.752112	0.019466
DNAJB4	0.520711	0.538377	0.789551	0.174932	1.363727	5.61E-06	1.977308	2.53E-15	1.491476	0.03925
CAT	0.27357901	0.834483581	-0.231848896	0.792764113	0.386629804	0.234448275	0.589527851	0.017308337	0.23119433	0.681651126
GPX4	-0.320340004	0.708795159	-0.194130057	0.813386874	-0.132036785	0.746925444	-0.990838268	1.25452E-05	-0.47850755	0.390982045
GPX1	-0.390845507	0.579344337	-0.266003357	0.673108837	-0.459526723	0.110531508	-1.223510953	4.70636E-08	-0.61487961	0.330455139
SOD1	-0.192060574	0.88052373	-0.218383456	0.766624636	0.396152355	0.19024511	0.251685917	0.339495407	0.05855277	0.909349003
COX1	0.061873	-0.63006	-0.87942	0.004394	-1.28186	6.16E-08	0.542933	0.02047	-0.63006	0.387811
COX2	0.001493	-0.50761	-0.40162	0.40119	-0.80657	0.001264	-0.09484	0.758751	-0.50761	1
COX3	-0.09433	-0.43701	-0.41972	0.37389	-0.53159	0.053944	-0.14182	0.618605	-0.43701	1
CYTB	0.006393	-0.43701	-0.35421	0.499885	-0.40934	0.162343	0.232357	0.372625	-0.43701	1
ND1	0.284463	-0.25962	-0.13505	0.911359	-0.44406	0.122474	-0.05626	0.875776	-0.25962	1
ND2	0.054776	-0.29986	0.589868	0.130454	0.488546	0.083206	-0.50793	0.031953	-0.29986	0.10354

doi:10.6342/NTU202402516

ND3	-0.37244	-0.63753	-0.58074	0.137583	-0.56939	0.036063	-0.57677	0.013555	-0.63753	1
ND4L	-0.29764	-0.13102	-0.02306	1	-0.39089	0.189712	0.285865	0.261653	-0.13102	1
ND5	-0.16833	-0.41813	-0.58014	0.139384	-1.05749	1.15E-05	0.907427	6.43E-05	-0.41813	1
ND6	0.587103	0.103254	1.078485	0.000126	0.642198	0.015386	-1.25601	1.81E-08	0.103254	0.002419
RNR2	0.011811	-0.26486	-0.52693	0.195954	-0.51987	0.060705	0.506444	0.031637	-0.26486	1
ATP8	0.270893	-0.14063	0.361018	0.499367	-0.08955	0.854062	-0.54215	0.022532	-0.14063	0.042438
ATP6	0.403571	-0.17655	0.238349	0.725387	-0.20666	0.549692	-0.41186	0.086737	-0.17655	1
CLU	1.234858802	9.74629E-06	0.951886871	0.005967972	0.752724821	0.011318933	-1.24084355	4.11008E-08	-0.59025217	0.777016794
CREBRF	0.895609082	0.033948609	0.030939636	0.007658806	0.0001524	0.00375096	-1.854837029	1.50685E-13	1.30109745	0.030050768
EDEM3	0.541554951	0.341051557	0.788233759	0.028075419	1.284293405	1.98481E-07	2.292829375	1.56095E-23	1.51518557	0.014368445
SEPTIN7	0.542521375	0.310622787	0.564518813	0.197505313	1.519222346	3.64396E-10	2.315315743	1.81657E-24	1.62661484	0.018966644
GRIA2	1.42749363	0.003324495	0.013212191	1	4.582111202	0.484937557	2.039070371	2.0328E-13	1.54115637	0.689397242
SYBU	-0.99329555	0.017227995	0.651300104	0.082159211	1.526827796	0.235716186	1.487869292	0.916132029	-0.46794156	0.533779853
NEFL	0.446083	0.471724892								
NEFM	1.543813894	2.00562E-09	-0.357740052	0.004119596	0.177783	0.323593167	-0.315748921	1.73399E-11	0.54051566	0.846159213
NEFH	-0.05024	0.01130893								
IFI6	-1.674770489	3.53237E-11	-0.436120745	0.522984914	-0.110833858	0.861579277	-0.720962752	0.00412274	-0.57761487	0.459471511
IFIT1	-1.636058888	0.924905981	1.248142088	1	0.584763114	0.521295738	0.846873058	0.04778507	0.78606225	-
TBK1	0.765599604	0.131710047	0.641805562	0.24173163	0.928113933	0.000970447	2.009230115	2.14683E-16	1.257842483	0.034992973
NFE2L2	0.330146305	0.727741675	0.757702368	0.070352661	0.989841326	0.00012206	1.731902041	2.42515E-13	1.115990896	0.030009355

[1]Log 2-Fold Change and p-adjusted values of selected genes were generated using EdgeR and DeSeq2, comparing between TAOK1-overexpressing SH-SY5Y and matched clone without TAOK1 overexpression.

doi:10.6342/NTU202402516